

# Thirty years of the finite volume method for solid mechanics

P. Cardiff<sup>1\*</sup>, I. Demirdžić<sup>2</sup>

<sup>1</sup>University College Dublin, Bekaert University Technology Centre, School of Mechanical and Materials Engineering, Belfield, Ireland

<sup>2</sup>Mašinski fakultet Sarajevo, Vilsonovo šetalište 9, 71000 Sarajevo, Bosnia-Herzegovina

## SUMMARY

Since early publications in the late 1980s and early 1990s, the finite volume method has been shown suitable for solid mechanics analyses. At present, there are several flavours of the method, which can be classified in a variety of ways, such as grid arrangement (cell-centred vs staggered vs vertex-centred), solution algorithm (implicit vs explicit), and stabilisation strategy (Rhie-Chow vs Jameson-Schmidt-Turkel vs Godunov upwinding). This article gives an overview, historical perspective, comparison and critical analysis of the different approaches where a close comparison with the *de facto* standard for computational solid mechanics, the finite element method, is given. The article finishes with a look towards future research directions and steps required for finite volume solid mechanics to achieve more widespread acceptance.

Received ...

KEY WORDS: finite volume methods; solid mechanics; stress analysis; finite element methods

## 1. INTRODUCTION

“Now however I recognise the FVM/FEM dichotomy as being comparable with those between Protestant and Catholic, or Sunni and Shia. That is to say that it promotes needless conflict; and expense; and loss of opportunity.” [1] With these words, Brian Spalding highlighted the, at times, unproductive nature of the debate around the relative merits of the finite volume (FVM) and finite element (FEM) methods. Although accepted in the Computational Fluid Dynamics (CFD) field, there remains a reluctance and general confusion around the application of the finite volume method to solid mechanics. The aim of this article is to clarify this confusion, by: providing an overview of the significant developments within the field; linking variants of the finite volume method for solid mechanics analyses; comparing finite volume methods with standard finite element methods; and, finally, identifying future directions for the field.

Building on the foundations of the finite difference method, the finite volume method is a generalisation in terms of geometry and topology: simple finite volume schemes reduce to finite

---

\*Correspondence to: I. Demirdžić, Mašinski fakultet Sarajevo, Vilsonovo šetalište 9, 71000 Sarajevo, Bosnia Herzegovina. E-mail: i.demirdzic@yahoo.com

difference schemes. Whereas the finite difference method is based on nodal relations for *differential* equations, the finite volume method balances forces acting on control volumes, directly discretising the *integral* form of the conservation laws. A number of prior developments within CFD provided the foundation for the earliest paper on the cell-centred finite volume method for solid mechanics by Demirdžić et al. [2]. In the subsequent three decades the finite volume method for solid mechanics has developed in a number of directions, differing in terms of discretisation, solution methodology and overall philosophy. The varied approaches may be classified in a number of ways, including, for example:

- *Grid arrangement*: cell-centred [2, 3] vs vertex-centred [4–12] vs staggered-grid [13–19], as well as more recently face-centred [20, 21] and meshless [22, 23];
- *Solution algorithm*: implicit [3, 24, 25] vs explicit (matrix-free) [26–28];
- *Stabilisation approach*: Rhie-Chow [29, 30] vs Jameson-Schmidt-Turkel [31] vs Godunov *two-sided* upwinding [27, 32].

There are countless other ways to classify the approaches, for example, based on force discretisation at the control volume face, however, the current article will base its discussion primarily around the three classification types above.

The essential characteristic of a finite volume method is the integration of the governing conservation equation over finite control volumes. In this sense, the *cell-centred* vs *vertex-centred* vs *staggered-grid* approaches primarily differ in *how* these control volumes are constructed. Cell-centred approaches use the primary mesh control volumes, whereas vertex-centred approaches construct a *dual mesh* with control volumes surrounding the vertices of the primary mesh. On the other hand, staggered-grid approaches create multiple secondary meshes, one for each scalar component of the primary solution vector, constructed about the primary mesh faces. Despite their close relationship, as explored further in Section 3, approaches based on differing grid arrangements often differ greatly in terms of philosophy: as noted by Baliga and Atabaki [33], the cell-centred method is often thought of as a control-volume finite difference method, combining ideas borrowed from finite volume and finite difference methods; whereas, the vertex-centred approach is viewed as a control-volume finite element method, formulated by amalgamating concepts native to finite volume and finite element methods.

Regardless of the chosen grid arrangement, spatio-temporal integration of the governing equations may adopt an *implicit* or *explicit* solution algorithm. Implicit algorithms are characterised by the solution of a linear system of equations and are unconditionally stable with respect to the time increment size. In contrast, explicit or matrix-free algorithms avoid the need to construct such a system of linear equations but the time increment size is restricted by the classic Courant-Friedrichs-Lewy constraint [34]. The choice of solution algorithm often depends on the problems of interest, with implicit methods favoured for elliptic and parabolic cases (steady-state and quasi-steady-state) and explicit methods for hyperbolic (high rates, wave propagation). Once the grid arrangement and solution algorithm are selected, care must be taken in the construction of a stable discretisation that does not suffer from unphysical instabilities in the solution field. To this end, a variety of stabilisation approaches have been proposed. Generally, each approach can be viewed upon as adding some form of diffusion to the surface force discretisation with the purpose of quelling high-frequency oscillations. Rhie-Chow-style stabilisation is common in the implicit approaches

originating from the work of Demirdžić and Muzaferija [29], while Godunov upwinding and Jameson-Schmidt-Turkel approaches are more commonly seen in the explicit approaches, rooted in the solution of compressible gas flow Euler equations.

From afar, each of these main variants of finite volume method can seem quite distinct; however, upon closer inspection, they share many similarities in terms of discretisation and solution algorithm. Nevertheless, the fragmented nature of the finite volume solid mechanics community is evident from many recent publications in the area, where authors, reviewers and editors tend to be unaware of developments within the field, for example, see [35]. In addition, and more generally, there is a lack of awareness in the computational mechanics community around the capabilities of the finite volume method for solid mechanics. Accordingly, a comparative and critical review of the finite volume method for solid mechanics is timely, relevant and essential for the future progress of the field. Within this domain, there are a number of open questions: What are the strengths and weaknesses of the various approaches? Which approaches show the greatest potential and widest applicability? Are there possibilities for the various methods to be combined to produce superior methods? How do the finite volume approaches relate to finite element methods? Are there directions of development which are missing? This article will attempt to provide answers to these questions, as well as providing a unifying framework for the discussion of finite volume methods for solid mechanics, and their relationship with finite element methods. Given the scale of the field, it is outside the scope of the article to provide an exhaustive review of all formulations; instead, the article aims to provide detailed analysis on the main variants of approach common in the literature. The primary novel contributions of the current article are twofold: (i) The first detailed review of the finite volume solid mechanics field is presented; and (ii) The first analysis of similarities and differences between all main variants of the finite volume method for solid mechanics is detailed. (ii) A unique analysis of the finite volume method for solid mechanics is performed, cumulating in the description of a unified approach.

The remainder of the article is constructed as follows: Section 2 provides a chronological overview of the prominent finite volume developments for solid mechanics. Section 3 compares and contrasts the three main flavours of the finite volume method for solid mechanics. In Section 4, the finite volume method for solid mechanics is compared to the “standard” continuous Bubnov-Galerkin finite element method, highlighting similarities and differences in terms of discretisation, solution methodology and overall philosophy. Section 5 reviews the variety of structural applications to which the finite volume method has been applied in its thirty year history. The penultimate section briefly reviews software that use, or have previously used, the finite volume method for solid mechanics simulations. Finally, Section 7 summarises the main conclusions of the article and considers the current challenges facing the field.

## 2. HISTORY OF THE FINITE VOLUME METHOD FOR COMPUTATIONAL SOLID MECHANICS

The development of the finite volume method for solid mechanics has occurred independently in a number of forms, with finite difference methods, computational fluid mechanics algorithms, and finite element methods providing much of the inspiration. This section gives an overview of the

historical development of these finite volume methods. The treatise is primarily partitioned based on the grid arrangement, where comments regarding the solution algorithm and stabilisation scheme are given where appropriate. In-depth dissections of the technical details are left to Section 3. While the field is small and fragmented, there are a number of notable reviews worth mentioning, including those of Maneeratana [36], Vaz Jr. et al. [37] and Cavalcante et al. [38].

Before delving into details of influential publications, it is insightful to first consider the literature landscape as a whole. To this end, Figure 1 presents a histogram of the publications in the area to-date, separated into journal articles, conferences, Ph.D. theses, Masters theses and books. Of course, exact records of each publication type are difficult to track and consequently the data should be taken as indicative. To complement this, Figure 2 lists the most popular international journals for

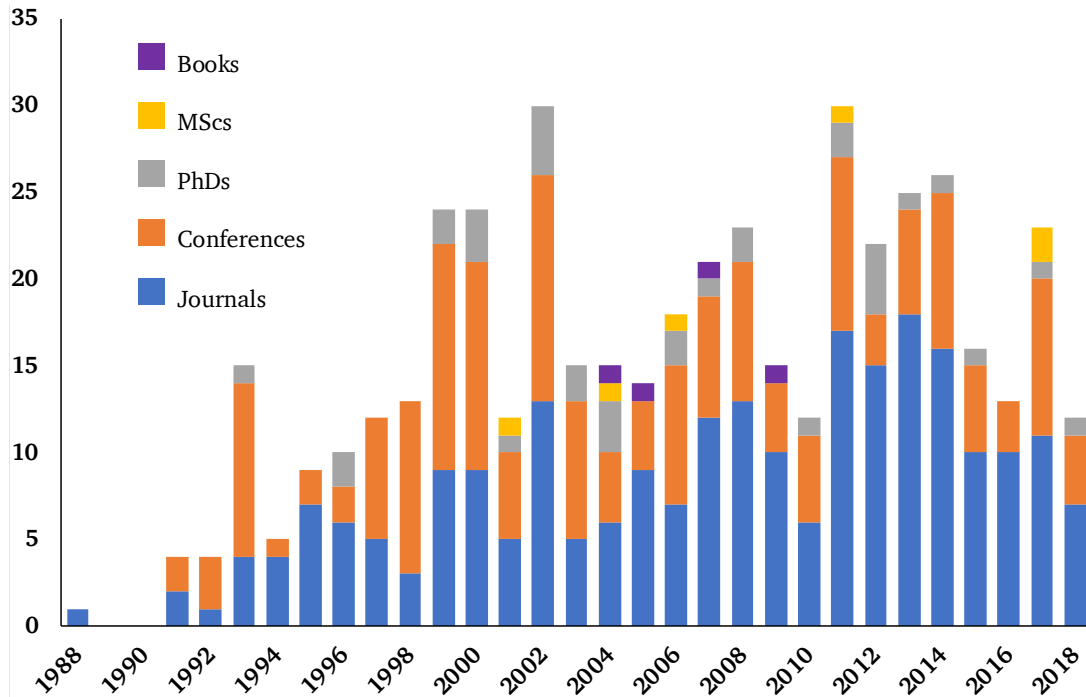


Figure 1. Histogram of the finite volume method for solid mechanics publications to-date

publishing finite volume solid mechanics articles; only journals with greater than five articles have been included. Furthermore, a table of the most cited articles related to the finite volume method for solid mechanics can be found in Appendix A.

A perspective on the literature landscape is gained from the *co-authorship network* presented in Figure 3, which has been generated using the VOSviewer software [39]. A co-authorship network is a visual method to assess research collaborations within a field, as well as observe detached regions of research. Referring to Figure 3, the three larger sub-networks broadly correspond to: implicit cell-centred approaches indicated by the red sub-network centred on *demirdžić* and *ivanković*; implicit vertex-centred approaches indicated by the green sub-network centred on *cross*, *bailey* and *fallah*; and a specialised form of finite volume method for microstructural analysis indicated by the blue sub-network centred on *aboudi*, *pindera* and *cavalcante*. Although the co-authorship graph is not a direct measure of contribution to the field, it does provide insight into the collaboration between authors and subdivisions within the domain. In the graph, individual authors are represented by

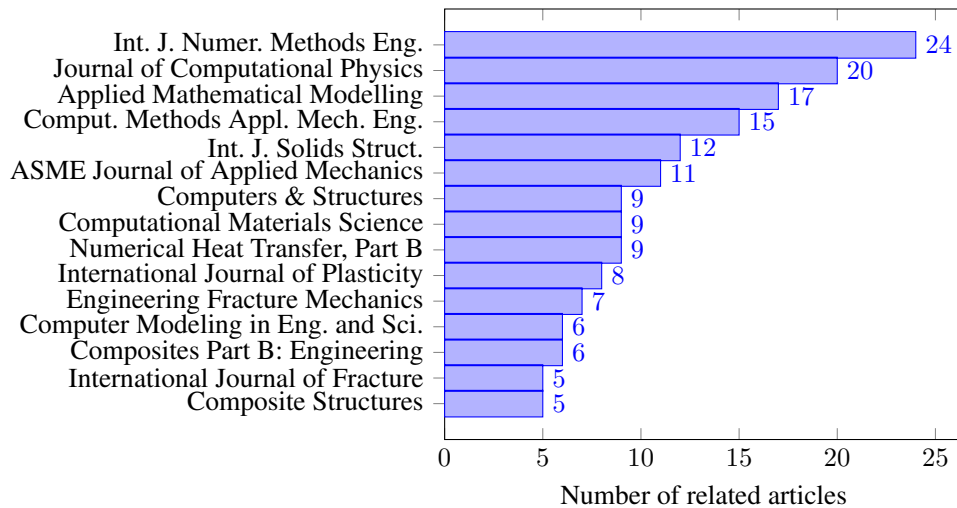


Figure 2. Number of publications per journal related to computational solid mechanics using the finite volume method, based on the cited references, where only journals with greater than five articles have been counted

filled circles, and a co-authored publication between two individual authors is symbolised by a line connecting the two filled circles; the line thickness increases with increasing number of co-authored publications; the size of an author's filled circle is directly proportional to the number of their related publications. To maintain interpretability, only authors with five or more related publications have been included in the network, and only peer-reviewed publications have been incorporated.

Finally, before considering individual contributions, we will clarify the meaning of a number of terms in the current context to avoid any confusion. For the domain spatial discretisation, this will be referred to interchangeably as the “mesh” or “grid”; each sub-domain in a finite volume mesh will be equivalently referred to as a “control volume”, a “cell”, or even an “element”; similarly, each sub-domain in the finite element mesh will be referred to as an “element” or “cell”. The term “node” indicates the mesh location where the solution variable is stored, which could be a vertex, face-centre or cell-centre depending on the method.

### 2.1. Cell-centred approaches

Thirty years ago, Demirdžić et al. [2] proposed the first application of the cell-centred finite volume method in its modern form to solid mechanics. Subsequently, cell-centred developments have primarily focussed on two relatively disconnected approaches:

- *Implicit* cell-centred approaches based on the original approach of Demirdžić et al. [2], and
- *Explicit* Godunov-type cell-centred approaches stemming from the work of Trangenstein and Colella [40].

The cell-centred approach takes its name from the dependent variable(s) residing at the cell centres (control volume centroids); equivalently, the approach has been termed the *colocated*, *co-located* or *collocated* finite volume method, as the dependent variables share their location at the cell centres/centroids.

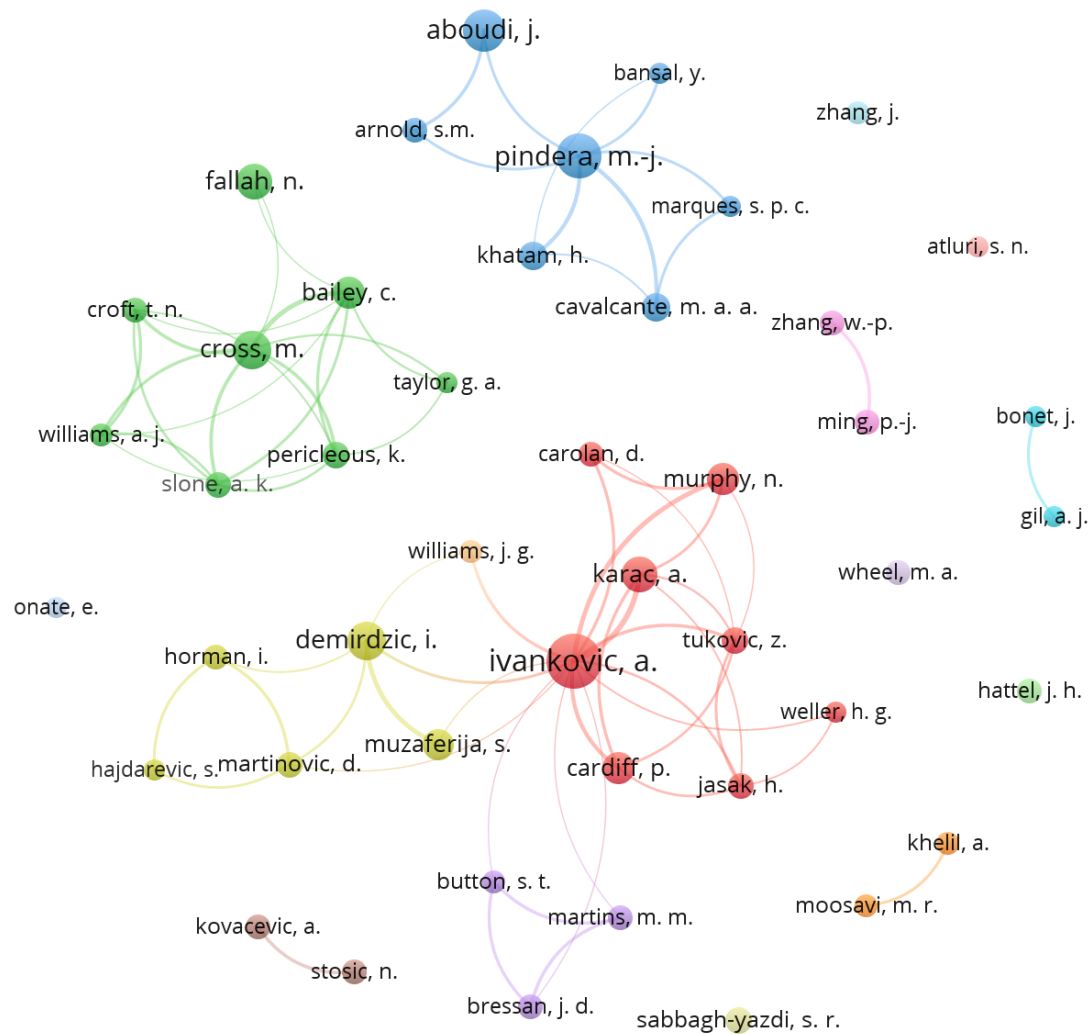


Figure 3. Co-authorship network of the finite volume method for solid mechanics, generated using the VOSviewer software [39]. To maintain interpretability, only authors with five or more related peer-reviewed publications have been included in the network. The network provides insight into collaborations within the field but is not a direct measure of contribution.

**Implicit cell-centred methods** Considering first the implicit methods: in the original approach of Demirdžić et al. [2], a structured rectangular 2-D method was applied to the simulation of thermal deformations in welded workpieces (Fig. 4(a)). The displacement was assumed to vary linearly between computational nodes, and the small strain material behaviour was described by the *Duhamel-Neumann* form of Hooke's law. A distinguishing feature of the proposed solution algorithm was the partitioning of the surface force term into a compact-stencil *implicit* term and a larger stencil *explicit* term. As a result, the linear momentum *vector* equation was temporarily decoupled into three *scalar* component equations that were independently solved, where outer fixed-point/Gauss-Seidel/Picard iterations provided the required coupling. This form of solution methodology is termed a *segregated* approach, as the governing conservation of linear momentum equation is segregated into three scalar equations during solution. This style of implicit segregated

solution algorithm was inspired by the methods adopted in similar CFD procedures, where the restrictive computer memory sizes available at the time necessitated memory efficient procedures.

The original 2-D method was later generalised to 3-D convex polyhedral cells by Demirdžić and Muzaferija [41] (Fig. 4(b)). This form of the cell-centred approach has since been extended to deal

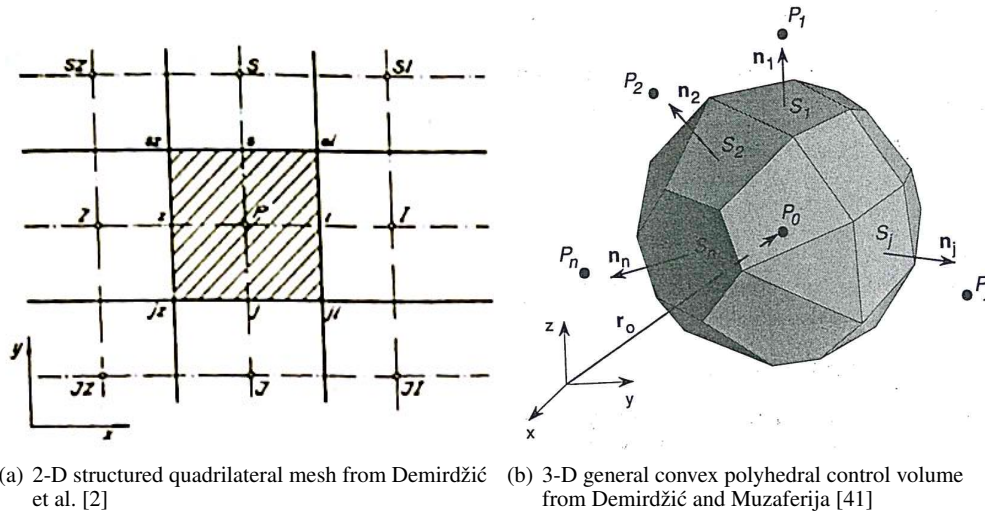


Figure 4. Original 2-D structured quadrilateral mesh of Demirdžić et al. [2] (left) and the subsequent generalisation to 3-D unstructured convex polyhedra [41] (right)

with a wide variety of solid and multi-physics phenomena, including:

- Elastoplasticity [3, 25, 36, 42–54] and viscoelasticity [55–60];
- Thermo-elasticity [2, 41, 61–65] and hygro-thermo-elasticity [66–77];
- Poro-elasticity [78–85];
- Anisotropy [66, 67, 69, 72–75, 86–89] and heterogeneous material properties [79, 84, 90–92].
- Incompressibility and quasi-incompressibility [93–100];
- Contact mechanics [25, 101–105];
- Finite strains and rotations [25, 36, 88, 95, 106–117];
- Fracture mechanics [60, 79, 80, 82, 84, 91, 118–132];
- Casting, melting, solidification and residual stresses [44, 45, 133–137];
- Fluid-solid interaction [29, 93, 94, 96, 98, 99, 113, 138–166];
- Beams, plates and shells [59, 89, 145, 146, 150, 167–187];
- Solid-electrostatic interaction [188, 189] and wave propagation [42, 190–192];

Of particular note are the developments of Weller et al. [193] and Jasak and Weller [194], where the same implicit cell-centred form has been demonstrated to be well-suited to running on distributed-memory supercomputers. The *domain decomposition method* was used where the solution domain is decomposed into a number of sub-domains, each solved on a separate Central Processing Unit (CPU) core; necessary coupling between the sub-domains is performed using a message-passing protocol, initially Parallel Virtual Machine, but Message Passing Interface in later publications. The Weller et al. [193] and Jasak and Weller [194] implementations form a component of the popular open-source C++ library OpenFOAM, formerly commercial software FOAM. Many

of the subsequent developments in the implicit cell-centred field have been based on the OpenFOAM platform, for example, [25, 30, 77, 78, 83, 88, 90, 104, 112, 113, 131, 195]. It should, however, be noted that the explicit Godunov-type approaches have also been implemented in OpenFOAM [28, 196].

The essence of the implicit cell-centre finite volume method has been the use of a displacement approach combined with a segregated algorithm; however, alternative solution methodologies have also been developed, including geometric multi-grid procedures [86, 120, 142, 143, 197], block-coupled algorithms [30, 188, 189, 198, 199], hybrid/mixed pressure-displacement formulations [46, 95, 97, 100, 138, 139, 200, 201], Aitken acceleration [78, 160, 199], and curvilinear formulations [43, 202]. In addition, fourth-order accuracy variants have been proposed [203] as well as novel gradient and tractions calculation methods [25, 157, 160, 199, 204–208]. Apart from the standard *continuum* approaches, a number of authors have proposed implicit cell-centred finite volume methods for beams, plates and shells [59, 89, 145, 146, 150, 167, 173, 174, 181, 185, 186, 209, 210].

**Explicit cell-centred methods** Explicit Godunov-type finite volume methods were first proposed for the solution of hyperbolic problems characterised by waves and shocks [32, 211, 212], and have been popularised for the solution of Euler compressible gas flow equations. The typical approach, which casts the conservation laws as a system of first-order hyperbolic equations, is characterised by the solution of a Riemann problem (propagation of a solution discontinuity) at the control volume faces to determine forces. The resulting discretisation evaluates the force at a control volume face as a weighted average of the force evaluated at each side of the face. Godunov-type methods were first applied to structural problems by Trangenstein and Colella, when they modelled the 1-D propagation of waves in elasto-plastic solids [40, 213, 214]; in their approach, the primitive conservation variables were the linear momentum vector and the deformation gradient (or displacement gradient) tensor. Subsequently, the method has been extended to unstructured 3-D grids in a variety of forms, differing in terms of discretisations and primitive variables [20, 21, 26–28, 32, 196, 215–236], for example, see Figure 5. Although cell-centred formulations are the most common form of Godunov-type method, vertex-centred [31, 237] and, recently, face-centred approaches [20, 21] have also been explored.

To-date, Godunov-type approaches have been used to model a wide range of physical mechanisms:

- Linear elasticity [21, 40, 213, 232];
- Material nonlinearity [26, 28, 196, 216, 218, 222–224, 226–236];
- Fracture and cavitation [216, 226];
- Finite strains [28, 196, 222–224, 226–229, 231, 233–236];
- Material heterogeneity [217, 219];
- Wave propagation and impacts [32, 40, 213–219, 222–229, 231–236].

A distinctive characteristic of Godunov-type methods is the adoption of fully explicit solution algorithms, where the time increment size is restricted by the standard Courant-Friedrichs-Lewy constraint [34].

From an implementation and philosophy perspective, the implicit approaches stemming from Demirdžić et al. [2] differ greatly from the explicit approaches deriving from Trangenstein and

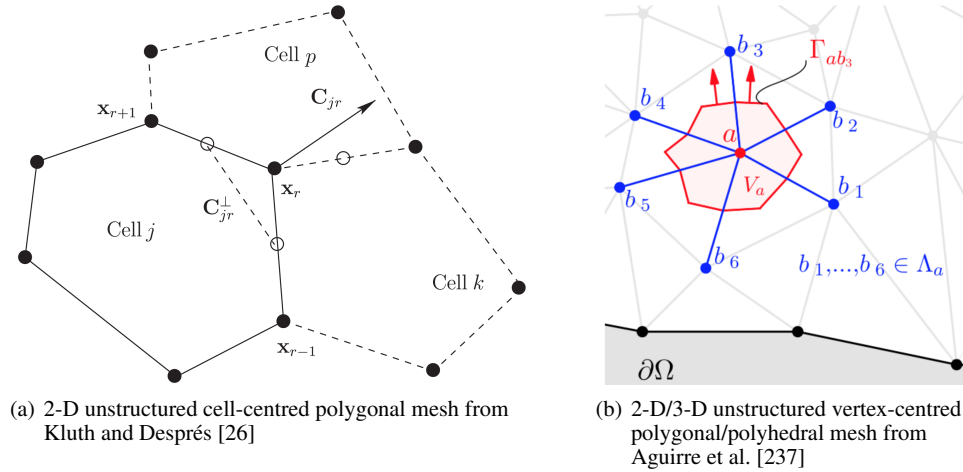


Figure 5. Forms of mesh employed by Kluth and Després [26] and Aguirre et al. [237]

Colella [40]. The most obvious difference is the need of the implicit approach to form and solve a linear system of equations, and the time increment size restriction for explicit methods. In addition to this, the implicit methods have typically assumed a smooth variation of the primitive variable within each cell (or across cell faces); in contrast, the explicit approaches have aimed to directly approximate the propagation of solution discontinuities. Many of these technical distinctions are discussed further in Section 3. It should be noted that *explicit* cell-centred approaches that do *not* adopt a Godunov approach are also possible, for example, as developed by Selim et al. [238, 239].

## 2.2. Vertex-centred approaches

**Implicit vertex-centred methods** Fryer et al. [5] was the first to propose a vertex-centred finite volume method for solid mechanics. The approach, initially termed a *control volume-unstructured mesh* procedure, could analyse complex 2-D geometry using both quadrilateral and triangular cells (Fig. 6(a)). The method of Fryer et al. [5] followed closely the approach of Baliga and Patankar [240] from a decade earlier, who developed a so-called *control-volume-based finite element method* for convection-diffusion equations on unstructured triangular grids.

In addition to the designation *vertex-based finite volume method*, the formulation is referred to by a number of other names, including *vertex-centred finite volume method*, *cell-vertex finite volume method*, *control volume procedure*, *control-volume finite element method*, *control-volume-based finite-element method*, and *element-based finite volume method*.

In contrast to cell-centred and staggered-grid approaches, vertex-centred approaches store the primary unknowns at the *primary* mesh vertices and integrate the governing equation over secondary/*dual* mesh control volumes surrounding each *primary* mesh vertex.

The original 2-D approach of Fryer et al. [5] was subsequently extended to three dimensions by Bailey and Cross [24] (Fig. 6(b)) and has since been applied to a wide range of physical phenomena:

- Compressible and incompressible elasticity [24, 242–250];
- Elasto-plasticity, elasto-visco-plasticity, creep and material nonlinearity [179, 183, 241, 251–253];

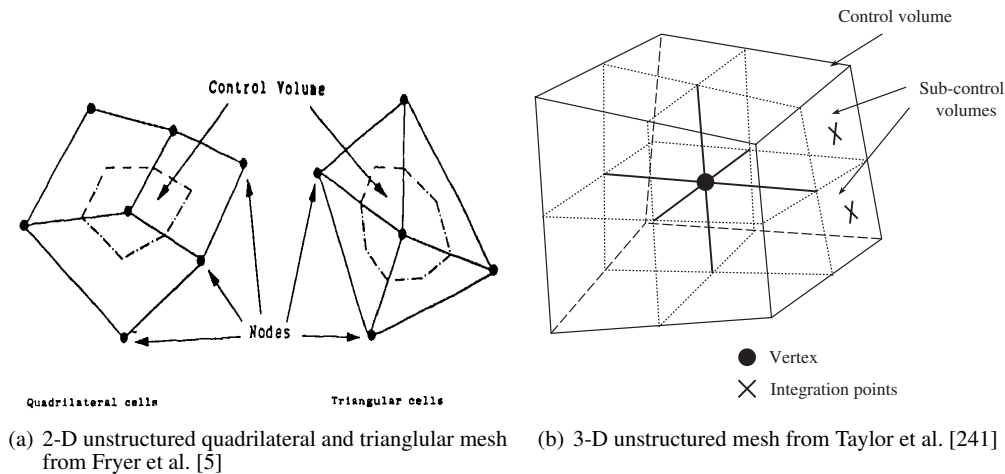


Figure 6. Vertex-based finite volume formulation of Fryer et al. [5] (left) showing the construction of control volumes around a mesh vertex for quadrilateral and triangular 2-D cells, and of Taylor et al. [241] showing the extension to 3-D cells.

- Finite strains and geometric nonlinearity [254–260];
- Beams, plates and shells [168, 261, 262];
- Multi-physics and fluid-solid interaction [249, 263–280];
- Casting [4, 7, 9, 10, 264–267, 281–284], extrusion and forging [285–287];
- Welding [288–290];
- Contact mechanics [291];
- Functionally graded solids [292, 293] and wood drying [294, 295];
- Micropolar/Cosserat elasticity (shear stress may not be symmetric) [296, 297];
- Vibrations, acoustics and wave propagation [178, 298–300].

Alternative solution methodologies have been examined, including mixed displacement-rotation approaches [301–303], and addressing parallelisation on distributed memory supercomputers [304, 305]. Also of note are the developments of Maitre et al. [306] and Souhail [307], who proposed a higher order extension of the vertex-based approach.

It is important to note the distinction between *overlapping* and *non-overlapping* vertex-centred methods: the more common approach involves non-overlapping control volumes, where the control volumes about each primary mesh vertex do not overlap with the control volumes of neighbouring primary mesh vertices. In the less popular overlapping control volumes approaches, for example, as discussed by Oñate et al. [12], primary mesh vertices partly share control volumes with primary mesh neighbouring vertices, resulting in the governing equations being integrated more than once over regions of the domain; this overlapping local integration domain approach is more similar to the finite element method. Additionally, Tsui et al. [249] proposed a variation on the common approach to construct the control volumes: the primary mesh cell centres are joined together to make the control volumes, rather than joining the cell-centres to the face-centres as per the classic vertex-based method.

**Explicit vertex-centred methods** Similar to cell-centred methods, both implicit and explicit solution algorithms have been developed, although explicit vertex-centred methods have seen less development. Within the category of explicit vertex-centred methods, there exists a variety of subclasses, including: so-called dual-time-stepping explicit methods, where the solution is calculated in an explicit manner and a linear system is not directly formed [248, 249, 277, 279, 298]; Godunov-type approaches [31, 237] similar to those seen in cell-centred approaches, as noted in Section 2.1; and the so-called *grid method* [308–313]. Regarding the grid-method, the originators of the method, Zhang and Liu [308], argue for the distinction between the grid method and the vertex-based finite volume method, however, the authors of the current article believe this distinction is unwarranted: like other finite volume methods, the grid method starts from the governing momentum equation in strong integral form and approximates the forces over the boundaries of the control volumes; although there are minor differences in the techniques used to approximate the surface forces, for example, comparing Dormy and Tarantola [314] and Zhang and Liu [309], the *grid method* still remains a form of vertex-centred finite volume method.

### 2.3. Staggered-grid approaches

In staggered-grid approaches, as originally proposed for CFD by Harlow and Welch [315], the components of the primary solution variable, for example, the  $x$  and  $y$  components of displacement, are stored at different locations. In addition, different sets of control volumes are used when integrating the discretised governing equation in each Cartesian direction. For example, the  $x$ -momentum component equation employs a different grid to the  $y$ -momentum component equation. The primary motivation for such staggered-grid approaches is the avoidance of solution instabilities, namely the “checker-boarding” phenomenon, where high frequency variations appear in the solution variables that are unobservable to the discretisation. Consequently, staggered-grid approaches do not need to explicitly included a stabilisation term, as is common in cell-centred methods. The extension of staggered-grid approaches to general unstructured 3-D meshes is, however, not trivial; and consequently, this major limitation has resulted in declining popularity for such approaches in solid mechanics.

The first application of a staggered-grid formulation to solid mechanics was by Beale and Elias [13, 14], who showed how the finite volume CFD code PHOENICS could be applied to stress analysis problems. In their method, Beale and Elias used the analogy between the stream functions in creeping-fluid-flow and the Airy stress functions in solid mechanics, where the stress components were the primary unknowns. This method was later generalised by Spalding, Bukhari, Qin, Hamill and co-workers [15, 17, 316–322], where a displacement, rather than a force analogy, was adopted, having the major advantage of being more general in three dimensions. Spalding noted that a CFD solution procedure designed for computing velocities is suitable for computing displacements if the convection terms are set to zero and the volume/dilatation stress term is introduced by inclusion of a pressure- and temperature-dependent source term. As a consequence, the resulting solution method used an *implicit* SIMPLE algorithm [323, 324], still popular in modern CFD codes. The employed primitive variables were displacement and pressure, as opposed to velocity and pressure in standard fluid flow analyses.

The use of mixed displacement-pressure approaches, however, is not a requirement of staggered-grid approaches. Hattel, Hansen and collaborators [16, 18, 19, 325–337] demonstrated a staggered-grid approach where the sole primary variable was displacement. Hattel and Hansen [16] initially proposed their staggered-grid approach for the analysis of thermally induced stresses in casting problems, and subsequently extended it for a variety of thermo-elasto-plasticity problems. They termed their approach “a control volume based finite difference method”, further indicating the close-relationship with finite difference methods. The authors noted that their method resulted in an elegant formulation for non-constant material properties, a benefit of the staggered grid approach.

In addition to the displacement and displacement-pressure approaches, a number of alternative staggered grid formulations have also been proposed: Spalding [320] proposed a staggered formulation where *rotation* and displacement were the primitive variables; Spalding surmised that the rotation-based method may provide a more efficient solution algorithm in certain situations. The approach is described in documentation from an early version of the PHOENICS software; however, issues with boundary conditions are noted and no further articles appear on the formulation. A similar idea was subsequently proposed by Wenke, Wheel, Pan and Qin [301–303] in the framework of vertex-based finite volume methods, where both displacements and rotations are considered the primitive variables. More recently, Wang and Melnik [338] put forward a staggered finite volume approach for analysis of shape memory alloys, defined on 2-D structured rectangular grids. In contrast to the majority of staggered grid approaches, which employ implicit solution algorithms, Rajagopal et al. [339] proposed a one-step explicit staggered grid finite volume approach to investigate the response of a layered viscoelastic plate.

#### 2.4. Other approaches

Across the spectrum of finite volume methods for solid mechanics, not all procedures align with the previously discussed divisions.

**Approaches for periodic heterogenous microstructures** Although arguably not a fundamental class of finite volume method, there has been significant development related to specialised versions of the finite volume method for periodic microstructures. Depending on the formulation, the related methods can be referred to by a number of names, including: the *higher-order theory for functionally graded material* (HOTFGM) [340], the *high-fidelity generalised method of cells* (HFGMC) [341–344], the *finite volume direct averaging micromechanics* (FVDAM) theory [345, 346], or some variant thereof. Although there is some disagreement over the naming convention [343, 344, 346], these methods have a common origin in the *method of cells* and the *generalised method of cells* developed by Aboudi and Paley [347–349]. Recent discussions around the development of these methods can be found in Haj-Ali and Aboudi [344], Cavalcante et al. [38], Gong et al. [292], and Cavalcante and Pindera [350], along with reviews of the high fidelity generalised method of cells approaches by Aboudi [351] and of microstructural analysis approaches by Pindera et al. [352] and Charalambakis and Murat [353]. Reviews of the application of such methods can be found in Aboudi et al. [354] and Aboudi [355]. A brief overview of the discretisation used in HOTFGM/HFGMC/FVDAM approaches is given in Appendix B.

**Meshless finite volume approaches** Meshless methods have been proposed in order to overcome the drawbacks of mesh-based finite element and finite volume methods, particularly related to large deformations and cracking. Atluri and Shen [356] were the first to propose a meshless finite volume formulation, based on the earlier generalised *Meshless Local Petrov-Galerkin (MLPG) method* by Atluri and Zhu [357]. The approach has subsequently been extended and applied to a variety of problems in elasto-statics, elasto-dynamics and fracture mechanics [358–375]. Based on the initial development of Atluri and co-workers, Moosavi and Khelil [367] proposed a novel meshless form of the finite volume method for elasto-static analysis, that combined the finite volume concept with the meshless local Petrov-Galerkin approach with moving least squares interpolation. Moosavi and co-workers have since extended the method to elasto-dynamics, beams, plates, shells and crack problems [368–370, 374, 375], where the method has been named the *orthogonal meshless finite volume method*. Whereas the Atluri and Shen [356] approach uses overlapping control volumes, the meshless finite volume method developed by Ebrahimnejad et al. [22, 376, 377] employs non-overlapping control volumes. The method has been applied to 2-D elasticity with adaptive mesh refinement, and was later extended to problems with material discontinuities [23, 378], to free vibration analysis of laminated composite plates [379, 380], and to fractures in orthotropic media [381].

**Eulerian approaches** There are many solid mechanics problems which can be equivalently considered from the fluid mechanics perspective, for example, in the analysis of extrusion and drawing. Eulerian “fluid” approaches are often used to solve such problems, for example, [46, 48, 50–52, 54, 286, 287, 382–394]. These methods are more closely related to CFD procedures and are not discussed further here.

**Miscellaneous** Teng et al. [395] and Chen et al. [396] developed a finite volume method to simulate the draping of woven fabrics, where the governing nonlinear equations were solved using a single-step full Newton-Raphson method. Martin and Pascal [397, 398] proposed a novel *discrete duality finite volume* method for solving linear elasticity problems on unstructured meshes; the main characteristic of the discretisation is the integration of the governing equations over two meshes: the given primal mesh and also over a dual mesh built from the primal one. Pietro et al. [399] proposed a novel discretisation scheme for linear elasticity with only one degree of freedom per control-volume face, corresponding to the normal component of the displacement.

### 3. COMPARING VARIANTS OF THE FINITE VOLUME METHOD FOR COMPUTATIONAL SOLID MECHANICS

The finite volume method, like other related numerical approaches, consists of the following main components:

- a) Discretisation of space and time;
- b) Discretisation of the mathematical model equations;
- c) Solution algorithm.

To facilitate comparison between the major variants, three popular formulations will be considered here:

- Implicit cell-centred approach originating from the work of Demirdžić et al. [2];
- Implicit vertex-centred approach of Fryer et al. [5] and Bailey and Cross [24];
- Explicit cell-centred approach emanating from Trangenstein and Colella [40].

Analysis and insight into the similarities and differences between these variants is provided.

### 3.1. Mathematical model for dynamic linear elasticity

To allow a clear comparison of the methods, the dynamic behaviour of a body with volume  $\Omega$  and surface  $\Gamma$  is analysed (Fig. 7), where part of its boundary is subjected to a specified displacement,  $\mathbf{u}_b$ , and the remainder is subjected to a specified traction,  $\mathbf{T}_b$ .

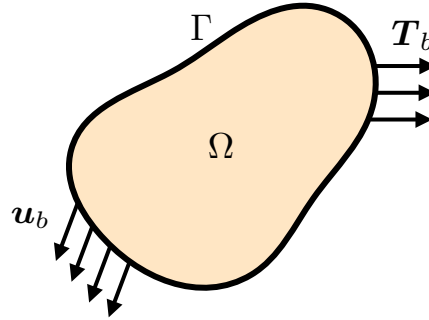


Figure 7. Generic solid body, with volume  $\Omega$  and surface  $\Gamma$ , subjected to boundary displacements,  $\mathbf{u}_b$ , and boundary tractions,  $\mathbf{T}_b$

Assuming the relationship between stress and strain to be described by Hooke's law, the governing conservation of linear momentum equation, a generalisation of Newton's second law, can be given in strong integral form as:

$$\underbrace{\int_{\Omega} \rho \frac{\partial^2 \mathbf{u}}{\partial t^2} d\Omega}_{\text{Inertia forces}} = \underbrace{\oint_{\Gamma} \mathbf{n} \cdot [\mu \nabla \mathbf{u} + \mu (\nabla \mathbf{u})^T + \lambda \text{tr}(\nabla \mathbf{u}) \mathbf{I}] d\Gamma}_{\text{Surface forces}} + \underbrace{\int_{\Omega} \rho \mathbf{f}_b d\Omega}_{\text{Body forces}} \quad (1)$$

Small deformations are assumed *i.e.* no distinction is made between the initial and deformed configurations;  $\rho$  is the initial density,  $\mathbf{u}$  is the unknown total displacement vector,  $\mathbf{n}$  is the outward-pointing surface unit normal vector,  $\nabla$  is the del operator,  $\lambda$  is the first Lamé parameter,  $\mu$  is the second Lamé parameter, synonymous with the shear modulus,  $\mathbf{I}$  is the second-order identity tensor, and  $\mathbf{f}_b$  is a body force acceleration. To avoid unnecessary complexity, the material properties ( $\rho$ ,  $\mu$  and  $\lambda$ ) are assumed to be uniform and isotropic; however, this assumption is not required. It should be noted that the finite volume method directly discretises this strong integral form of the governing equation, without requiring weighting functions, the weak form of the equation or the use of the Gauss divergence theorem.

### 3.2. Implicit cell-centred approach

In this sub-section, the implicit cell-centred approach stemming from Demirdžić et al. [2] is described.

**Discretisation of time** For all described variants of the finite volume method, discretisation of the solution domain comprises time discretisation and space discretisation. The total specified simulation time is divided into a finite number of time increments,  $\Delta t$ , and the discretised governing equations are solved in a time-marching manner.

**Discretisation of space** For the implicit cell-centred approach, the spatial domain is divided into a finite number of contiguous convex polyhedral cells bounded by polygonal faces that do not overlap and fill the space completely. A typical control volume is shown in Figure 8, with the computational node  $P$  located at the cell centre/centroid, and the cell volume is  $\Omega_P$ ;  $N_f$  is the centroid of a neighbouring control volume, which shares face  $f$  with the current control volume;  $\Gamma_f$  is the area vector of face  $f$ , vector  $\mathbf{d}_f$  joins  $P$  to  $N_f$ , and  $\mathbf{x}$  is a positional vector. No distinction is made between different cell volume shapes, as all general convex polyhedra are discretised in the same fashion.

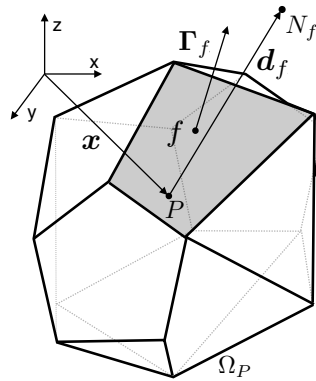


Figure 8. General convex polyhedral control volume (adapted from [25, 29, 155])

**Discretisation of the mathematical model equations** The governing conservation law (Equation 1) is applied to each polyhedral cell in the mesh. The discretisation of each of the three terms (inertia, surface forces, body forces) within the equation is now discussed in turn.

Considering first the spatial discretisation of the inertia term in Equation 1. The term can be approximated by making an assumption about the variation of the displacement vector  $\mathbf{u}$  over the cell; typically in the implicit cell-centred approach a linear variation is assumed. This linear variation can be expressed in terms of a truncated Taylor series expansion about the cell centre:

$$\mathbf{u}(\mathbf{x}) = \mathbf{u}_P + (\mathbf{x} - \mathbf{x}_P) \cdot (\nabla \mathbf{u})_P \quad (2)$$

This expression says that the displacement  $\mathbf{u}(\mathbf{x})$  at any point in the cell can be calculated using the cell-centre displacement  $\mathbf{u}_P$  and the constant gradient of displacement within the cell  $(\nabla \mathbf{u})_P$ . This approximation is second-order order in space *i.e.* as the mesh spacing is reduced, the error in this

approximation reduces at second-order rate. In principle, any other distribution could be used; for example, Demirdžić [203] extended the approach to use a fourth-order cubic distribution.

Using the approximation in Equation 2, the inertia term can be calculated using the midpoint rule as a function of the cell-centred values:

$$\int_{\Omega} \rho \frac{\partial^2 \mathbf{u}}{\partial t^2} d\Omega \approx \rho \left( \frac{\partial^2 \mathbf{u}}{\partial t^2} \right)_P \Omega_P \quad (3)$$

where the subscript  $P$  on the density has been dropped as a uniform density field is assumed *i.e.*  $\rho_P = \rho$ .

The acceleration  $\partial^2 \mathbf{u} / \partial t^2$  may be discretised in time using any appropriate finite difference scheme; in the original cell-centred approach of Demirdžić et al. [2], the bounded first-order backward Euler method was used:

$$\left( \frac{\partial^2 \mathbf{u}}{\partial t^2} \right)_P \approx \frac{\mathbf{u}_P - 2\mathbf{u}_P^{[m-1]} + \mathbf{u}_P^{[m-2]}}{\Delta t^2} \quad (4)$$

where  $m$  is the time-step counter; the superscript on the unknown current time value of displacement has been dropped for brevity. Here it is assumed that the time-step size  $\Delta t$  is constant; however, the method can be generalised to variable time-step sizes. There are numerous other temporal discretisations that may be used; for example, the unbounded second-order backward Euler scheme [194], the second-order trapezoidal rule [199], or the second-order Newmark schemes that are popular with the finite element method.

The final discretised inertia term is:

$$\int_{\Omega} \rho \frac{\partial^2 \mathbf{u}}{\partial t^2} d\Omega \approx \rho \frac{\mathbf{u}_P - 2\mathbf{u}_P^{[m-1]} + \mathbf{u}_P^{[m-2]}}{\Delta t^2} \Omega_P \quad (5)$$

In a similar fashion, the body force term (second term on the right-hand side of Equation 1) is approximated by assuming  $\mathbf{f}_b$  to vary over the cell according to Equation 2. Consequently, the term can be approximated in terms of the cell-centre values using the midpoint rule as:

$$\int_{\Omega} \rho \mathbf{f}_b d\Omega \approx \rho \mathbf{f}_{b_P} \Omega_P \quad (6)$$

Towards the discretisation of the surface force term, the closed surface integral in Equation 1 is converted into a sum of surface integrals over each polygonal face:

$$\oint_{\Gamma} \mathbf{n} \cdot [\mu \nabla \mathbf{u} + \mu (\nabla \mathbf{u})^T + \lambda \text{tr}(\nabla \mathbf{u}) \mathbf{I}] d\Gamma = \sum_{f=1}^{n_{Faces}} \int_{\Gamma_f} \mathbf{n} \cdot [\mu \nabla \mathbf{u} + \mu (\nabla \mathbf{u})^T + \lambda \text{tr}(\nabla \mathbf{u}) \mathbf{I}] d\Gamma \quad (7)$$

where  $n_{Faces}$  is the number of faces in the cell. This form represents a force balance for the cell. To approximate the stress term  $[\mu \nabla \mathbf{u} + \mu (\nabla \mathbf{u})^T + \lambda \text{tr}(\nabla \mathbf{u}) \mathbf{I}]$  at each cell face, the assumed variation of displacement in Equation 2 is once again used; accordingly, the stress can be calculated in terms

of the displacement gradient values at the face centre (centroid):

$$\sum_{f=1}^{nFaces} \int_{\Gamma_f} \mathbf{n} \cdot [\mu \nabla \mathbf{u} + \mu (\nabla \mathbf{u})^T + \lambda \text{tr}(\nabla \mathbf{u}) \mathbf{I}] \, d\Gamma \approx \sum_{f=1}^{nFaces} \mathbf{n}_f \cdot [\mu (\nabla \mathbf{u})_f + \mu (\nabla \mathbf{u})_f^T + \lambda \text{tr}[(\nabla \mathbf{u})_f] \mathbf{I}] |\Gamma_f| \quad (8)$$

where subscript  $f$  indicates a quantity at a face centre, for example,  $(\nabla \mathbf{u})_f$  is the gradient of displacement tensor at the centre of face  $f$ . The approach used to approximate this face displacement gradient is one of the principal differences between variants of the finite volume method. In addition, polygonal faces may not be flat and approaches have been examined to accommodate for this; for example, Tuković et al. [208] proposed decomposing all faces into triangles before evaluating the forces.

As a consequence of the assumed variation (Equation 2), the gradient of displacement  $\nabla \mathbf{u}$  is constant within each cell and so the displacement gradient at a face, between two cells, is discontinuous; to resolve this, the standard cell-centred approach expresses the displacement gradient at a face  $(\nabla \mathbf{u})_f$  as a weighted mean of the displacement gradient at the two adjacent cell-centres:

$$(\nabla \mathbf{u})_f \approx \gamma_f (\nabla \mathbf{u})_P + (1 - \gamma_f) (\nabla \mathbf{u})_{N_f} \quad (9)$$

where subscript  $P$  indicates a quantity at the current cell-centre, subscript  $N_f$  indicates a quantity at the neighbour cell-centre adjacent to face  $f$ , and  $0 < \gamma_f < 1$  is the interpolation weight. Typically, the interpolation weight is calculated using an inverse distance method:

$$\gamma_f = \frac{|\mathbf{x}_{N_f} - \mathbf{x}_f|}{|(\mathbf{x}_f - \mathbf{x}_P) + (\mathbf{x}_{N_f} - \mathbf{x}_f)|} \quad (10)$$

In addition to the standard cell-centred method for approximating the face centre displacement gradient given in Equation 9, a number of alternative methods have also been examined, for example, temporary elements with isoparametric formulations [204] or using a compact stencil for the normal gradient as in the original discretisation of Demirdžić et al. [2]; in this compact stencil form, the normal component is calculated using central differencing:

$$\begin{aligned} (\nabla \mathbf{u})_f \approx & \underbrace{\mathbf{n}_f \mathbf{n}_f \cdot \left[ |\Delta_f| \frac{\mathbf{u}_{N_f} - \mathbf{u}_P}{|d_f|} + (\Gamma_f - \Delta_f) \cdot (\nabla \mathbf{u})_f \right]}_{\text{normal component}} \\ & + \underbrace{(\mathbf{I} - \mathbf{n}_f \mathbf{n}_f) \cdot [\gamma_f (\nabla \mathbf{u})_P + (1 - \gamma_f) (\nabla \mathbf{u})_{N_f}]}_{\text{tangential component}} \end{aligned} \quad (11)$$

where  $\mathbf{n}_f = \boldsymbol{\Gamma}_f / |\boldsymbol{\Gamma}_f|$  are the face unit normals, and:

$$\boldsymbol{\Delta}_f = \frac{\mathbf{d}_f}{\mathbf{d}_f \cdot \mathbf{n}_f} |\boldsymbol{\Gamma}_f| \quad (12)$$

At this point, it is worth noting the locally conservative nature of the discretisation: adjacent cells share integration points at the face centres, resulting in the force at cell faces being locally and hence globally conserved. This is a characteristic shared by all finite volume methods.

To complete the discretisation of the surface force in terms of displacement  $\mathbf{u}$ , the cell-centred displacement gradients need to be expressed in terms of the cell-centred displacements. For its accuracy on unstructured grids and ease of implementation, the least-squares method is the most popular:

$$(\nabla \mathbf{u})_P \approx \left[ \sum_{f=1}^{nFaces} w_f^2 \mathbf{d}_f \mathbf{d}_f \right]^{-1} \cdot \sum_{f=1}^{nFaces} [w_f^2 \mathbf{d}_f (\mathbf{u}_{N_f} - \mathbf{u}_P)] \quad (13)$$

As shown previously in Figure 8, vector  $\mathbf{d}_f$  joins cell-centre  $P$  to the neighbour cell-centre  $N_f$ . The scalar weighting function can be taken as unity ( $w_f = 1$ ) [29] or as the inverse distance ( $w_f = 1/|\mathbf{d}_f|$ ) [194]. Alternative gradient calculation methods, such as the Gauss divergence method or point Gauss divergence method [208] have also been proposed. With respect to the Gauss divergence method of gradient calculation, this approach stems from the Lawrence Livermore Laboratory ‘hydrocodes’ of the 1960s developed by Wilkins [400, 401]. Zienkiewicz and Oñate [6, 12] claimed this Gauss divergence cell-gradient method to be “*an early attempt to use FV concepts in CSM*”; this link is, however, tenuous; the Gauss divergence cell-gradient calculation is not a core postulate of the finite volume method and is in fact not required. For descriptions of subsequent finite difference developments based on the original Wilkins [400] approach, the interested reader is referred to [402] and [403].

Although the discretisation of the surface force in terms of displacement  $\mathbf{u}$  is complete, the presented discretisation is unstable and known to suffer from so-called *checker-boarding* errors. Without an appropriate stabilisation term, oscillations in the displacement field, which are twice the period of the cell size, will go unnoticed. These unstable oscillations are analogous to the spurious singular modes that appear in reduced-integration finite element discretisations, also known as zero-energy modes or *hourglassing*. Typically the implicit cell-centred approach adds the so-called Rhie-Chow stabilisation term to the discretised divergence of stress (Equation 8), as introduced to solid mechanics by Demirdžić and Muzaferija [29]:

$$\begin{aligned} \mathcal{R}_{\text{Rhie-Chow}} &= \sum_{f=1}^{nFaces} \left\{ K_f \left[ |\boldsymbol{\Delta}_f| \frac{\mathbf{u}_{N_f} - \mathbf{u}_P}{|\mathbf{d}_f|} + (\boldsymbol{\Gamma}_f - \boldsymbol{\Delta}_f) \cdot (\nabla \mathbf{u})_f \right] - \boldsymbol{\Gamma}_f \cdot [K_f (\nabla \mathbf{u})_f] \right\} \\ &= \sum_{f=1}^{nFaces} K_f \left[ |\boldsymbol{\Delta}_f| \frac{\mathbf{u}_{N_f} - \mathbf{u}_P}{|\mathbf{d}_f|} - \boldsymbol{\Delta}_f \cdot (\nabla \mathbf{u})_f \right] \end{aligned} \quad (14)$$

This third-order diffusion term corresponds to the difference between two ways of calculating the normal gradient of displacement at a face, resulting in an ability to ‘sense’ high-frequency

oscillations in  $\mathbf{u}$ . The approach was first proposed by Rhie and Chow [404] in the context of cell-centred finite volume methods for incompressible fluid flow, and is commonly used in cell-centred finite volume fluid formulations. The  $K_f$  coefficient controls the magnitude of the smoothing effect and is typically taken as  $K_f = \mu$  [29],  $K_f = \mu + \lambda$  [194] or  $K_f = 2\mu + \lambda$  [30]. The third-order diffusion term also serves a purpose towards choice of implicit components within the segregated solution algorithm: this is discussed further below. Alternative forms of diffusion/smoothing terms have been also been proposed, for example, the fourth-order Jameson-Schmidt-Turkel [405] term employed in Godunov-type approaches [31, 237], which takes the form of a Laplacian of a Laplacian:

$$\mathcal{D}_{\text{JST}} = \nabla^2 [K_{\text{JST}} (\nabla^2 \mathbf{u})] \quad (15)$$

The scalar coefficient  $K_{\text{JST}}$  gives the correct dimension to the dissipation as well as controlling its magnitude.

The final discretised form of the governing momentum equation, employing the Rhie-Chow form of stabilisation and  $K_f = 2\mu + \lambda$ , is expressed as:

$$\begin{aligned} \rho \frac{\mathbf{u}_P - 2\mathbf{u}_P^{[m-1]} + \mathbf{u}_P^{[m-2]}}{\Delta t^2} \Omega_P &= \sum_{f=1}^{nFaces} \mathbf{n}_f \cdot [\mu(\nabla \mathbf{u})_f + \mu(\nabla \mathbf{u})_f^T + \lambda \text{tr}[(\nabla \mathbf{u})_f] \mathbf{I}] |\Gamma_f| \\ &+ \sum_{f=1}^{nFaces} (2\mu + \lambda) \left[ |\Delta_f| \frac{\mathbf{u}_{N_f} - \mathbf{u}_P}{|\mathbf{d}_f|} - \Delta_f \cdot (\nabla \mathbf{u})_f \right] \\ &+ \rho \mathbf{f}_{b_P} \Omega_P \end{aligned} \quad (16)$$

where the face displacement gradients  $(\nabla \mathbf{u})_f$  are calculated using Equations 9, 10 and 13. The primitive unknown variables are the cell-centre displacement vectors  $\mathbf{u}_P$  at time  $t$  (time index  $[m]$ ).

Boundary conditions are incorporated through appropriate modification of the surface force term discretisation at faces coinciding with the boundary of the solution domain. In the case of a displacement condition  $\mathbf{u}_b$  (Dirichlet boundary condition), the face displacement gradients are calculated at the face, while in the case of a traction condition  $\mathbf{T}_b$  (Neumann boundary condition), the specified traction directly replaces the surface stress expression. Initial conditions, in the form of the displacement field at  $t = 0$ ,  $t = -\Delta t$ , and  $t = -2\Delta t$ , must also be specified.

**Solution algorithm** In order to solve the discretised governing equation (Equation 16) for the unknown displacement vector, the typical cell-centre approach uses a *segregated* solution procedure, where the central-differencing component in Equation 16,  $(2\mu + \lambda)|\Delta_f|(\mathbf{u}_{N_f} - \mathbf{u}_P)/|\mathbf{d}_f|$ , and  $\rho(\mathbf{u}_P/\Delta t^2)\Omega_P$  within the inertia term are treated implicitly; all other terms are calculated explicitly using the latest available displacement field. The purpose of the segregated approach is to temporarily decouple/segregate the three scalar components of the vector momentum equation so that they can be solved sequentially; outer fixed-point/Gauss-Seidel/Picard iterations provide the necessary coupling, where the displacement gradient terms are explicitly updated each outer iteration using the latest available displacement field. Employing this implicit-explicit split, the

discretised equation for each cell can be written in the form of a linear algebraic equation:

$$a_P \mathbf{u}_P - \sum_{f=1}^{nFaces} a_{N_f} \mathbf{u}_{N_f} = \mathbf{b}_P \quad (17)$$

where

$$a_P = \frac{\rho \Omega_P}{\Delta t^2} + \sum_{f=1}^{nFaces} a_{N_f} \quad (18)$$

$$a_{N_f} = (2\mu + \lambda) \frac{|\Delta_f|}{|\mathbf{d}_f|} \quad (19)$$

$$\begin{aligned} \mathbf{b}_P = & \rho \frac{2\mathbf{u}_P^{[m-1]} - \mathbf{u}_P^{[m-2]}}{\Delta t^2} \Omega_P \\ & + \sum_{f=1}^{nFaces} \mathbf{n}_f \cdot \{ \mu(\nabla \mathbf{u})_f + \mu(\nabla \mathbf{u})_f^T + \lambda \text{tr}[(\nabla \mathbf{u})_f] \mathbf{I} \} |\Gamma_f| \\ & - \sum_{f=1}^{nFaces} (2\mu + \lambda) \Delta_f \cdot (\nabla \mathbf{u})_f + \rho \mathbf{f}_{b_P} \Omega_P \end{aligned} \quad (20)$$

In contrast, typical implicit vertex-centred and implicit finite element solution algorithms treat the entire divergence of stress term implicitly within the linear system matrix, or a linearisation of it when nonlinearities are present. This so-called *block-coupled* approach has also been proposed for the cell-centred approach [25, 59]: in this case,  $a_P$  and  $a_{N_f}$  in Equation 17 are second-order tensors.

The algebraic equations (Equation 17) can be assembled for all  $M$  cells in the domain into the form of three decoupled linear systems:

$$[\mathbf{K}] [\mathbf{U}] = [\mathbf{F}] \quad (21)$$

where  $[\mathbf{K}]$  is a  $M \times M$  sparse matrix with diagonal coefficients  $a_P$  and off-diagonal coefficients  $a_{N_f}$ ,  $[\mathbf{U}]$  is a vector of the unknown cell-centre displacement vectors, and  $[\mathbf{F}]$  is the source vector containing contributions from  $\mathbf{b}_P$ . In finite element parlance,  $[\mathbf{K}]$  is the global stiffness matrix and  $[\mathbf{F}]$  is the global force vector. The segregated cell-centred discretisation ensures that matrix  $[\mathbf{K}]$ , has the following properties [29]:

- It is sparse with the number of non-zero elements in each row equal to the number of nearest neighbours cells (those sharing a face with the cell) plus one;
- It is symmetric;
- It is positive definite;
- It is diagonally dominant ( $|a_P| \geq \sum_{f=1}^{nFaces} |a_{N_f}|$ ), which makes the linear system efficiently solved by a number of iterative methods, which retain the sparsity of matrix  $[\mathbf{K}]$ : this results in significantly lower memory requirements than equivalent direct linear solvers, for example, see [25]. The most common iterative method used is the conjugate gradient method with incomplete Cholesky preconditioning [406].

It is worth noting that the segregated solution algorithm has been shown to suffer from slow convergence for slender geometry undergoing bending [25]; in that case, a block-coupled algorithm

is significantly faster [25]; and  $[K]$  is a  $M \times M$  sparse matrix, where each coefficient is a second-order tensor.

For the segregated approach, the linear system (Equation 30) need not be solved to a tight tolerance as coefficients and source terms are approximated from the previous outer iteration; instead, a reduction in the residuals of one order of magnitude is typically sufficient. Outer iterations are performed until the predefined solution tolerance has been achieved. Under-relaxation of the displacement field and/or the linear system may improve convergence, depending on the boundary conditions and mesh. Acceleration of the approach can be achieved through geometric multi-grid procedures [86, 120, 197], block-coupled algorithms [30, 188, 189, 199], Aitken acceleration [78, 160, 199], and/or parallelisation on distributed memory clusters [88, 194]. A favourable characteristic of the solution procedure is the straightforward extension to nonlinearity: nonlinear terms (material, geometric or boundary conditions) are resolved *on the fly*; after each outer iteration the coefficients and the source terms are updated and the procedure continues as in the linear case, for example, compare the linear elasticity approach of Jasak and Weller [194] with the finite strain elasto-plastic frictional contact procedure of Cardiff et al. [30].

In addition to the displacement-based approach described above, alternative solution algorithms, where pressure and displacement are the primary variables, have been proposed by Bijelonja et al. [95, 97, 100] and Fowler and Yee [200]; the benefit of such approaches is their ability to deal with incompressible and quasi-incompressible solids in a straightforward manner, while avoiding pressure instabilities.

### 3.3. *Implicit vertex-centred approach*

**Discretisation of space** Like the other approaches, the vertex-centred approach divides the spatial domain into a finite number of contiguous cells that do not overlap and fill the space completely. When compared with the *typical* cell-centred approach, there are two key differences related to the mesh arrangement:

- The vertex-centred approach integrates the governing equations over cells in a secondary-grid, with cells that are typically constructed around the vertices/points in the primary grid (Figure 9). The resulting secondary grid cells may not preserve convexity;
- The primitive unknowns are stored at the vertices/points of the primary grid, corresponding to the approximate, but not necessarily exact, centre of the secondary-grid cells.

However, in essence vertex-centred approaches can be viewed as a form of cell-centred method integrated over a secondary mesh.

In principal, the primary mesh can consist of arbitrary convex polyhedral cells; however, depending on the chosen discretisation (for example, if shape functions are used), the method may be limited to triangular/quadrilateral meshes in 2-D and tetrahedral/hexahedral meshes in 3-D; in fact, no vertex-centred solid mechanics examples using polyhedral meshes were found when preparing this article.

In addition to this form of the vertex-centred approach, a variant exists where the primary mesh cells around a vertex are used to perform the integration, for example, as discussed by Oñate et al. [12]; this produces overlapping regions of integration, where neighbouring vertices share part of their integrated volume. Secondary-grid cells can also be created by joining the mesh cell centres

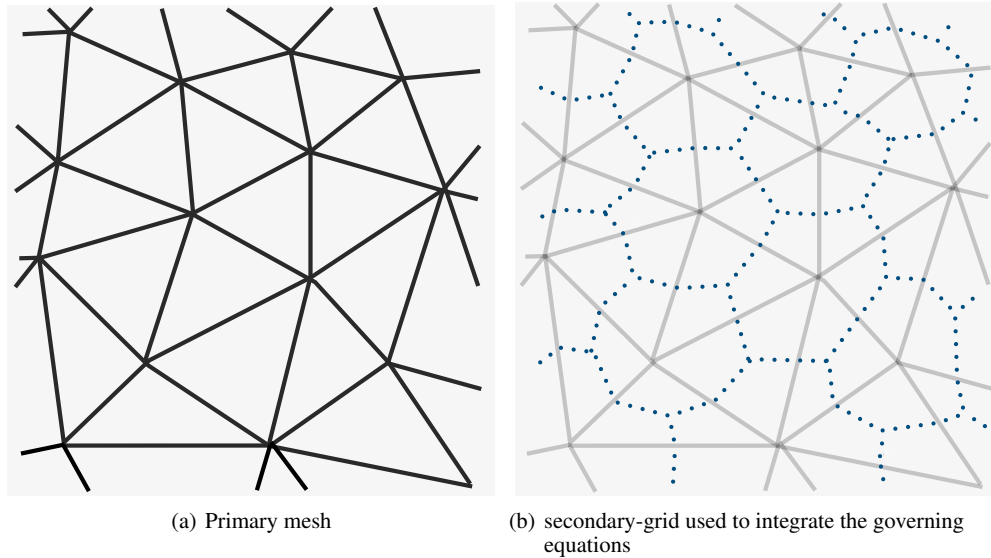


Figure 9. 2-D vertex-centred grid showing the (a) primary mesh, (b) secondary-grid used to integrate the governing equations. Figure adapted from Hassan [407]

together [249], rather than joining the cell-centres to the face-centres as per the classic vertex-based method.

**Discretisation of the mathematical model equations** The vertex-centred approach starts from the strong integral form of the governing momentum equation (Equation 1), which is integrated over a secondary-grid [5]. The vertex-centred approach discretises each term of the governing equation over the cells in the secondary-grid. An example secondary-grid cell is shown in Figure 10, where each vertex  $i$  in the primary grid is uniquely associated with a cell in the secondary-grid.

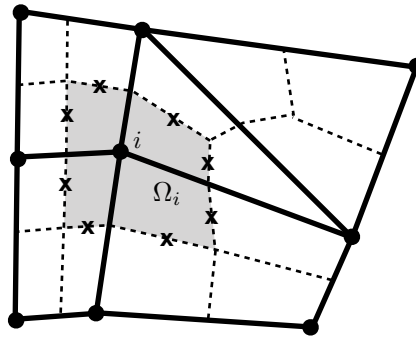


Figure 10. A typical control volume constructed around vertex  $i$ , with a volume  $\Omega_i$ . The solid lines show the primary grid and the dashed lines show the secondary-grid. When calculating the momentum balance for a secondary-grid cell (shaded), the displacement gradient is calculated at the boundary edge centres (boundary face centres in 3-D) of the secondary-grid cell (marked by “x”). Figure adapted from Bailey and Cross [24]

As with the cell-centred variant, the discretisation of each of the three terms (inertia, surface forces, body forces) in the governing conservation law (Equation 1) will now be discussed in turn.

To approximate the volume integral temporal term, the displacement  $\mathbf{u}$  within each secondary-grid cell is assumed to be constant [24, 240, 273]. Consequently, for a volume about vertex  $i$ , the

term may be approximated in terms of the acceleration at vertex  $i$  and the secondary-grid cell volume  $\Omega_i$  about vertex  $i$ :

$$\int_{\Omega} \rho \frac{\partial^2 \mathbf{u}}{\partial t^2} d\Omega \approx \rho \left( \frac{\partial^2 \mathbf{u}}{\partial t^2} \right)_i \Omega_i \quad (22)$$

As with other finite volume approaches, the acceleration term  $\partial^2 \mathbf{u} / \partial t^2$  may be discretised in time using any appropriate finite difference scheme. For example, Slone et al. [273] employed the Newmark finite difference scheme, which is popular in the finite element community. For ease of comparison with the cell-centred approach (Equations 5), a first-order Euler scheme is assumed here, giving the final discretised term as:

$$\int_{\Omega} \rho \frac{\partial^2 \mathbf{u}}{\partial t^2} d\Omega \approx \rho \frac{\mathbf{u}_i - 2\mathbf{u}_i^{[m-1]} + \mathbf{u}_i^{[m-2]}}{\Delta t^2} \Omega_i \quad (23)$$

Comparing this expression with the equivalent cell-centred expression (Equation 5), the only difference is the mesh location where the unknown displacement is stored. A conceptual difference comes from the fact that vertex  $i$  is not in general situated at the centre of the secondary-grid cell volume  $\Omega_i$ ; consequently, in the approximation of the inertia term, the cell-centred approach allows a local linear displacement distribution, whereas the vertex-centred approach requires a constant displacement distribution.

The volume integral body force term is discretised in a similar manner to the temporal term, where the body force  $\mathbf{f}_b$  is assumed to be constant within each secondary-grid cell and equal to the value at vertex  $i$ :

$$\int_{\Omega} \rho \mathbf{f}_b d\Omega \approx \rho \mathbf{f}_{b_i} \Omega_i \quad (24)$$

Once again the discretised term differs from the the equivalent cell-centred term in that a constant rather than a linear local variation is assumed. In the case that vertex  $i$  does lie at the centroid of the control volume, then the vertex-centred and cell-centred terms are the same.

To discretise the surface force term, the closed surface integral in Equation 1 is converted into a sum of surface integrals over the faces of the secondary-grid cell, taking the same form as Equation 7. Approximation of the stress term at each face requires an assumption about the local displacement distribution. In contrast to the standard cell-centred approach, *most* vertex-centred approaches explicitly use shape functions to describe the local displacement field variation. Following the standard finite element notation, these shape (or interpolation) functions refer to the displacement within each cell of the primary mesh:

$$\mathbf{u}(\mathbf{x}) = \sum_{i=1}^{nVertices} N_i(\mathbf{x}) \mathbf{u}_i = [\mathbf{N}] [\mathbf{u}] \quad (25)$$

where  $nVertices$  is the number of vertices in the primary mesh cell of interest,  $N_i(\mathbf{x})$  is the shape function associated with vertex  $i$  within the cell,  $\mathbf{u}_i$  is the displacement at vertex  $i$ , and  $[\mathbf{N}]$  and  $[\mathbf{u}]$  represent a vector of all shape functions and nodal displacements within the cell respectively. It

should be emphasised that these shape functions refer to the vertices and cells of the primary mesh, as opposed to of the secondary mesh cells.

As is standard in the conventional continuous Bubnov-Galerkin finite element method, the shape functions, which are defined in the reference domain and mapped to the physical domain, approximate the displacement field as a continuous piecewise distribution. As the shape functions describe the displacement distribution between the vertices on the primary mesh, this allows convenient calculation of the displacement gradients at the secondary-grid cell boundaries when applying the momentum balance (Figure 10). Although shape functions are a key characteristic of the vertex-centred approaches presented in literature, they are *not* essential. As shown by Tsui et al. [249], it is possible to develop a vertex-centred finite volume approach that does not directly use shape functions; similar to many cell-centred approaches, Tsui et al. [249] applied the Gauss divergence theorem to calculate secondary-grid cell displacement gradients; these gradients were then interpolated to secondary-grid cell faces. In the cell-centred approach, the truncated Taylor series expansion about the cell centres (Equation 2) fulfills the role of shape functions. As shape functions are specific to the cell geometry (*e.g.* triangle, quadrilateral, tetrahedral), shape function based approaches are limited in their choice of element shape, whereas all convex polyhedral meshes are valid for cell-centred approaches.

To approximate the stress at the faces of a secondary-grid cell, the gradient of displacement must be calculated. The use of shape functions allows this spatial gradient of displacement to be conveniently calculated as:

$$\nabla \mathbf{u} \approx \sum_{i=1}^{nVertices} \nabla N_i(\mathbf{x}) \mathbf{u}_i = [\mathbf{B}] [\mathbf{u}] \quad (26)$$

where  $[\mathbf{B}]$  is a vector of the shape functions gradients. Substituting Equation 26 into Equation 7 allows the surface force term to be expressed in terms of the unknown displacements at the primary mesh vertices:

$$\begin{aligned} \sum_{f=1}^{nFaces} \int_{\Gamma_i} \mathbf{n} \cdot [\mu \nabla \mathbf{u} + \mu (\nabla \mathbf{u})^T + \lambda \text{tr}(\nabla \mathbf{u}) \mathbf{I}] \, d\Gamma \approx \\ \sum_{f=1}^{nFaces} \sum_{v=1}^{nVertices} \mathbf{n}_f \cdot [\mu \nabla N_{vf} \mathbf{u}_v + \mu \mathbf{u}_v \nabla N_{vf} + \lambda \text{tr}(\nabla N_{vf} \mathbf{u}_v) \mathbf{I}] \end{aligned} \quad (27)$$

where  $nVertices$  refers to the number of vertices in the primary-grid cell in which the secondary-grid face  $f$  is situated;  $N_{vf}$  refers to the corresponding shape function for vertex  $v$  within the primary-grid cell. Consequently, the surface force term for a secondary-grid cell surrounding vertex  $v$  will be a function of the displacement at vertex  $v$  as well as the displacement at all vertices that share a primary-grid cell with vertex  $v$ . For example, for the secondary-grid cell shown in Figure 10, the surface force term will be a function of the displacements at all vertices shown except for the vertex in the top-right.

The final discretised form of the governing momentum equation for the vertex-centred approach is expressed for a secondary-grid cell as:

$$\rho \frac{\mathbf{u}_i - 2\mathbf{u}_i^{[m-1]} + \mathbf{u}_i^{[m-2]}}{\Delta t^2} \Omega_i = \sum_{f=1}^{nFaces} \sum_{v=1}^{nVertices} \mathbf{n}_f \cdot [\mu \nabla N_{vf} \mathbf{u}_v + \mu \mathbf{u}_v \nabla N_{vf} + \lambda \text{tr}(\nabla N_{vf} \mathbf{u}_v) \mathbf{I}] + \rho \mathbf{f}_{b_v} \Omega_v \quad (28)$$

As with the other finite volume approaches, boundary conditions are incorporated through appropriate modification of the surface force term, and initial conditions must be specified for dynamic cases.

**Solution algorithm** The discretised equation for each secondary-grid cell can be written in the form of an algebraic equation:

$$\mathbf{A}_i \cdot \mathbf{u}_i - \sum_{v=1}^{nVertices} \mathbf{A}_v \cdot \mathbf{u}_v = \mathbf{b}_i \quad (29)$$

where  $\mathbf{u}_i$  is the displacement at the primary-grid vertex associated with the secondary-grid cell, and  $nVertices$  indicates all vertices which share a primary-grid cell with vertex  $i$ .  $\mathbf{A}_i$  and  $\mathbf{A}_v$  are the corresponding block coefficients (second-order tensors in 3-D).

In earlier publications [5], the vertex-centred approach followed a similar solution algorithm to the standard cell-centred approach, where the surface force term was partitioned into *implicit* and *explicit* components and a segregated solution algorithm was employed. In later publications [24], a block-coupled solution procedure is used, where the entire surface force term is discretised implicitly. As noted previously, similar coupled solution algorithms were later proposed for the cell-centred variant by Das et al. [188] and Cardiff et al. [25].

Following the block-coupled approach, the algebraic equations (Equation 29) can be assembled for all  $M$  secondary-grid cells (primary-grid vertices) in the domain to form a system of linear equations:

$$[\mathbf{K}] [\mathbf{U}] = [\mathbf{F}] \quad (30)$$

where the  $M \times M$  global stiffness matrix  $[\mathbf{K}]$  is sparse with block diagonal coefficients  $\mathbf{A}_i$  and off-diagonal block coefficients  $\mathbf{A}_v$ ,  $[\mathbf{U}]$  is a vector of the unknown primary-grid vertex displacement vectors, and the global force source vector  $[\mathbf{F}]$  contains contributions from  $\mathbf{b}_i$ .

This linear system can then be solved using direct or iterative linear solvers, where iterative conjugate gradient solvers with diagonal/Jacobi scaling have been favoured in literature, for example, [5, 24]. Parallelisation on distributed memory supercomputers has been addressed by McManus et al. [304, 305], and mixed displacement-rotation approaches have also been employed [301–303].

### 3.4. Explicit cell-centred Godunov-type approach

Godunov-type procedures are specialised approaches for analysis of problems that involve wave propagation, shocks and solution discontinuities. Features that distinguish this variant of finite volume approach from the others are the use of acoustic Riemann solvers, solution reconstruction procedures, slope limiters for gradient calculations, occasionally nodal integration, as well as representing the governing equations as a coupled system of first-order equations; in addition, explicit time marching solution algorithms are employed.

**Discretisation of space** The majority of Godunov-type approaches are spatially discretised using cell-centred approaches, for example, [26–28, 196, 220, 222, 223, 225–229, 231–236]; consequently, this section will focus on such approaches; however, Godunov-type approaches have also used vertex-centred [31, 237], staggered grid [224, 228] and face-centred [20, 21] formulations. To-date, many of the developments have been limited to one and two dimensions, but in general the procedures can be extended to three dimensions. Like the *implicit* cell-centred approach described in Section 3.2, the solution spatial domain is divided into a finite number of contiguous convex polyhedral cells bounded by polygonal faces that do not overlap and fill the space completely.

**Discretisation of the mathematical model equations** In a notable deviation from the other finite volume variants, Godunov-type approaches portray the second-order governing momentum equation (Equation 1) as a coupled system of first-order equations:

$$\int_{\Omega} \rho \frac{\partial \mathbf{v}}{\partial t} d\Omega = \oint_{\Gamma} \mathbf{n} \cdot \boldsymbol{\sigma} d\Gamma + \int_{\Omega} \rho \mathbf{f}_b d\Omega \quad (31)$$

$$\int_{\Omega} \frac{\partial \mathbf{F}}{\partial t} d\Omega = \oint_{\Gamma} \mathbf{v} \mathbf{n} d\Gamma \quad (32)$$

where  $\mathbf{v}$  is the velocity vector and the deformation gradient,  $\mathbf{F}$ , defines the local deformation as:

$$\mathbf{F} = \mathbf{I} + (\nabla \mathbf{u})^T \quad (33)$$

Equation 32 is obtained by taking the time-derivative of Equation 33 and employing the Gauss divergence theorem.

To ensure the compatibility conditions are satisfied, the deformation gradient at the initial time should be curl free:

$$\nabla \times \mathbf{F}^{[m=0]} = \mathbf{0} \quad (34)$$

In addition, the discrete evolution of  $\mathbf{F}$  (or  $\nabla \mathbf{u}$ ) should not allow curl errors to escalate. For further discussion of this point, see [27, 28, 40, 214, 225]. It is also possible to employ the evolution of the displacement gradient  $\nabla \mathbf{u}$  directly rather than the deformation gradient, as shown by Trangenstein and Colella [40]; however, this is less popular in literature.

The governing system of coupled first-order equations (Equations 31 and 32) can be expressed concisely as:

$$\int_{\Omega} \frac{\partial \mathbf{U}}{\partial t} d\Omega = \oint_{\Gamma} \mathcal{F}_n d\Gamma + \int_{\Omega} \mathcal{S} d\Omega \quad (35)$$

where  $\mathbf{U}$  is the primary unknown vector,  $\mathcal{F}_n$  is the flux vector, and  $\mathcal{S}$  is the source vector, given as:

$$\mathbf{U} = \begin{pmatrix} \mathbf{v} \\ \mathbf{F} \end{pmatrix}, \quad \mathcal{F}_n = \begin{pmatrix} \mathbf{t}/\rho \\ \mathbf{v}\mathbf{n} \end{pmatrix}, \quad \mathcal{S} = \begin{pmatrix} \mathbf{f}_b \\ \mathbf{0} \end{pmatrix} \quad (36)$$

and the traction vector,  $\mathbf{t}$ , gives the stress on a plane as  $\mathbf{t} = \mathbf{n} \cdot \boldsymbol{\sigma}$ . To close the system, we give the constitutive relation (Hooke's law) in terms of the deformation gradient:

$$\boldsymbol{\sigma} = \mu \mathbf{F}^T + \mu \mathbf{F} + \lambda \text{tr}(\mathbf{F}) \mathbf{I} - (2\mu + 3\lambda) \mathbf{I} \quad (37)$$

We next describe the discretisation of the three terms in Equation 35: the time derivative term, the diffusion term and the body force term.

Assuming the primary unknowns ( $\mathbf{v}$  and  $\mathbf{F}$ ) vary linearly within each cell according to Equation 2, the volume integrals can be expressed in terms of the cell-centre values (subscript  $P$ ) and the surface integral becomes a sum over the face-centre values (subscript  $f$ ); consequently, Equation 35 becomes:

$$\frac{\partial \mathbf{U}_P}{\partial t} \Omega_P = \sum_{f=1}^{nFaces} \mathcal{F}_{n_f} |\Gamma_f| + \mathcal{S}_P \Omega_P \quad (38)$$

Similar to the other approaches, discretisation of the time-rate term can be achieved using a variety of finite difference methods. Here we assume a first-order *forward* Euler discretisation to allow straight-forward comparison with the other methods:

$$\frac{\mathbf{U}_P - \mathbf{U}_P^{[m-1]}}{\Delta t} \Omega_P = \sum_{f=1}^{nFaces} \mathcal{F}_{n_f}^{[m-1]} |\Gamma_f| + \mathcal{S}_P \Omega_P \quad (39)$$

where, as before,  $m$  is the time-step counter, which for brevity has been dropped on the unknown current time value. Of course, as an explicit time-marching solution algorithm will be employed, the time step size is limited by the Courant-Friedrichs-Lewy constraint [34]; this condition is necessary for stability but is not sufficient. It is also necessary that the time integrator avoids the creation of new local extrema, known as the Total Variation Diminishing property or the local maximum principle; the first-order forward Euler approach is one such method that obeys this condition.

Alternatively, the flux calculation in Equation 39, which sums over the cell faces, can be expressed as a sum over the cell points/vertices according to:

$$\frac{\mathbf{U}_P - \mathbf{U}_P^{[m-1]}}{\Delta t} \Omega_P = \sum_{v=1}^{nVertices} \mathcal{F}_{n_v}^{[m-1]} |\mathbf{C}_v| + \mathcal{S}_P \Omega_P \quad (40)$$

where the calculation of point/vertex/nodal area vector,  $\mathbf{C}_v$ , is given in Carré et al. [221] and Kluth and Després [26] or equivalently in Maire et al. [222].

Up to this point, the presented discretisation coincides with the cell-centred approach described in Section 3.2, apart from the introduction of a system of first-order conservation equation and the use of the forward Euler method as opposed to the backward Euler method; however, in the discretisation of the face flux,  $\mathcal{F}_n$ , Godunov-type methods deviate from the other approaches. As a result of the assumed piecewise linear distribution (Equation 2), there is a discontinuity at the cell internal faces. A distinguishing characteristic of Godunov-type methods is the acknowledgement of this discontinuity in the solution field, known as a Riemann problem, and the development of appropriate methods (Riemann solvers) to deal with the propagation of this discontinuity. Accordingly, the face flux,  $\mathcal{F}_n$ , is defined as a function of the solution variable at either side of the interface:

$$\mathcal{F}_{n_f} = f(\mathbf{U}_{P_f}, \mathbf{U}_{N_f}) \quad (41)$$

The solution at either side of the interface ( $\mathbf{U}_{P_f}$  and  $\mathbf{U}_{N_f}$ ) is determined via extrapolation from the adjacent cell centres:

$$\begin{aligned} \mathbf{U}_{P_f} &= \mathbf{U}_P + \mathbf{G}_P \cdot (\mathbf{x}_f - \mathbf{x}_P) \\ \mathbf{U}_{N_f} &= \mathbf{U}_N + \mathbf{G}_N \cdot (\mathbf{x}_f - \mathbf{x}_N) \end{aligned} \quad (42)$$

where  $\mathbf{G}_P$  is the gradient of  $\mathbf{U}$  within cell  $P$ , and  $\mathbf{G}_N$  is the gradient within cell  $N$ . A critical component of Godunov-type methods is the definition of this solution *reconstruction*, such that the local maximum principle is preserved *i.e.* the value of  $\mathbf{U}$  at face  $f$  should not be greater than the value at adjacent cell centres  $P$  and  $N$ . There are a number of ways to define such discrete gradients; here, as a typical example, the Monotone Upstream Scheme for Conservation Law (MUSCL) scheme is described [27]. The MUSCL approach consists of two steps: first, the gradient is predicted based on local neighbouring values, then this gradient is corrected/limited to respect the local maximum principle.

To predict the gradient, the second-order least-squares method described in Section 3.2 can be used; this approach does not prohibit overshoots and undershoots at the faces, and hence does not satisfy the local maximum principle. To remedy this, a so-called *slope limiter* is used to restrict the value of the gradient,  $\mathbf{G}$ . The slope limiter is included through modification of the reconstruction expression (Equation 42):

$$\begin{aligned} \mathbf{U}_{P_f} &= \mathbf{U}_P + \phi_P \mathbf{G}_P \cdot (\mathbf{x}_f - \mathbf{x}_P) \\ \mathbf{U}_{N_f} &= \mathbf{U}_N + \phi_N \mathbf{G}_N \cdot (\mathbf{x}_f - \mathbf{x}_N) \end{aligned} \quad (43)$$

where  $0 \leq \phi \leq 1$  is a scalar slope limiter. When  $\phi = 1$ , no limiting is applied, whereas when  $\phi = 0$ , full limiting is applied and the value near the face is assumed equal to the cell-centre value. Choosing the value of  $\phi$  is a balance between stability (lower value of  $\phi$ ) and accuracy (higher value of  $\phi$ ). For the MUSCL procedure,  $\phi$  is determined as described by Lee et al. [27]:

1. Find the smallest and largest values among the current and adjacent cells:

$$\mathbf{u}^{\min} = \min(\mathbf{u}_P, \mathbf{u}_{N_i}), \quad \mathbf{u}^{\max} = \max(\mathbf{u}_P, \mathbf{u}_{N_i}) \quad (44)$$

where  $\mathbf{u}_{N_i}$  represents the values at neighbour cells, which share an internal face with cell  $P$ .

2. Calculate the un-restricted reconstructed value  $\mathbf{u}_{P_f}$  with  $\phi_P = 1$  at each internal face within cell  $P$ .
3. Find the maximum allowable value of  $\phi_{P_f}$  for each face in cell  $P$ :

$$\phi_{P_f} = \begin{cases} \min\left(1, \frac{\mathbf{u}^{\max} - \mathbf{u}_P}{\mathbf{u}_{P_f} - \mathbf{u}_P}\right), & \text{if } \mathbf{u}_{P_f} - \mathbf{u}_P > 0 \\ \min\left(1, \frac{\mathbf{u}^{\min} - \mathbf{u}_P}{\mathbf{u}_{P_f} - \mathbf{u}_P}\right), & \text{if } \mathbf{u}_{P_f} - \mathbf{u}_P < 0 \\ 1, & \text{if } \mathbf{u}_{P_f} - \mathbf{u}_P = 0 \end{cases}$$

4. Select  $\phi_P = \min_f(\phi_{P_f})$
5. Calculate the reconstructed value at each internal face using  $\phi_P$  determined in step 4 and Equation 43.

To complete the discretisation, all that remains is to express the flux vector,  $\mathcal{F}_{n_f}$ , in terms of the solution vector,  $\mathbf{u}$ . To achieve this, the Rankine-Hugoniot jump conditions [32] are employed. These jump conditions describe the relationship between the states on both sides of a shock wave. The jump conditions corresponding to Equations 31 and 32 are [27]:

$$U[\mathbf{v}] = - (1/\rho) \mathbf{n} \cdot [\boldsymbol{\sigma}] \quad (45)$$

$$U[\mathbf{F}] = -[\mathbf{v}]\mathbf{n} \quad (46)$$

where the operator  $[\cdot]$  represents the jump across the shock, for example,  $[\mathbf{u}_f] = \mathbf{u}_{N_f} - \mathbf{u}_{P_f}$ . The wave speed is indicated by  $U$ . Using equations 45 and 46 and assuming a constant wave speed, the face flux can be expressed as the sum of an average flux and a stabilisation flux [27, 28]:

$$\mathcal{F}_{n_f} = \mathcal{F}_{n_f}^{\text{average}} + \mathcal{F}_{n_f}^{\text{stab}} \quad (47)$$

where the average flux is:

$$\mathcal{F}_{n_f}^{\text{average}} = \frac{1}{2} [\mathcal{F}_n(\mathbf{u}_{P_f}) + \mathcal{F}_n(\mathbf{u}_{N_f})] \quad (48)$$

and the so-called upwinding stabilisation term is:

$$\mathcal{F}_{n_f}^{\text{stab}} = \left[ \begin{array}{l} \frac{\rho}{2} [c_s \mathbf{I} + (c_p - c_s) \mathbf{n}_f \mathbf{n}_f] \cdot (\mathbf{v}_{N_f} - \mathbf{v}_{P_f}) \\ \frac{1}{2} \left[ \frac{1}{c_s} \mathbf{I} + \left( \frac{1}{c_p} - \frac{1}{c_s} \right) \mathbf{n}_f \mathbf{n}_f \right] \cdot (\mathbf{n}_f \cdot [\boldsymbol{\sigma}_{N_f} - \boldsymbol{\sigma}_{P_f}]) \end{array} \right] \quad (49)$$

The volumetric and shear wave speeds are indicated by  $c_p$  and  $c_s$ . Jameson-Schmidt-Turkel stabilisation has been used as an alternative to this upwinding stabilisation, and in principal Rhie-Chow stabilisation could also be used.

The final discretised governing equations, given in terms of unknowns  $\mathbf{v}_P^{[m]}$  and  $\mathbf{F}_P^{[m]}$  at time-step  $m$ , are expressed as:

$$\begin{aligned} \frac{\mathbf{v}_P^{[m]} - \mathbf{v}_P}{\Delta t} \Omega_P &= \sum_{f=1}^{nFaces} \frac{1}{2\rho} \mathbf{n}_f \cdot \left[ \mu \mathbf{F}_{P_f}^T + \mu \mathbf{F}_{P_f} + \lambda \operatorname{tr}(\mathbf{F}_{P_f}) \mathbf{I} - (2\mu + 3\lambda) \mathbf{I} \right] |\Gamma_f| \\ &+ \sum_{f=1}^{nFaces} \frac{1}{2\rho} \mathbf{n}_f \cdot \left[ \mu \mathbf{F}_{N_f}^T + \mu \mathbf{F}_{N_f} + \lambda \operatorname{tr}(\mathbf{F}_{N_f}) \mathbf{I} - (2\mu + 3\lambda) \mathbf{I} \right] |\Gamma_f| \\ &+ \sum_{f=1}^{nFaces} \frac{1}{2} [c_s \mathbf{I} + (c_p - c_s) \mathbf{n}_f \mathbf{n}_f] \cdot (\mathbf{v}_{N_f} - \mathbf{v}_{P_f}) |\Gamma_f| \\ &+ \mathbf{f}_{b_P} \Omega_P \end{aligned} \quad (50)$$

$$\begin{aligned} \frac{\mathbf{F}_P^{[m]} - \mathbf{F}_P}{\Delta t} \Omega_P &= \sum_{f=1}^{nFaces} \frac{1}{2} (\mathbf{v}_{P_f} \mathbf{n}_f + \mathbf{v}_{N_f} \mathbf{n}_f) |\Gamma_f| \\ &+ \sum_{f=1}^{nFaces} \frac{1}{2} \left[ \frac{1}{c_s} \mathbf{I} + \left( \frac{1}{c_p} - \frac{1}{c_s} \right) \mathbf{n}_f \mathbf{n}_f \right] \cdot [\mathbf{n}_f \cdot (\boldsymbol{\sigma}_{N_f} - \boldsymbol{\sigma}_{P_f})] |\Gamma_f| \end{aligned} \quad (51)$$

where the  $m-1$  time index on  $\mathbf{F}$  and  $\mathbf{v}$  has been omitted for brevity *i.e.*  $\mathbf{F} \equiv \mathbf{F}^{[m-1]}$  and  $\mathbf{v} \equiv \mathbf{v}^{[m-1]}$ . The stress either side of a face is calculated according to Equation 37.

**Solution algorithm** The solution of the governing discretised equations (Equations 50 and 51) proceeds in an explicit manner as follows:

1. Increase the total time by  $\Delta t = \alpha_{\text{CFL}} \frac{h_{\min}}{c_p}$ , according to the Courant-Friedrichs-Lewy [34] condition, where  $h_{\min}$  is the shortest length within the mesh and  $\alpha_{\text{CFL}}$  is typically chosen to be less than  $1/2$
2. Store the old-time solution values:  $\mathbf{v}^{[m-1]} \leftarrow \mathbf{v}^{[m]}$  and  $\mathbf{F}^{[m-1]} \leftarrow \mathbf{F}^{[m]}$
3. Calculate the reconstructed solution values,  $\mathbf{v}_{N_f}$ ,  $\mathbf{v}_{P_f}$ ,  $\mathbf{F}_{N_f}$  and  $\mathbf{F}_{P_f}$ , at each cell face according to Equation 43
4. Solve Equation 50 for  $\mathbf{v}^{[m]}$
5. Solve Equation 51 for  $\mathbf{F}^{[m]}$
6. Repeat steps 1 to 4 until the end time has been reached

Like all explicit methods, this approach does not require the solution of an implicit linear system of equations and hence each time-step can be evaluated more rapidly than in the previously discussed implicit methods; however, the time-step size limit essentially restricts explicit methods to hyperbolic-style problems. Finally, the explicit nature of the algorithm allows straight-forward and efficient parallelisation on distributed memory supercomputer.

### 3.5. Discussion

The field of finite volume solid mechanics comprises more approaches than those presented above, however, the selected three variants capture the primary differences in the approaches. It can be seen that the distinction between the variants can be narrowed down to four components:

1. Control volume construction;
2. Face gradient calculation;
3. Stabilisation approach;
4. Solution methodology.

Each of these components is briefly reviewed below, followed by the natural definition of a unified approach linking all variants.

**Control volume construction** There are predominantly four ways to construct control volumes (Figure 11): 1) cell-centred, 2) vertex-centred with non-overlapping volumes; 3) vertex-centred with overlapping control volumes, 4) and a staggered-grid. In terms of the relative merits of the different approaches, a number of observations can be made:

1. The staggered-grid is restricted to structured quadrilateral/hexahedral meshes in 2-D/3-D;
2. The vertex-centred approach with non-overlapping control volumes requires the construction and storage of a second mesh;
3. The vertex-centred approaches have nodes on the boundary, whereas the cell-centre approach typically does not;
4. The cell-centred approach allows convenient approximation of the face normal gradients but requires interpolation to approximate the tangential gradients;
5. In contrast, the vertex-centred approach with overlapping volumes allows convenient approximation of the tangential gradients but requires interpolation to approximate the normal gradients.

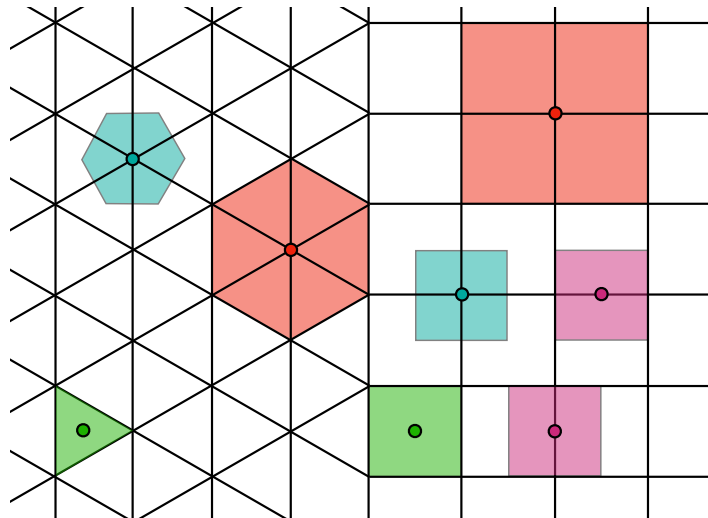


Figure 11. Illustration of the four ways to construct control volumes on a primary mesh: 1) cell-centred (green); 2) vertex-centred with non-overlapping control volumes (blue); 3) vertex-centred with overlapping control volumes (red); and 4) staggered-grid (purple). The nodal locations are indicated by filled circles.

**Face gradient calculation** Once the control volume is constructed, all approaches must approximate the traction at each control volume face. To achieve this, the gradient of displacement

at the face  $(\nabla \mathbf{u})_f$  is approximated in terms of the nodal displacement values. Neglecting any additional stabilisation terms (addressed in the next section), the most common approaches are:

1. Interpolate the gradient from the adjacent cell-centres:

$$(\nabla \mathbf{u})_f = \frac{|\mathbf{d}_{Pf}|(\nabla \mathbf{u})_P + |\mathbf{d}_{Nf}|(\nabla \mathbf{u})_N}{|\mathbf{d}_f|} \quad (52)$$

where  $\mathbf{d}_f$  is the vector from the centre of cell  $P$  to the centre of cell  $N$ ,  $\mathbf{d}_{Pf}$  is the vector from the centre of cell  $P$  to the centre of face  $f$ , and  $\mathbf{d}_{Nf}$  is the vector from the centre of cell  $N$  to the centre of face  $f$ . These interpolation weights may differ depending on the specific approach.

2. Calculate the normal gradient using central-differencing, and interpolate the tangential gradient from the adjacent cell-centres:

$$(\nabla \mathbf{u})_f = \mathbf{n}_f \frac{\mathbf{u}_N - \mathbf{u}_P}{|\mathbf{d}_f|} + (\mathbf{I} - \mathbf{n}_f \mathbf{n}_f) \cdot \frac{|\mathbf{d}_{Pf}|(\nabla \mathbf{u})_P + |\mathbf{d}_{Nf}|(\nabla \mathbf{u})_N}{|\mathbf{d}_f|} \quad (53)$$

3. Calculate the normal gradient using central-differencing, and calculate the tangential gradient using the point or edge values. In the case of a staggered-grid, these point or edge values correspond to nodes and no interpolation is necessary. For the cell-centred approach, these point or edge values are interpolated from the cell-centred nodes, and an appropriate face tangential gradient calculation method used; for example, the face-Gauss method [25, 208] is a generalisation of the approach used in the original Demirdžić et al. [2] approach:

$$(\nabla \mathbf{u})_f = \mathbf{n}_f \frac{\mathbf{u}_N - \mathbf{u}_P}{|\mathbf{d}_f|} + \sum_{e=1}^{nEdges} \mathbf{m}_e \mathbf{u}_e L_e \quad (54)$$

where  $\mathbf{m}_e$  is the outward-facing bi-normal at edge  $e$ ,  $L_e$  is the length of edge  $e$ , and  $\mathbf{u}_e$  is the displacement at the centre of edge  $e$ , which has been interpolated from adjacent cell-centres.

4. Extrapolate the gradient from each adjacent cell-centre, and take the average:

$$(\nabla \mathbf{u})_f = \frac{(\nabla \mathbf{u})_P + \mathbf{d}_{Pf} \cdot \nabla (\nabla \mathbf{u})_P + (\nabla \mathbf{u})_N + \mathbf{d}_{Nf} \cdot \nabla (\nabla \mathbf{u})_N}{2} \quad (55)$$

5. For each of the previous face gradient calculation methods, a limiter can be applied to preserve the local maximum principle, as discussed in Section 3.4.
6. Use shape functions to evaluate the face gradient. As an example, taking a vertex-based method and a 2-D triangular grid with linear shape functions, the face gradient is given in Voigt notation as:

$$[(\nabla \mathbf{u})_f] = \begin{bmatrix} \partial u_x / \partial x \\ \partial u_y / \partial y \\ \partial u_x / \partial y \\ \partial u_y / \partial x \end{bmatrix} = \frac{1}{x_{13}y_{23} - x_{23}y_{13}} \underbrace{\begin{bmatrix} y_{23} & 0 & y_{31} & 0 & y_{12} & 0 \\ 0 & x_{32} & 0 & x_{13} & 0 & x_{21} \\ x_{32} & 0 & x_{13} & 0 & x_{21} & 0 \\ 0 & y_{23} & 0 & y_{31} & 0 & y_{12} \end{bmatrix}}_{\text{Derivative of shape functions}} \cdot \begin{bmatrix} u_{x1} \\ u_{y1} \\ u_{x2} \\ u_{y2} \\ u_{x3} \\ u_{y3} \end{bmatrix} \quad (56)$$

where suffixes 1, 2 and 3 refer to the three nodes in the triangle, and the relative coordinates are given as  $x_{ab} = x_a - x_b$ . Here we are referring to the vertex-centred method, however, shape functions could in principle be used with any control volume construction.

7. Use a higher-order approach, for example, the fourth-order approach proposed by Demirdžić [203].

To provide additional insight, let us consider the face gradient calculations on a simple grid. Taking a uniform quadrilateral mesh (Figure 12), we will calculate the gradient at a face using the most popular of the methods above. The discretised governing equation for the cell in Figure 12 can

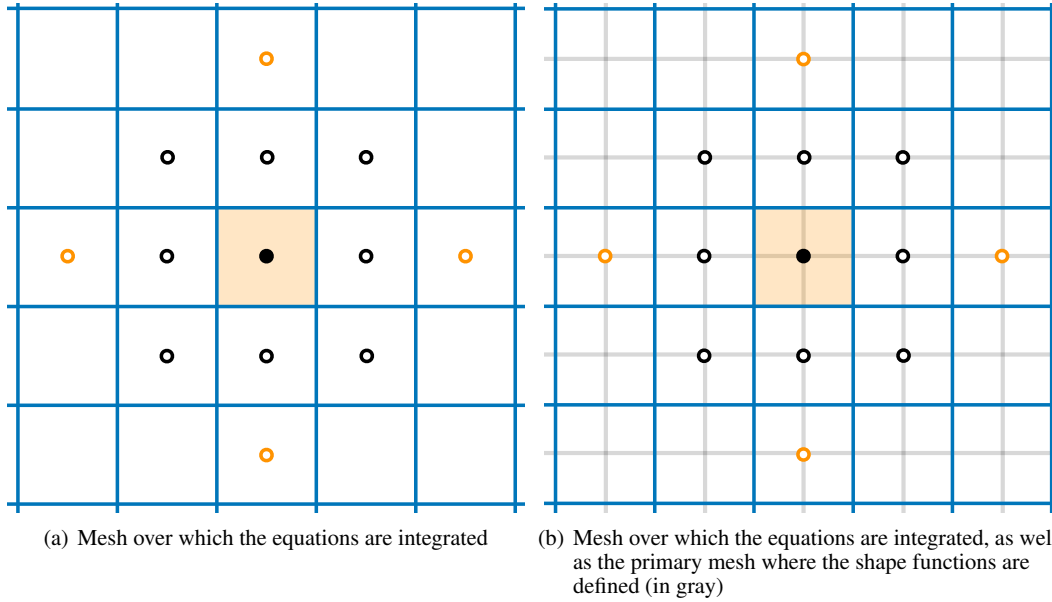


Figure 12. Local integration domain (shaded orange) and computational stencil (white-filled dots) for a node (black-filled dot) in a 2-D quadrilateral mesh. All methods include close neighbours (white-filled dots with black border) within their stencil, while method 1 additionally includes distant neighbours (white-filled dots with orange border).

be written in the form of a tensor algebraic equation:

$$\sum_{i=1}^{i=13} \mathbf{A}_i \cdot \mathbf{u}_i = \mathbf{0} \quad (57)$$

which corresponds to a block row in the resulting stiffness matrix, assuming a block-coupled solution methodology is used. It is possible to present the coefficients  $\mathbf{A}_i$  of this equation graphically to allow direct comparison between the different face gradient calculation approaches: Figure 13 compares the resulting coefficients from using methods 1, 2, 3 and 6, neglecting any stabilisation terms. Noting that boundary conditions have not been considered, a number of observations can be made:

- Methods 2, 3 and 6 employ the same compact computational stencil, whereas method 1 (interpolated gradient) uses a larger stencil, including second face-neighbours;
- All coefficients are symmetric;

		$\begin{pmatrix} \mu/4 & 0 \\ 0 & (2\mu+\lambda)/4 \end{pmatrix}$	
	$\begin{pmatrix} 0 & -(\mu+\lambda)/4 \\ -(\mu+\lambda)/4 & 0 \end{pmatrix}$	$\begin{pmatrix} 0 & 0 \\ 0 & 0 \end{pmatrix}$	$\begin{pmatrix} 0 & (\mu+\lambda)/4 \\ (\mu+\lambda)/4 & 0 \end{pmatrix}$
$\begin{pmatrix} (2\mu+\lambda)/4 & 0 \\ 0 & \mu/4 \end{pmatrix}$	$\begin{pmatrix} 0 & 0 \\ 0 & 0 \end{pmatrix}$	$\begin{pmatrix} -(3\mu+\lambda)/2 & 0 \\ 0 & -(3\mu+\lambda)/2 \end{pmatrix}$	$\begin{pmatrix} 0 & 0 \\ 0 & 0 \end{pmatrix}$
	$\begin{pmatrix} 0 & (\mu+\lambda)/4 \\ -(\mu+\lambda)/4 & 0 \end{pmatrix}$	$\begin{pmatrix} 0 & 0 \\ 0 & 0 \end{pmatrix}$	$\begin{pmatrix} 0 & -(\mu+\lambda)/4 \\ -(\mu+\lambda)/4 & 0 \end{pmatrix}$
		$\begin{pmatrix} \mu/4 & 0 \\ 0 & (2\mu+\lambda)/4 \end{pmatrix}$	

(a) Method 1: Interpolate gradients from adjacent cell-centres

		$\begin{pmatrix} 0 & 0 \\ 0 & 0 \end{pmatrix}$	
	$\begin{pmatrix} 0 & -(\mu+\lambda)/4 \\ -(\mu+\lambda)/4 & 0 \end{pmatrix}$	$\begin{pmatrix} \mu & 0 \\ 0 & 2\mu+\lambda \end{pmatrix}$	$\begin{pmatrix} 0 & (\mu+\lambda)/4 \\ (\mu+\lambda)/4 & 0 \end{pmatrix}$
$\begin{pmatrix} 0 & 0 \\ 0 & 0 \end{pmatrix}$	$\begin{pmatrix} 2\mu+\lambda & 0 \\ 0 & \mu \end{pmatrix}$	$\begin{pmatrix} -6\mu-2\lambda & 0 \\ 0 & -6\mu-2\lambda \end{pmatrix}$	$\begin{pmatrix} 2\mu+\lambda & 0 \\ 0 & \mu \end{pmatrix}$
	$\begin{pmatrix} 0 & (\mu+\lambda)/4 \\ -(\mu+\lambda)/4 & 0 \end{pmatrix}$	$\begin{pmatrix} \mu & 0 \\ 0 & 2\mu+\lambda \end{pmatrix}$	$\begin{pmatrix} 0 & -(\mu+\lambda)/4 \\ -(\mu+\lambda)/4 & 0 \end{pmatrix}$
		$\begin{pmatrix} 0 & 0 \\ 0 & 0 \end{pmatrix}$	

(b) Method 2: Calculate the normal gradient at the face using central-differencing, and interpolate the tangential gradient from the adjacent cell-centres

		$\begin{pmatrix} 0 & 0 \\ 0 & 0 \end{pmatrix}$	
	$\begin{pmatrix} 0 & -(\mu+\lambda)/4 \\ -(\mu+\lambda)/4 & 0 \end{pmatrix}$	$\begin{pmatrix} \mu & 0 \\ 0 & 2\mu+\lambda \end{pmatrix}$	$\begin{pmatrix} 0 & (\mu+\lambda)/4 \\ (\mu+\lambda)/4 & 0 \end{pmatrix}$
$\begin{pmatrix} 0 & 0 \\ 0 & 0 \end{pmatrix}$	$\begin{pmatrix} 2\mu+\lambda & 0 \\ 0 & \mu \end{pmatrix}$	$\begin{pmatrix} -6\mu-2\lambda & 0 \\ 0 & -6\mu-2\lambda \end{pmatrix}$	$\begin{pmatrix} 2\mu+\lambda & 0 \\ 0 & \mu \end{pmatrix}$
	$\begin{pmatrix} 0 & (\mu+\lambda)/4 \\ -(\mu+\lambda)/4 & 0 \end{pmatrix}$	$\begin{pmatrix} \mu & 0 \\ 0 & 2\mu+\lambda \end{pmatrix}$	$\begin{pmatrix} 0 & -(\mu+\lambda)/4 \\ -(\mu+\lambda)/4 & 0 \end{pmatrix}$
		$\begin{pmatrix} 0 & 0 \\ 0 & 0 \end{pmatrix}$	

(c) Method 3: Calculate the normal gradient at the face using central-differencing, and calculate the tangential gradient at the face using the point or edge values

		$\begin{pmatrix} 0 & 0 \\ 0 & 0 \end{pmatrix}$	
	$\begin{pmatrix} (3\mu+\lambda)/4 & -(\mu+\lambda)/4 \\ -(\mu+\lambda)/4 & (3\mu+\lambda)/4 \end{pmatrix}$	$\begin{pmatrix} -(\mu+\lambda)/2 & 0 \\ 0 & (\mu+\lambda)/2 \end{pmatrix}$	$\begin{pmatrix} (3\mu+\lambda)/4 & -(\mu+\lambda)/4 \\ (\mu+\lambda)/4 & (3\mu+\lambda)/4 \end{pmatrix}$
$\begin{pmatrix} 0 & 0 \\ 0 & 0 \end{pmatrix}$	$\begin{pmatrix} (\mu+\lambda)/2 & 0 \\ 0 & -(\mu+\lambda)/2 \end{pmatrix}$	$\begin{pmatrix} -(3\mu+\lambda) & 0 \\ 0 & -(3\mu+\lambda) \end{pmatrix}$	$\begin{pmatrix} (\mu+\lambda)/2 & 0 \\ 0 & -(\mu+\lambda)/2 \end{pmatrix}$
	$\begin{pmatrix} (3\mu+\lambda)/4 & -(\mu+\lambda)/4 \\ (\mu+\lambda)/4 & (3\mu+\lambda)/4 \end{pmatrix}$	$\begin{pmatrix} -(\mu+\lambda)/2 & 0 \\ 0 & (\mu+\lambda)/2 \end{pmatrix}$	$\begin{pmatrix} (3\mu+\lambda)/4 & -(\mu+\lambda)/4 \\ -(\mu+\lambda)/4 & (3\mu+\lambda)/4 \end{pmatrix}$
		$\begin{pmatrix} 0 & 0 \\ 0 & 0 \end{pmatrix}$	

(d) Method 6: Use shape functions with reduced integration

Figure 13. A comparison of the block coefficients in the stiffness matrix for the centre node/cell, where different face gradient calculation methods are employed. A unit thickness is assumed and stabilisation terms have been disregarded.

- All methods show geometric symmetries, for example, the top-right coefficient is equal to the bottom-left coefficient; this is a consequence of the momentum/force being conserved between nodes;
- In methods 1, 2, and 3, the normal forces are calculated entirely from the central cell displacement as well as the left, right, top and bottom cell displacements (far-left/right/top/bottom cells in the case of method 1). Similarly, the shear forces are calculated entirely from the top-left, top-right, bottom-left and bottom-right cell displacements;

- Methods 2 (interpolated tangential gradient) and 3 (tangential gradient calculated at the face) are equivalent for this simple grid. For meshes including skewness and non-orthogonality, this may not be the case;
- Method 1 differs from methods 2 and 3 in only one way: the left, right, top and bottom cell coefficients have been moved to a more distant neighbour and scaled in magnitude; in addition, the central coefficient has been scaled in magnitude. This corresponds to the normal component being calculated using a larger stencil (interpolated gradient) in method 1 vs methods 2 and 3 (central differencing at the face);
- Method 6 (shape functions) requires the force to be integrated over 8 faces compared with 4 faces for methods 1, 2 and 3; this comes from the way in which the mesh is constructed from a primary mesh;
- Half the components of the corner coefficients are zero for methods 1, 2 and 3, while they are all non-zero for method 6.

It should be noted that the coefficients that appear in the linear system matrix depend on the chosen solution algorithm; for block-coupled approaches, the coefficients will be as shown, whereas for segregated approaches, the coefficients will be more sparse and will not contain inter-component couplings (the off-diagonal components of the coefficients will be zero). For example, the matrix coefficients corresponding to method 2 (and equivalently method 3) are given for the segregated approach in Figure 14. In contrast to the coefficients given in Figure 13(b), the segregated

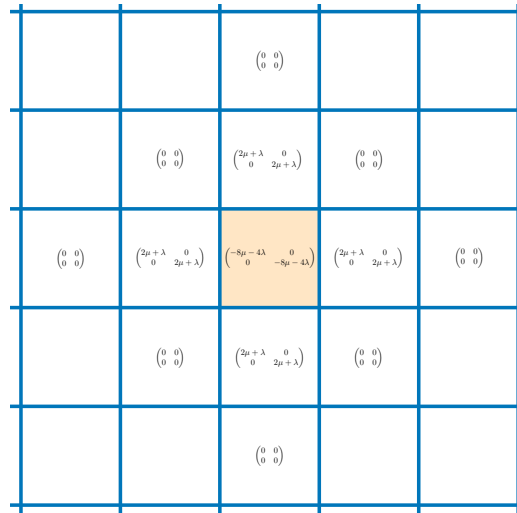


Figure 14. Stiffness matrix coefficients for methods 2 and 3 when a segregated solution algorithm is used; the inter-component coupling terms are included via the source vector in a deferred correction manner

coefficients (Figure 14) differ in the following ways:

- As noted, all inter-component coupling is zero *i.e.* all block off-diagonal coefficients are zero; this allows the two scalar displacement equations to be solved separately;
- The matrix has greater sparsity than the other approaches, leading to reduced memory requirements;
- The coefficients produce a matrix which is *weakly* diagonally dominant: the magnitude of the centre node coefficient is equal to the sum of the magnitudes of the other nodes. Such a

weakly diagonally dominant system (which becomes strongly diagonally dominant with the inclusion of Dirichlet/essential boundary conditions) promotes the convergence of iterative linear solvers.

**Stabilisation approach** For the discretisations that require stabilisation, three distinct forms of stabilisation term can be found; these can be expressed as a stabilisation traction  $\mathbf{t}^{\text{stab}}$  applied at the control volume face:

$$\mathbf{t}^{\text{stab}} = \begin{cases} \alpha^{\text{stab}} K_f \left( \frac{\mathbf{u}_N - \mathbf{u}_P}{|\mathbf{d}_f|} - \mathbf{n}_f \cdot \frac{|\mathbf{d}_{Nf}| \nabla \mathbf{u}_N + |\mathbf{d}_{Pf}| \nabla \mathbf{u}_P}{|\mathbf{d}_f|} \right) |\Gamma_f| & \text{Rhie-Chow} \\ -\alpha^{\text{stab}} \rho c_p |\mathbf{d}_f|^2 (\nabla^2 \mathbf{v}_N - \nabla^2 \mathbf{v}_P) |\Gamma_f| & \text{Jameson-Schmidt-Turkel} \\ \rho [c_s \mathbf{I} + (c_p - c_s) \mathbf{n}_f \mathbf{n}_f] \cdot \frac{\mathbf{v}_N + \mathbf{d}_{Nf} \cdot \nabla \mathbf{v}_N - \mathbf{v}_P - \mathbf{d}_{Pf} \cdot \nabla \mathbf{v}_P}{2} |\Gamma_f| & \text{Godunov upwinding} \end{cases} \quad (58)$$

where  $\alpha^{\text{stab}}$  is a user-defined scaling factor, the pressure wave speed of sound is  $c_p = \sqrt{\frac{2\mu + \lambda}{\rho}}$ , and the shear wave speed of sound is  $c_s = \sqrt{\frac{\mu}{\rho}}$ .

In Equation 58, Jameson-Schmidt-Turkel and Godunov-upwinding terms are given in a form that is only suitable for dynamic problems; however, it is possible to define similar stabilisation terms for quasi-static analyses:

$$\mathbf{t}^{\text{stab}} = \begin{cases} \alpha^{\text{stab}} K_f \left( \frac{\mathbf{u}_N - \mathbf{u}_P}{|\mathbf{d}_f|} - \mathbf{n}_f \cdot \frac{|\mathbf{d}_{Nf}| \nabla \mathbf{u}_N + |\mathbf{d}_{Pf}| \nabla \mathbf{u}_P}{|\mathbf{d}_f|} \right) |\Gamma_f| & \text{Rhie-Chow} \\ -\alpha^{\text{stab}} K_f |\mathbf{d}_f| (\nabla^2 \mathbf{u}_N - \nabla^2 \mathbf{u}_P) |\Gamma_f| & \text{Jameson-Schmidt-Turkel} \\ \alpha^{\text{stab}} \frac{K_f}{2} \frac{\mathbf{u}_N + \mathbf{d}_{Nf} \cdot \nabla \mathbf{u}_N - \mathbf{u}_P - \mathbf{d}_{Pf} \cdot \nabla \mathbf{u}_P}{|\mathbf{d}_f|} |\Gamma_f| & \text{Godunov upwinding} \end{cases} \quad (59)$$

where the Rhie-Chow term is given for comparison. A user-defined scaling factor  $\alpha^{\text{stab}}$  is added to the Godunov-type term in 59, as this form of the term does not have the same physical significance as the dynamic term in Equation 58. After some algebraic manipulation, where we include the  $(1/2)$  factor in  $\alpha^{\text{stab}}$  and note that  $\mathbf{d}_{Nf} = -|\mathbf{d}_{Nf}| \mathbf{n}_f$ , the Godunov upwinding-type stabilisation term is seen to be identical to Rhie-Chow stabilisation. This shows that even in its original dynamic form (Equation 58), it is in fact just a scaled version of Rhie-Chow stabilisation, and is equivalent for a specific choice of scaling parameters.

Using the 2-D square grid (Figure 12) as before, the computational stencil and coefficients resulting from the Rhie-Chow and Jameson-Schmidt-Turkel stabilisation terms can be graphed (Figure 15). Scale factors of  $\alpha^{\text{stab}} = (1/4)$  for the Jameson-Schmidt-Turkel term and  $\alpha^{\text{stab}} = 1$  for the Rhie-Chow term are chosen so that the magnitude of the terms is similar. For this grid, both approaches produce similar coefficients, however, the Jameson-Schmidt-Turkel approach differs in that it includes additional coupling in the corner coefficients. It can also be seen that both approaches require a large computational stencil, in that second face-neighbours are needed. When either of these stabilisation approaches is combined with one of the face gradient calculations methods discussed above, the stencil of coefficients are summed. For example, the computational

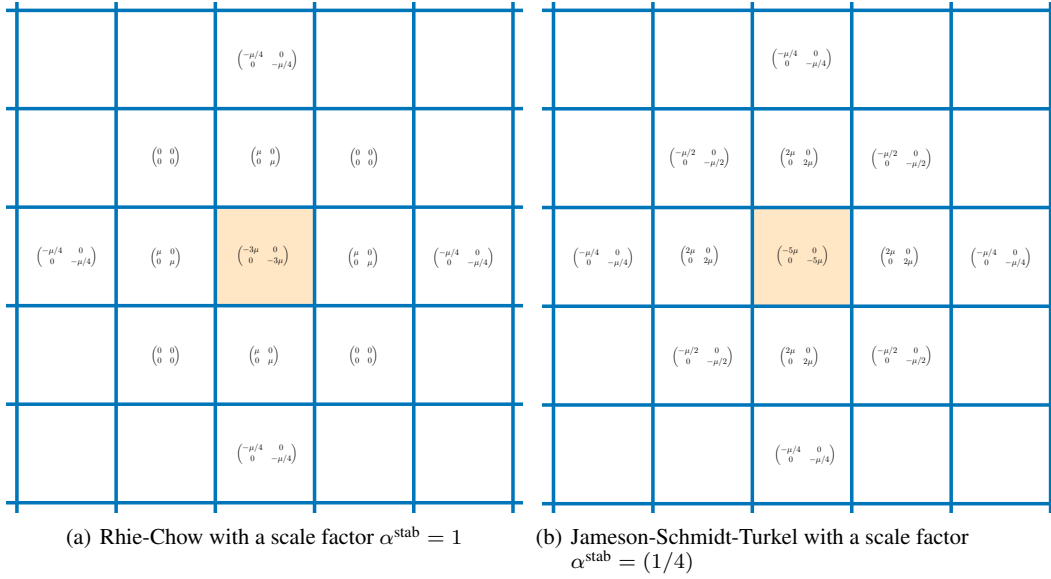


Figure 15. A comparison of the block coefficients in the stiffness matrix for the centre node/cell for two styles of stabilisation term: Rhie-Chow and Jameson-Schmidt-Turkel

stencil and coefficients from face gradient calculation method 1 with Rhie-Chow stabilisation are shown in Figure 16(a), and from face gradient calculation method 2 with Jameson-Schmidt-Turkel stabilisation in Figure 16(b).

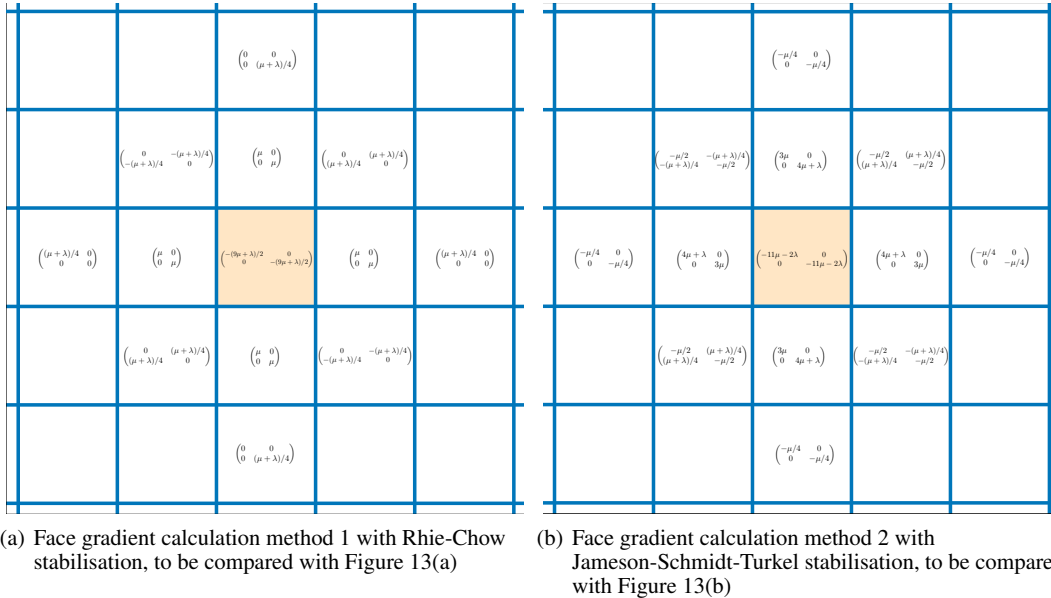


Figure 16. The effect on the stiffness matrix coefficients by including stabilisation terms

Within literature, a number of authors have described stabilisation techniques, however, stability analysis of finite volume discretisations for solid mechanics is not common. Of course, the stability of a formulation quickly becomes apparent in use, however, we can also take inspiration from

finite element approaches [408] and analyse the stiffness matrix eigenvalues. Taking a single unconstrained finite element, the number of zero eigenvalues of the stiffness matrix indicates the number of zero energy modes. For a stable formulation, the number of zero valued eigenvalues is equal to the number of rigid degrees of freedom; in 3-D, there are three rigid translations and three rigid rotations, whereas in 2-D there are two rigid translations and one rigid rotation. For an unstable formulation, there will be additional zero valued eigenvalues, where the corresponding eigenvector indicates the unstable mode. For the finite volume method, an equivalent analysis of an individual cell/element is less obvious. One such approach is to consider a periodic patch of finite volume cells, containing a central cell and all neighbour cells within its computational stencil (Figure 17), and analyse the eigenvalues of its (block-coupled) global stiffness matrix. In this case, as there

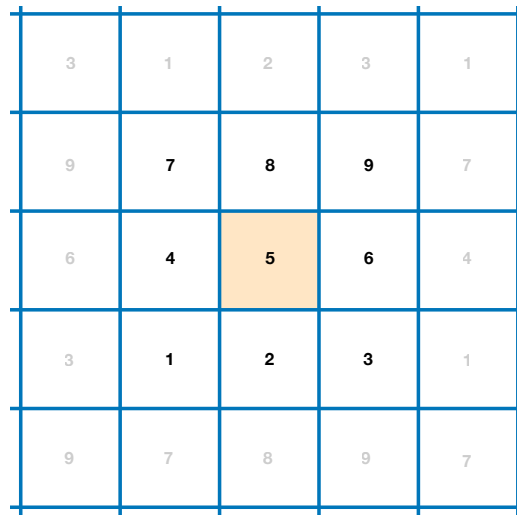


Figure 17. A periodic patch of finite volume cells, containing a central cell (cell 5) and all neighbour cells within its computational stencil. The periodic/cyclic neighbours are indicated as cells in grey numbering.

are 9 cells, each with 2 degrees of freedom, the global stiffness matrix is  $18 \times 18$ . As each cell contains all other eight cells in their stencil (due to the periodic conditions), the stiffness matrix is fully dense (no zero block entries). In this case, using face gradient calculation method 2, the stiffness matrix contains 2 zero eigenvalues, corresponding to the two rigid translation directions; the periodic conditions prohibit rigid rotation; this indicates that the discretisation is stable in this configuration. In addition to analysing a periodic patch of *internal* cells, it may also be necessary to examine a patch of cells adjacent to a boundary. The discretisation at boundary faces is typically different than at internal faces, and so boundaries may quell or excite spatial instabilities.

**Solution methodology** Like other popular numerical methods, the finite volume method can employ implicit or explicit solution algorithms. The relative merits of implicit vs explicit approaches are independent of the finite volume method; the interested reader can find numerous textbooks addressing this topic, for example, [408–410].

**A generalised finite volume method for solid mechanics** Based on these four components, it is possible to describe a generalised approach encompassing all individual variants, as shown in Figure 18. Common approaches are indicated by the coloured lines: implicit cell-centred (green),

implicit vertex-centred (blue), explicit Godunov-type (red), and staggered-grid (purple). This figure allows the relationship between the variants to be concisely expressed. What is also apparent from this figure is that there are avenues that have yet to be fully explored.

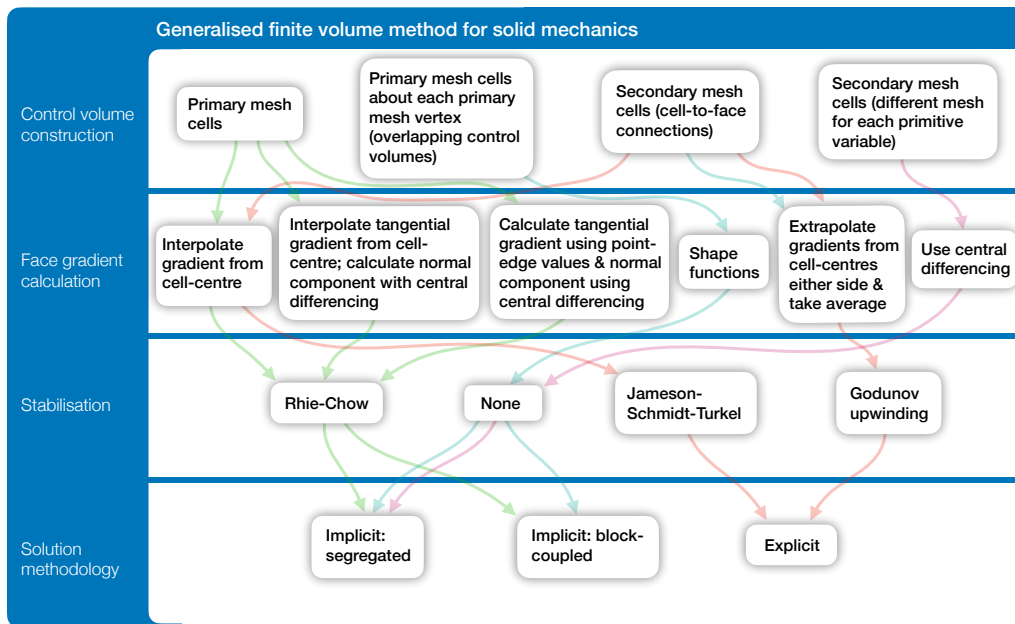


Figure 18. Generalisation of the finite volume method for solid mechanics, allowing the creation of any scheme through appropriate selection of four key components: 1) control volume construction method, 2) face gradient calculation approach, 3) stabilisation technique, and 4) solution methodology. Common approaches are indicated by the coloured lines: implicit cell-centred (green), implicit vertex-centred (blue), explicit Godunov-type (red), and staggered-grid (purple).

#### 4. COMPARING OF THE FINITE VOLUME METHOD FOR COMPUTATIONAL SOLID MECHANICS WITH THE FINITE ELEMENT METHOD

Within this section, the finite volume method for solids mechanics is compared with the “standard” continuous Bubnov-Galerkin finite element method, for example, as described by Bathe [409], Zienkiewicz and Taylor [411], and Belytschko et al. [408]. Following the approach taken in the previous section, the finite element method will be compared to the finite volume method in terms of: (a) discretisation of space and time; (b) discretisation of the mathematical model equations; and (c) solution algorithm.

##### 4.1. Discretisation of time and space

Like the finite volume method, the finite element method follows the standard time-marching temporal discretisation approach. Similarly, the solution domain space is divided into a finite number of convex cells (or elements) that do not overlap and fill the space completely. With regard to the mesh, the following differences can be noted between the finite element method and each of the finite volume variants:

- The cell-centred approach and vertex-centred approaches which *do not* use shape functions are applicable to general convex polyhedral in 3-D and general polygons in 2-D, whereas the standard finite element method is limited to standard element shapes, such as hexahedra/tetrahedra in 3-D and quadrilaterals/triangles in 2-D. A consequence of this it that ‘hanging nodes’ (Fig. 19) are common in finite volume analyses but not directly possible with the standard finite element method;
- The vertex-centred (and hypothetically cell-centred) approaches which *do* use shape function are limited to the same types of meshes used by the standard finite element method;

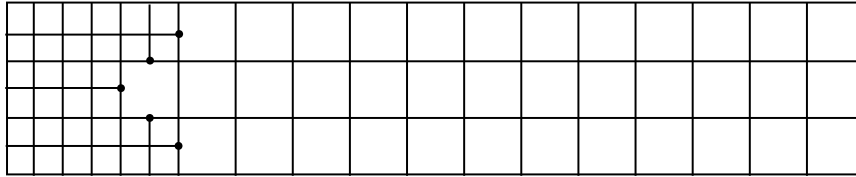


Figure 19. 2-D quadrilateral mesh of a beam, where ‘hanging nodes’ are shown as black dots.

#### 4.2. Discretisation of the mathematical model equations

In Section 3.1, the conservation of linear momentum in strong integral form (Equation 1) was taken as the starting point for the finite volume discretisation. In contrast, the finite element method requires the weak form of the governing equation, and hence begins with the strong differential form:

$$\rho \frac{\partial^2 \mathbf{u}}{\partial t^2} = \nabla \cdot [\mu \nabla \mathbf{u} + \mu (\nabla \mathbf{u})^T + \lambda \text{tr}(\nabla \mathbf{u}) \mathbf{I}] + \rho \mathbf{f}_b \quad (60)$$

This form is then multiplied by an arbitrary continuous weighting function  $\omega$  and integrated over the material volume to give the conservation of momentum in weak form:

$$\int_{\Omega} \omega \cdot \left\{ \rho \frac{\partial^2 \mathbf{u}}{\partial t^2} - \nabla \cdot [\mu \nabla \mathbf{u} + \mu (\nabla \mathbf{u})^T + \lambda \text{tr}(\nabla \mathbf{u}) \mathbf{I}] - \rho \mathbf{f}_b \right\} d\Omega = \mathbf{0} \quad (61)$$

Unsurprisingly a finite volume method is recovered if the weighting functions  $\omega$  are taken as unity within the control volumes and zero elsewhere.

To derive the finite element method, the weak form (Equation 61) is rearranged using integration by parts combined with the Gauss divergence theorem:

$$\int_{\Omega} \rho \omega \cdot \frac{\partial^2 \mathbf{u}}{\partial t^2} d\Omega + \int_{\Omega} \nabla \omega : \overbrace{[\mu \nabla \mathbf{u} + \mu (\nabla \mathbf{u})^T + \lambda \text{tr}(\nabla \mathbf{u}) \mathbf{I}]}^{\sigma} d\Omega = \int_{\Gamma_T} \omega \cdot \mathbf{T}_{\Gamma} d\Gamma + \int_{\Omega} \rho \omega \cdot \mathbf{f}_b d\Omega \quad (62)$$

where  $\Gamma_T$  is the region of the domain boundary where tractions  $\mathbf{T}_{\Gamma}$  are applied. In the second term on the left-hand side of Equation 62, the differential operator now acts on the weighting function  $\omega$ , in contrast to Equation 1 where it acts on the stress tensor  $\sigma$ . It is assumed that the weighting functions, also known as test functions, satisfy the following requirements [408]:

- They are *not* functions of time;
- They are  $C^0$  continuous;
- They vanish on displacement boundaries.

Interpreting the weighting functions  $\omega$  as *virtual displacements* allows Equation 62 to be viewed as the principle of virtual work. In this way, the original problem of trying to find a displacement field which satisfies the conservation of linear momentum can be reinterpreted as trying to find a displacement field which minimises the total energy.

The finite element method then assumes the displacement  $\mathbf{u}$  within each mesh element to vary according to *shape functions*, as presented previously in Equation 25. The standard *Bubnov-Galerkin* form of the finite element method is achieved by assuming that the weighting functions  $\omega$  in Equation 62 are approximated using the same shape functions as the displacement field:

$$\omega = \sum_{A=1}^{nVertices} N_A \bar{\omega}_A \quad (63)$$

where  $\bar{\omega}_A$  represents the discrete weighting function value at vertex  $A$ ; uppercase letter  $A$  is used as an index for vertices to avoid confusion with index notation  $i, j$  and  $k$ .

Combining Equations 25 (displacement shape functions), 63 and 62, the finite element equations are expressed as [412]:

$$\begin{aligned} & \underbrace{\int_{\Omega} \rho \sum_{A=1}^{nVertices} N_A \bar{\omega}_A \cdot \sum_{B=1}^{nVertices} N_B \frac{\partial^2 \mathbf{u}_B}{\partial t^2} d\Omega}_{\text{Inertial force term}} \\ & + \underbrace{\int_{\Omega} \sum_{A=1}^{nVertices} \nabla N_A \bar{\omega}_A : \left[ \mu \sum_{B=1}^{nVertices} \nabla N_B \mathbf{u}_B + \mu \sum_{B=1}^{nVertices} \mathbf{u}_B \nabla N_B + \lambda \text{tr} \left( \sum_{B=1}^{nVertices} \nabla N_B \mathbf{u}_B \right) \mathbf{I} \right]}_{\text{Internal force term}} d\Omega \\ & = \underbrace{\oint_{\Gamma_T} \sum_{A=1}^{nVertices} N_A \bar{\omega}_A \cdot \mathbf{T}_{\Gamma} d\Gamma}_{\text{External (surface) force term}} + \underbrace{\int_{\Omega} \sum_{A=1}^{nVertices} N_A \bar{\omega}_A \cdot \rho \mathbf{f}_b d\Omega}_{\text{External (body) force term}} \end{aligned} \quad (64)$$

To proceed, we will switch to index notation, not referring to spatial directions  $i$  and  $j$  or nodes  $A$  and  $B$ , but instead to the degrees of freedom [412]. For this, the index for a global degree of freedom  $P$  can be given uniquely in terms of the spatial index and node index:

$$P = f(i, A) \quad (65)$$

Examining Equation 64 term by term and using both index notation and degree of freedom notation, the inertial force term can be expanded as:

$$\begin{aligned}
& \int_{\Omega} \rho \sum_{A=1}^{nVertices} N_A \bar{\omega}_A \cdot \sum_{B=1}^{nVertices} N_B \frac{\partial^2 \mathbf{u}_B}{\partial t^2} d\Omega \\
&= \sum_{A=1}^{nVertices} \sum_{i=1}^{nDims} \int_{\Omega} \rho N_A \bar{\omega}_{iA} \sum_{B=1}^{nVertices} N_B \frac{\partial^2 U_{iB}}{\partial t^2} d\Omega \\
&= \sum_{A=1}^{nVertices} \sum_{i=1}^{nDims} \bar{\omega}_{iA} \sum_{B=1}^{nVertices} \sum_{j=1}^{nDims} \int_{\Omega} \rho N_A \delta_{ij} N_B \frac{\partial^2 U_{iB}}{\partial t^2} d\Omega \\
&= \sum_{P=1}^{nDoF} \bar{\omega}_P \sum_{Q=1}^{nDoF} M_{PQ} \frac{\partial^2 U_Q}{\partial t^2} d\Omega \tag{66}
\end{aligned}$$

where  $nDims$  is the number of spatial dimensions,  $\delta_{ij}$  is the Kronecker delta, and  $nDoF = nDims \times nVertices$  is the number of global degrees of freedom. Matrix  $M_{PQ}$  is known as the mass matrix and is given as:

$$M_{PQ} = \int_{\Omega} \rho N_A \delta_{ij} N_B d\Omega \tag{67}$$

The volume integral in Equation can be calculated (or approximated) using Gaussian/numerical quadrature:

$$M_{PQ} \approx \sum_{p=1}^{nQuadPoints} w_p \rho(\xi_p) N_A(\xi_p) \delta_{ij} N_B(\xi_p) \tag{68}$$

where  $nQuadPoints$  is the number of quadrature points,  $w$  is the quadrature weight, and  $\xi$  is the quadrature location within the element. For example, using one-point quadrature, the quadrature locations are situated at the centroids of the elements; in that case, the density and the derivative of the shape functions are evaluated at element centroids.

Unlike finite volume approaches, the resulting mass matrix will not in general be diagonal; however, diagonalisation or *lumping* of the mass matrix is common, although often ad hoc [408]; for example, the row-sum technique calculates the diagonal elements as the sum of the coefficients for that row.

The internal force term in Equation 64 can be simplified as:

$$\begin{aligned}
& \int_{\Omega} \sum_{A=1}^{nVertices} \nabla N_A \bar{\omega}_A : \left[ \mu \sum_{B=1}^{nVertices} \nabla N_B \mathbf{u}_B + \mu \sum_{B=1}^{nVertices} \mathbf{u}_B \nabla N_B + \lambda \text{tr} \left( \sum_{B=1}^{nVertices} \nabla N_B \mathbf{u}_B \right) \mathbf{I} \right] d\Omega \\
&= \int_{\Omega} \sum_{A=1}^{nVertices} \sum_{i=1}^{nDims} \sum_{j=1}^{nDims} N_{A,j} \bar{\omega}_{iA} (\mu N_{B,j} U_{iB} + \mu N_{B,i} U_{jB} + \lambda N_{B,k} U_{kB} \delta_{ij}) d\Omega \\
&= \sum_{P=1}^{nDoF} \bar{\omega}_P K_{PQ} U_Q \tag{69}
\end{aligned}$$

where matrix  $K_{PQ}$  is known as the stiffness matrix:

$$K_{PQ} = \int_{\Omega} \sum_{j=1}^{nDims} N_{A,j} [\mu N_{B,j} + \mu N_{B,i} + \lambda N_{B,i} \delta_{ij}] d\Omega \quad (70)$$

The integral can once again be evaluated using Gaussian/numerical quadrature:

$$K_{PQ} \approx \sum_{p=1}^{nQuadPoints} \sum_{j=1}^{nDims} w_p N_{A,j}(\xi_p) [\mu(\xi_p) N_{B,j}(\xi_p) + \mu(\xi_p) N_{B,i}(\xi_p) + \lambda(\xi_p) N_{B,i}(\xi_p) \delta_{ij}] \quad (71)$$

Evaluating this integral exactly (using sufficient quadrature points) would naively appear to be the best approach; however, formulations that use *full* integration tend to suffer from locking [408], which can be described as an overly stiff behaviour in bending. Consequently, *reduced* integration is often favoured, where the local field is under-integrated. This reduced integration has the benefit of relieving this locking phenomena as well as reducing the computational time, due to the lower number of integration points.

A downside of reduced integration is the introduction of spatial instabilities into the discretisation. In essence, the element is capable of deforming in certain *modes* which offer no resistance. These spurious singular or zero energy modes produce an accordion-like deformation pattern known as hourglassing. Similar to the finite volume method, a stabilisation term is included in the formulation to suppress such spatial instabilities. For the finite element method, this hourglass stabilisation is incorporated through the inclusion of a stabilisation stiffness within the element stiffness matrix, or a viscous stabilisation term for dynamic problems [408]. For static problems a variety of stabilisation methods have been proposed, but typically a *stabilisation stiffness* term  $K_{PQ}^{stab}$  is added to the element stiffness matrix of the form [408, 413]:

$$K_{PQ}^{stab} = \alpha_{stab} \mu N_{A,j}^{stab} N_{B,j}^{stab} \Omega \quad (72)$$

where  $N_{A/B,j}^{stab}$  represents the gradient interpolators used to define the hourglass deformation modes. The  $\alpha_{stab}$  is a scaling factor typically set between 0.005 and 0.1 [408, 413], depending on the form of  $N_{A,j}^{stab}$ . For volumetric spatial instabilities,  $\mu$  is replaced by the bulk modulus,  $\kappa = (2/3)\mu + \lambda$ , and  $N_{A,j}^{stab}$  represents the gradient interpolators for the volumetric/pressure hourglass mode.

Finally, the two external force terms in Equation 64 are expressed as:

$$\oint_{\Gamma_T} \sum_{A=1}^{nVertices} N_A \bar{\omega}_A \cdot \mathbf{T}_\Gamma d\Gamma + \int_{\Omega} \sum_{A=1}^{nVertices} N_A \bar{\omega}_A \cdot \rho \mathbf{f}_b d\Omega = \sum_{P=1}^{nDoF} \bar{\omega}_P F_P \quad (73)$$

where vector  $F_P$  is known as the global force vector:

$$F_P = \oint_{\Gamma_T} \sum_{A=1}^{nVertices} N_A T_{i\Gamma} d\Gamma + \int_{\Omega} \sum_{A=1}^{nVertices} \rho N_A f_{ib} d\Omega \quad (74)$$

and once again the integrals are evaluated using quadrature.

Equation 64 can now be expressed as:

$$\bar{\omega}^T \left( M \frac{\partial^2 \mathbf{U}}{\partial t^2} + \mathbf{K} \mathbf{U} - \mathbf{F} \right) = \mathbf{0} \quad (75)$$

where the global vectors of dimension  $nDoF \times 1$  are:

$$\bar{\omega} = [\bar{\omega}_P], \quad \mathbf{U} = [U_P], \quad \mathbf{F} = [F_P] \quad (76)$$

and global matrices of dimension  $nDoF \times nDoF$  are:

$$\mathbf{M} = [M_P], \quad \mathbf{K} = [K_P] \quad (77)$$

As Equation 75 is satisfied for all values of  $\bar{\omega}$ , this requires that the bracketed term is equal to zero. This gives the semi-discrete form (discrete in space, not in time) of the finite element equations:

$$M \frac{\partial^2 \mathbf{U}}{\partial t^2} + \mathbf{K} \mathbf{U} = \mathbf{F} \quad (78)$$

To complete the discretisation, the acceleration term  $\frac{\partial^2 \mathbf{U}}{\partial t^2}$  is discretised using a finite difference scheme. Similar to the finite volume approaches, many finite difference schemes can be used, where Newmark schemes are popular. The simple Euler backward scheme is given here for comparative purposes:

$$M \frac{U - 2U^{[m-1]} + U^{[m-2]}}{\Delta t^2} + \mathbf{K} \mathbf{U} = \mathbf{F} \quad (79)$$

Boundary tractions/forces have already been included in  $\mathbf{F}$  via the external (surface) force term in Equation 64. For the incorporation of displacement conditions, this signifies that some of the degrees of freedom in  $\mathbf{U}$  are known; these equations can hence be disregarded. As in the case with the finite volume methods, initial conditions, in the form of the displacement field at  $t = 0$ ,  $t = -\Delta t$ , and  $t = -2\Delta t$ , must also be specified.

### 4.3. Solution algorithm

Once known degrees of freedom have been incorporated, Equation 79 represents a system of  $nDoF - nKnownDof$  linear algebraic equations, where  $nKnownDof$  is the number of known degrees of freedom. Similar to the analogous matrices in the finite volume method, the mass matrix can be seen to be a function of the density and element geometry; the stiffness matrix is a function of the mechanical properties and element geometry; and the force vector  $\mathbf{F}$  contains surface and body force contributions as well as inertial terms and non-zero known degree of freedom contributions. Like the finite volume approaches, this system of algebraic equations can be solved using either an implicit or explicit time marching procedure.

For implicit approaches, Equation 79 can be rearranged and solved for  $\mathbf{U}$ :

$$\left( \frac{1}{\Delta t^2} M + \mathbf{K} \right) \mathbf{U} = \mathbf{F} + M \frac{2U^{[m-1]} - U^{[m-2]}}{\Delta t^2} \quad (80)$$

Assuming a stable discretisation, the matrix of the linear system  $(\frac{1}{\Delta t^2} \mathbf{M} + \mathbf{K})$  (or  $\mathbf{K}$  for quasi-static) has the following properties:

- It is sparse with the number of non-zero elements in each row equal to the number of vertices which share an element with the current vertex, plus one;
- It is symmetric;
- It is positive definite;
- In general, unlike for the cell-centred finite volume approaches where a segregated algorithm is used, it is not diagonally dominant; however, finite volume discretisations that employed block-coupled solution methodologies will produce a similar non-diagonally dominant matrix.

To solve Equation 80, typically a direct linear solver is employed, for example, Gaussian elimination, LU decomposition or multi-frontal methods; however, iterative methods such as preconditioned conjugate gradient are also possible [409].

#### 4.4. Discussion

**Overview** Given the close relationship between the finite volume and finite element methods, it is not surprising that both have been compared previously: some notable dissections include those from Oñate, Zienkiewicz, Idelsohn [6, 8, 11, 12, 414–417], Lahrman [418], Perré and Passard [294], Harrild and Henriquez [419], Zarrabi and Basu [55], Fang et al. [420], Yamamoto et al. [421], Jacquemet and Henriquez [422, 423], Vaz Jr. et al. [37], Filippini et al. [424], and recently Demirdžić [425]. The general consensus is that both methods share the same data structure and general strategy to assemble the corresponding characteristic matrices, with the main conceptual difference being in the local integration domain and local integration method. Although a number of authors have claimed superior accuracy of one method over the other [37, 418, 419], the majority of authors have found both methods to produce similar predictions with no significant differences [294, 420, 421, 423].

One generally accepted appeal of the finite volume method is the ease with which it can be followed and implemented: the finite volume method is simply based on balancing forces acting on a volume, requiring no knowledge of advanced mathematical frameworks. Comparing the derivations in Section 3.2 and 4.2, the finite element approach would appear to be more mathematically involved; however, proponents of the finite element method claim that the principle of virtual work and energy minimisation techniques are equally interpretable as the balance equation form.

**Weak vs strong forms of the conservation law and the implications** As discussed, finite volume and finite element methods differ in their philosophy: where the finite volume method deals with the strong balance form of the governing law, the finite element method deals with the equivalent weak virtual energy form. One consequence of this is the manner in which local conservation is enforced. As finite volume approaches discretise surface integrals at the (typically non-overlapping) control volume boundaries, strong local conservation is achieved: forces are equal and opposite at cell boundaries. As a consequence of this local conservation, global conservation within the domain is automatically achieved. In contrast, finite element methods discretise the surface force term as a volume integral using locally overlapping integration domains: this results in local conservation

in an average sense, rather than directly for each element. Global conservation is ensured in an average sense, assuming there are sufficient numbers of elements. An additional consequence of these contrasting approaches is how each method treats Neumann/natural boundary conditions: considering traction conditions, finite volume methods satisfy these conditions exactly regardless of the mesh density; whereas finite element approaches satisfy them in an approximate sense, and as the mesh is refined strong enforcement is approached.

As noted by a number of authors, for example, [11, 12, 24], by choosing unity weighting functions in the weak form of the governing equation (Equation 62), it is possible to recover the finite volume method. Spalding [322] alludes to this point by referring to finite volume approaches as *unity-weighting function methods* and to finite element approaches as *non-unity weighting function methods*.

**Geometric flexibility** As *standard* finite element methods use shape functions to define a continuous displacement distribution, this limits their application to meshes containing *standard* element shapes. Concretely, only standard shapes such as triangles and quadrilaterals are allowed in 2-D, and tetrahedra and hexahedra in 3-D. Similarly, finite volume approaches that explicitly use shape functions are constrained in the same way. More commonly finite volume methods describe the local solution distribution using a truncated Taylor expansion, resulting in discontinuous jumps at the cell interfaces. An outcome of this is the ability of finite volume approaches to deal with general convex polyhedral meshes. In this way, finite volume approaches are more flexible in terms of mesh generation and dynamic remeshing. In addition to hanging nodes, typical finite volume discretisations can deal with *overset/chimera* and immersed boundary meshes in a straight-forward manner.

**Mass matrix and stiffness matrix properties** A desirable property of finite volume methods for explicit implementation and parallelisation is that the mass matrix is automatically diagonal. For finite element methods, the lack of a diagonal consistent mass matrix results in the use of so-called *mass lumping* approaches, which are often ad-hoc, as noted previously. The stiffness matrix, however, bears many similarities between the methods.

To allow direct comparison, let us consider finite volume and finite element discretisations on a uniform equilateral-triangular grid (Figure 20). We will consider a typical domain of integration around a node, where a node represents a vertex in the finite element method and a cell-centre in the finite volume method. For ease of comparison, the dual mesh is used for the finite volume method. In the finite element case (Figure 20(a)), the local integration domain (shaded in orange) consists of all elements adjacent to the centre node (black-filled dot). Consequently, the computational stencil for the centre vertex consists of the six neighbouring vertices (indicated by white-filled dots), which share an element with the centre node. In the finite volume case (Figure 20(b)), the local integration domain (shaded in orange) is the cell itself containing the node at its centre (black-filled dot); the computational stencil includes all neighbouring cell-centres (white-filled dots). In this case, as both methods share the same computational stencil, the resulting stiffness matrices will share the same structure and sparsity, *assuming* that the same solution strategy is used, for example, block-coupled or segregated. For a triangular grid, *either* the nodal locations *or* the orientation of the local integration domains can be aligned between the methods, but not both; as such, the comparison of

coefficients from both methods is not entirely direct, however, it does still provide insight. Here it was chosen to align the nodal locations rather than the local integration domains: the finite volume cell can be seen to be rotated  $90^\circ$  relative to the finite element cell, as well as being one third the area.

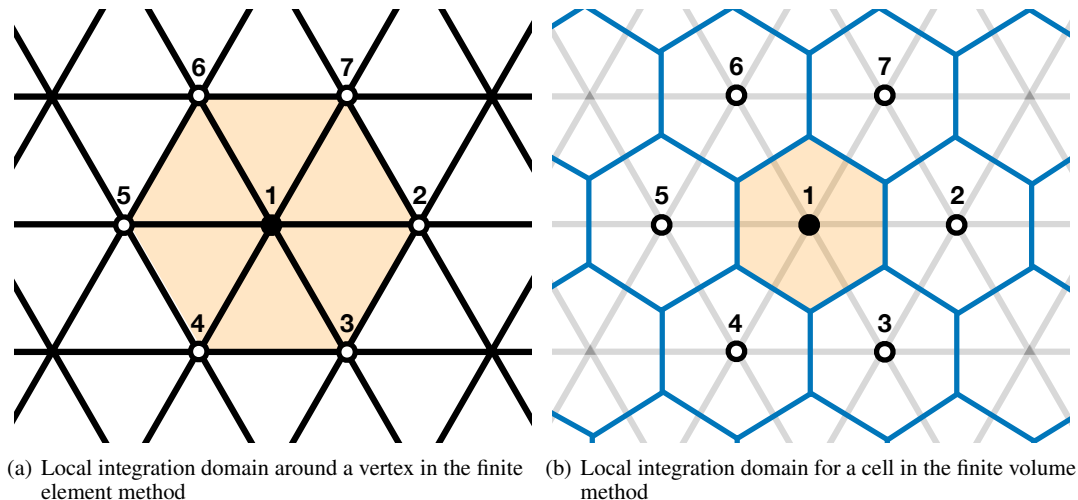


Figure 20. Uniform 2-D triangular grid showing the local integration domains and computational stencils for the finite element and finite volume methods. The centre node is shown as a black dot and all neighbouring nodes are shown as white-filled dots, where nodes are vertices in the finite element method, and are cell-centres in the finite volume method.

It is important to mention that the size and shape of the computational stencil in the finite volume method depend on the approach used to calculate the displacement gradients at the cell faces. Here face gradient calculation method 2 in Section 3.5 has been employed. Alternative face gradient calculation methods can result in the *second cell-neighbours* being included in the stencil; in contrast, a characteristic of the finite element method is that the integration domain is fixed regardless of local discretisation.

An additional observation is that the local integration domains overlap in the finite element method, but do not in the typical finite volume method *i.e.* integration domains for neighbouring finite element nodes overlap. An overlapping version of the vertex-centred finite volume method has been considered by Oñate et al. [12] but has not received significant attention.

Referring to the node numbering given in Figure 20, the block row for the centre node in the global mass matrix is given for the finite element method [408], consistent and lumped, as well as the finite volume method in Figure 21. The finite element mass-lumped approach can be seen to coincide with the finite volume approach; from this, we can see that the finite element lumped approach is essentially assigning the mass of the hexagon surrounding a node to the node itself, corresponding with the integration domain of the finite volume approach.

Considering next the stiffness matrix. Once again taking the same uniform 2-D triangular grid given in Figure 20, the block row for the centre node in the global stiffness matrix for the finite element method [408] is compared with the equivalent row from the finite volume method in Figure 22. For the finite volume method, the matrix using a block-coupled solution algorithm is given, as well as for the segregated approach. Examining the general structure of the coefficients for all three

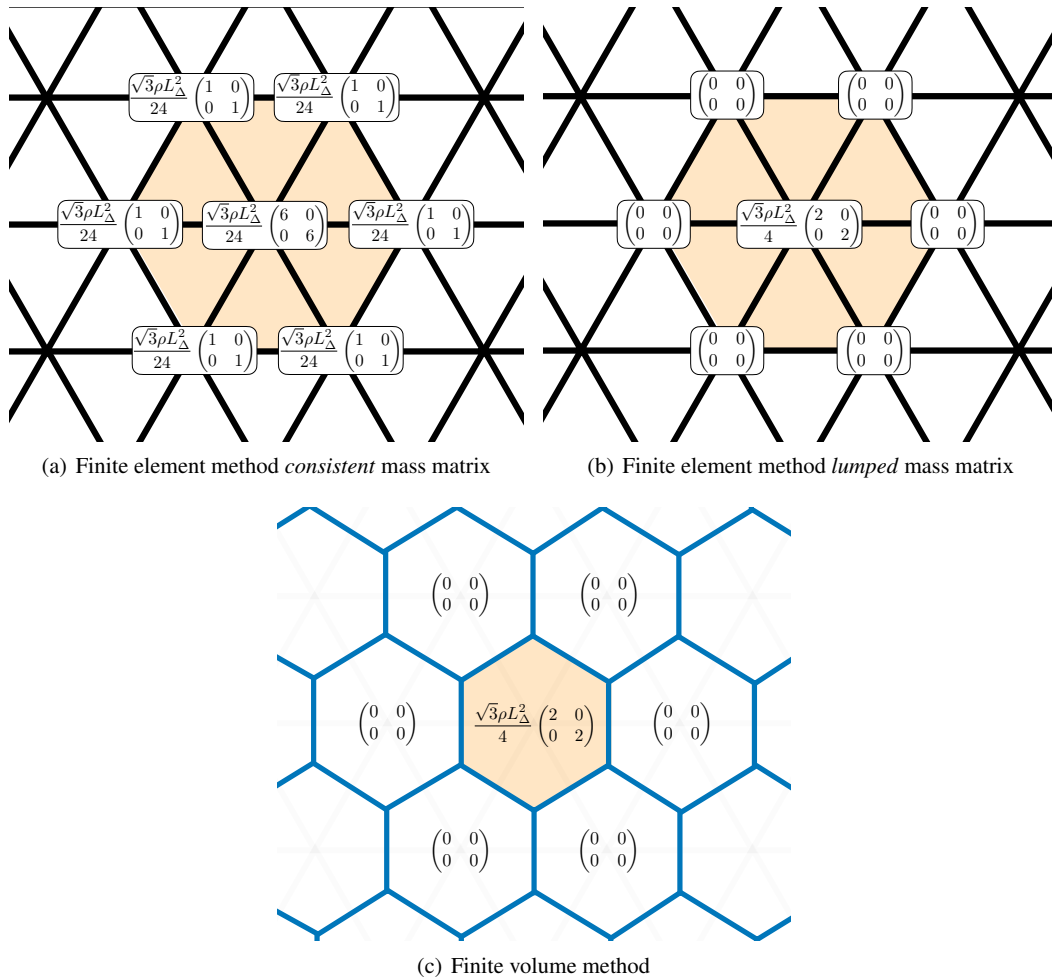


Figure 21. Block coefficients for a row in the mass matrix corresponding to the centre node, where  $L_\Delta$  is the triangle side-length, a unit thickness is assumed, and  $\frac{\sqrt{3}}{4}L_\Delta^2$  is the area of a triangular element. The area of the hexagonal finite volume cell is equal to  $\frac{\sqrt{3}}{2}L_\Delta^2$ .

methods (Figure 22(a), (b) and (c)), the following observations can be made:

- All three methods employ the same computational stencil;
- The coefficients are symmetric in all three cases, albeit the effect of boundary conditions has not been considered here;
- As expected, all three methods show geometric symmetries, for example, the top-right coefficient is equal to the bottom-left coefficient;
- The finite element and coupled finite volume approaches show the same sparsity structure *i.e.* there are zeros in the same locations; in addition, the coefficients have the same signs and show similar magnitudes, but do not have the same value, apart from for the central node;
- The segregated finite volume approach differs from the others by removing all inter-component coupling from the coefficients, as discussed in Section 3.5;
- The segregated finite volume approach produces a row of coefficients which is weakly diagonally dominant, also discussed in Section 3.5;

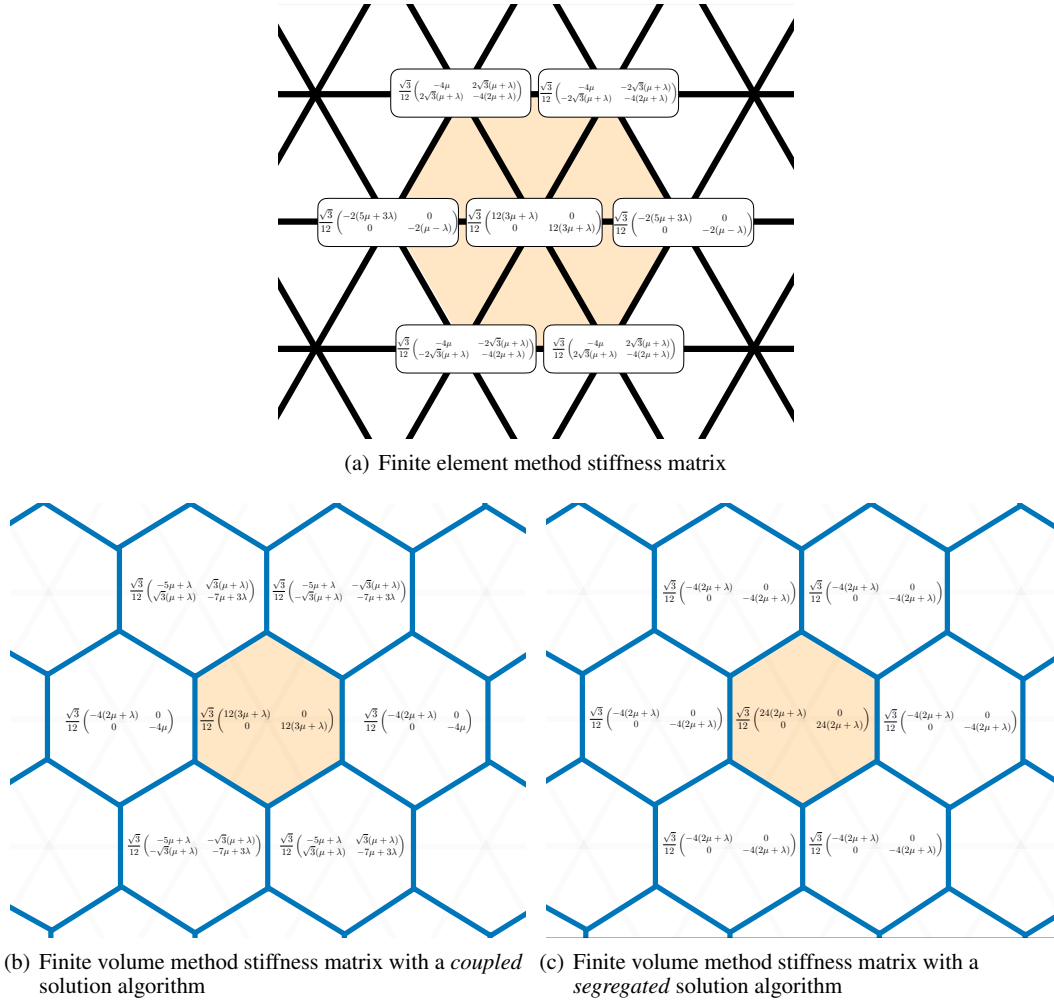


Figure 22. Block coefficients for a row in the stiffness matrix corresponding to the centre node, where  $L_{\Delta}$  is the triangle side-length and a unit thickness is assumed

- The momentum/force *between nodes* is conserved for all three methods (based on the symmetry of the coefficients), however, conservation of momentum/force *between elements/cells* is *not* directly enforced for the finite element method, whereas it *is* for the finite volume method.

**Discretisation stabilisation** As described in Section 4.2, finite element formulations which under-integrate the local domain require the inclusion of a stabilisation term, in the same way one is required in many finite volume formulations. In the finite element method, these spurious singular, zero energy modes produce an accordion-like deformation pattern known as hourglassing (Figure 23(a)), named due to its visual similarity to an hourglass timing device. These spatial instabilities are equivalent to checkerboarding instabilities that occur in finite volume formulations (Figure 23(b)); these checkerboarding pressure-type instabilities are also possible in finite element formulations. The origin of these spatial instabilities in both finite element and finite volume formulations is a *rank deficiency* in their respective stiffness matrices. Essentially, a stable discretisation should not

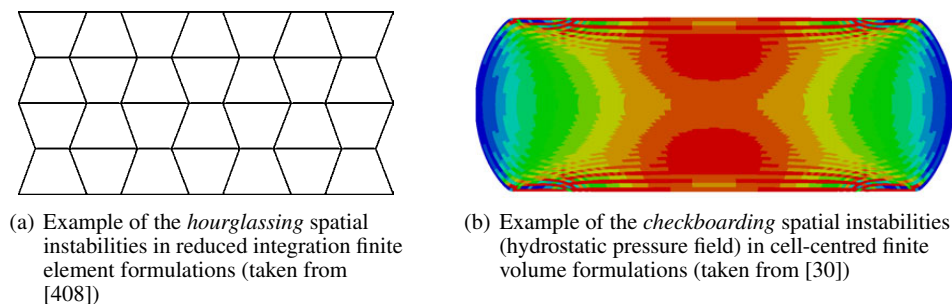


Figure 23. The equivalence of spatial instabilities in finite element and finite volume formulations

support any deformation modes which do not offer resistance, apart from rigid body translations and rotations. More precisely, rank deficiency refers to the fact that the discretised stiffness matrix has zero-valued eigenvalues which are not related to rigid body motions (as discussed in Section 3.5). For example, considering a 3-D element/cell, the stiffness matrix for a *full rank* formulation has six zero valued eigenvalues: three rigid translations and three rigid rotations; for a rank deficient formulation, additional zero valued eigenvalues are present corresponding to zero energy instability modes.

To address these spatial instabilities, both finite element and finite volume approaches add a stabilisation term to the discretised governing equations. In both cases, there are two primary constraints on the form of this stabilisation term [408]:

- It should not significantly affect the accuracy of the discretisation, and
- It should not affect the linear completeness of the discretisation; in other terms, the discretisation should still be able capable of describing a linear solution field exactly after the inclusion of the stabilisation term.

For both methods, a variety of techniques exist and the stabilisation *force* often takes a similar form:

$$\begin{aligned}
 \mathbf{f}^{\text{stab}} &= \alpha^{\text{stab}} C^{\text{stab}} \Omega (\nabla^2 \mathbf{u} - \nabla \cdot \nabla \mathbf{u}) && \text{Rhie-Chow stabilisation} \\
 &\quad - \alpha^{\text{stab}} C^{\text{stab}} \Omega \nabla^2 (\nabla^2 \mathbf{u}) && \text{Jameson-Schmidt-Turkel stabilisation} \quad (81) \\
 \mathbf{f}_P^{\text{stab}} &= \alpha^{\text{stab}} C^{\text{stab}} \Omega N_{A,j} N_{B,j} U_Q && \text{Hourglass stabilisation}
 \end{aligned}$$

where  $C^{\text{stab}}$  is some measure of mechanical property that gives an appropriate dimension to the dissipation, such as  $\mu$ ,  $2\mu + \lambda$ ,  $\mu + \lambda$ , or  $\kappa$ , for quasi-static analyses, or a function of the speed of sound for dynamic analyses. The  $\alpha^{\text{stab}}$  factor allows the magnitude of the stabilisation to be scaled.

**Performance of the methods** The differences in local integration domain and local integration method between the finite volume and finite element methods has consequences for the robustness, accuracy and efficiency of the resulting methods. Particularly for nonlinear analysis, the ideal discretisation is unclear due to a variety of numerical challenges which are yet to be fully resolved, including [426]: (1) spurious hourglassing and pressure checker-boarding, (2) bending difficulties, (3) shear and volumetric locking, (4) high frequency noise in the vicinity of shocks, (5) lower order of convergence for strains and stresses in comparison with displacements, and (6) sensitivity to mesh

distortions. It is these challenges that finite volume discretisations can potentially solve in a novel way.

Apart from this, a major motivation for finite volume solid mechanics schemes is the challenge of multi-physics problems. As long as the finite volume method is prominent in the world of computational fluid mechanics, there will be a demand for straight-forward finite volume solid mechanics implementations. These solid mechanics implementations can share the same computational framework, discretisation and solution methodologies as their fluid counterparts and can be integrated seamlessly into the code base.

Regarding accuracy and overly stiff behaviour, finite volume methods have not shown the same locking behaviour typical in fully integrated finite element methods. Given their similarity with reduced integrated finite elements, it is perhaps not surprising that this is the case; however, like finite elements, the absolute accuracy depends on the details of the formulation. Concerning order of accuracy, an attractive property of most finite volume methods is that the error in the strain and stress reduces at a second-order rate, like the displacement [37, 208]; this may not be the case for many finite element schemes, where the error in the strain and stress reduce at a rate closer to first order.

As models become larger and the availability of supercomputers and cloud computing increases, code parallelisation is becoming critical. Due to the widespread use of iterative linear solvers, finite volume methods (fluid and solid) commonly exploit hundreds or thousands of CPU cores, for example, the OpenFOAM software. In contrast, as direct linear solvers have often been the chosen solution approach for finite element schemes, parallel efficiency is inherently limited (relative to iterative solvers) and the use of large numbers of CPU cores has been less common; however, there are a number of projects focussed on the application of finite element methods to supercomputers using iterative solvers, for example, ParaFEM [427]. Apart from the choice between direct and iterative linear solver, cell-finite volume approaches possess a convenient advantage over vertex-centred methods (such as the finite element method) when it comes to domain decomposition parallelisation: each node (cell-centre) is uniquely located on one CPU core domain. As a result, duplication of nodal data at processor-to-processor boundaries is not required. In contrast, in the finite element method, nodes (vertices) that lie on a processor-to-processor boundary are present on at least two processor domains, requiring the use of *ghost elements* or similar data duplication techniques. A final point related to parallelisation is the debate around open-source vs commercial software, which equally affects both finite volume and finite element methods. For many, the current *per-CPU-core* pricing of some well known commercial codes may in fact be the greatest practical obstacle to parallel efficiency.

**Higher order discretisations** Apart from the size of the finite element solid mechanics community, arguably the next greatest advantage of the finite element method over the finite volume method is its straight-forward extension to higher-order discretisation. A key feature of the finite element method is that an element is completely characterised by the coordinates and degrees of freedom associated with its nodes/vertices [412]. This compact computational stencil allows uncomplicated inclusion of higher-order local distributions. As noted previously, higher-order finite volume approaches have been developed for solid mechanics [203], however, as the order increases,

so does the size of the computational stencil; this introduces significant challenges for unstructured polyhedral grids, and as such, higher-order schemes are not as common as in the finite element field.

For linear analyses, the power of higher-order schemes is undeniable, notwithstanding challenges with locking behaviour, however, for nonlinear analysis such higher order schemes are not commonly used in practice. For example, considering an elasto-plastic analysis, as noted by Belytschko et al. [408], the stress may have discontinuous derivatives at the surface separating elastic and plastic material. In this case, the errors in Gaussian quadrature of an element that contains an elastic-plastic interface are likely to be large; higher-order quadrature is not a solution as it often leads to stiff behaviour or locking. Additionally, finite element users are typically recommended to use lower order formulations for problems that include either contact, large strains or plasticity [413].

**Discontinuous Galerkin methods** The standard *continuous* Bubnov-Galerkin finite element method, as presented above, assumes a continuous distribution of the displacement between elements. In contrast, as shown in Figure 24, the finite volume method *typically* assumes discontinuous jumps in the displacement field at the interfaces between cells (although it does not have to). There is, however, a class of finite element approaches known as discontinuous Galerkin methods, introduced by Reed and Hill [428], which assume similar jumps in the solution field across element boundaries. In this way, the local integration method adopted by the discontinuous Galerkin method combines features of the finite volume and finite element methods. In particular, discontinuous Galerkin schemes bare the following desirable finite volume properties [429]:

- They produce mass matrices that are block-diagonal;
- They easily handle irregular meshes with hanging nodes;
- They are locally conservative, which is a property that is a critical property for computational fluid dynamics applications.

In addition, a potential advantage of discontinuous Galerkin schemes over finite volume schemes is their ease of extension to higher orders, and the mixing of lower and higher order elements.

Discontinuous Galerkin methods are, however, typically implemented using explicit solution algorithms. The reason they are less suitable for implicit implementations (and analysis of quasi-static type problems) is they possess large numbers of globally-coupled degrees of freedom. To overcome this disadvantage, the so-called *hybridisable* discontinuous Galerkin (HDG) method was introduced by Cockburn et al. [430]. The key characteristic of the hybridisable form was defining *traces* of field variables as single values at cell interfaces, allowing a significant reduction in the number of global unknowns. Detailed analysis of the HDG method is outside the scope of the current article and readers are referred to recent articles on the application of HDG to solid mechanics [431–434].

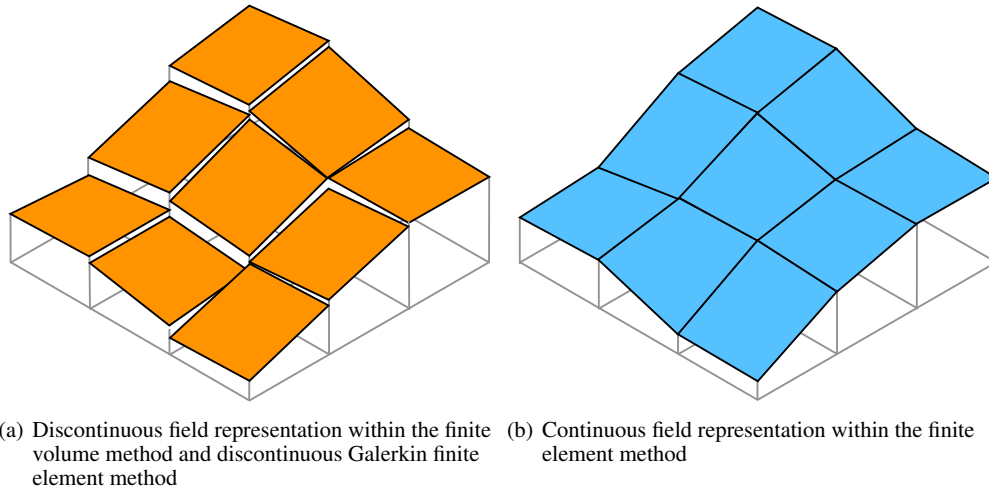


Figure 24. A comparison between the representation of the displacement field in the finite volume method (and discontinuous Galerkin finite element method) and the finite element method (adapted from Lee et al. [27])

## 5. APPLICATIONS OF THE FINITE VOLUME METHOD FOR COMPUTATIONAL SOLID MECHANICS

Some of the main areas where finite volume methods have been applied to solid mechanics are summarised below, including example images.

### 5.1. Fluid-solid interaction

Example cases are shown in Figure 25, and examples references include: [29, 94, 96, 98, 99, 113, 120, 121, 138–140, 142–145, 147, 149, 152–160, 162, 164, 199, 208, 216, 239, 249, 268, 271, 272, 274–277, 277–280, 310, 435–469];

### 5.2. Fracture and adhesive joints

Example cases are shown in Figure 26, and examples references include: [84, 119–132, 140, 381, 447, 458, 459, 470–502];

### 5.3. Microstructure analysis

Example cases are shown in Figure 27, and examples references include: [38, 49, 340–346, 348–355, 494–496, 498, 499, 503–560];

### 5.4. Metal forming and casting

Example cases are shown in Figure 28, and examples references include: [30, 44, 46, 47, 50, 51, 51–54, 110, 135–137, 276, 281, 285–287, 332, 335, 337, 386, 387, 389, 390, 392, 561–569];

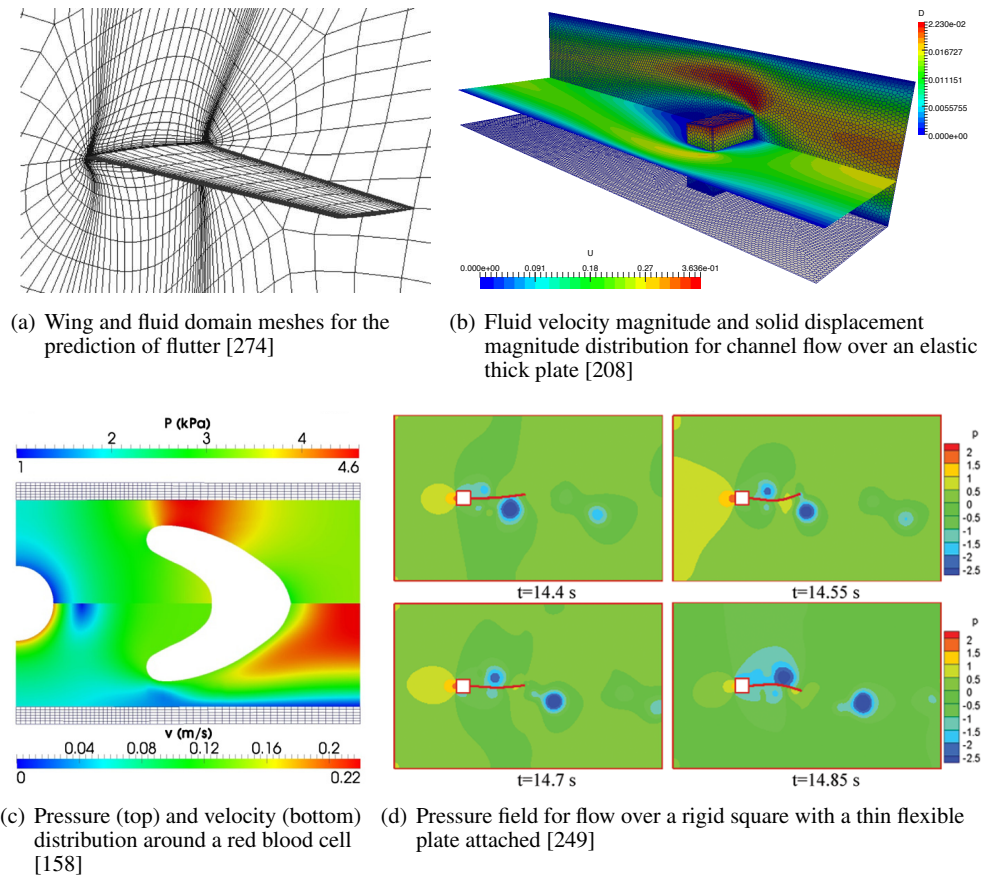


Figure 25. Fluid-solid interaction examples

### 5.5. Biomechanics

Example cases are shown in Figure 29, and examples references include: [60, 102, 105, 138, 156, 158, 196, 259, 278, 338, 419, 422, 456, 460, 466, 467, 570–589].

### 5.6. Screw compressors

Example cases are shown in Figure 30, and examples references include: [147, 148, 151–153, 161, 590–596];

### 5.7. Geomechanics and poroelasticity

Example cases are shown in Figure 31, and examples references include: [78, 80–82, 84, 149, 308–314, 597].

## 6. SOFTWARES EMPLOYING THE FINITE VOLUME METHOD FOR SOLID MECHANICS

A number of software have, or previously have, implemented versions of the finite volume method for solid mechanics; these software, in alphabetical order, include:

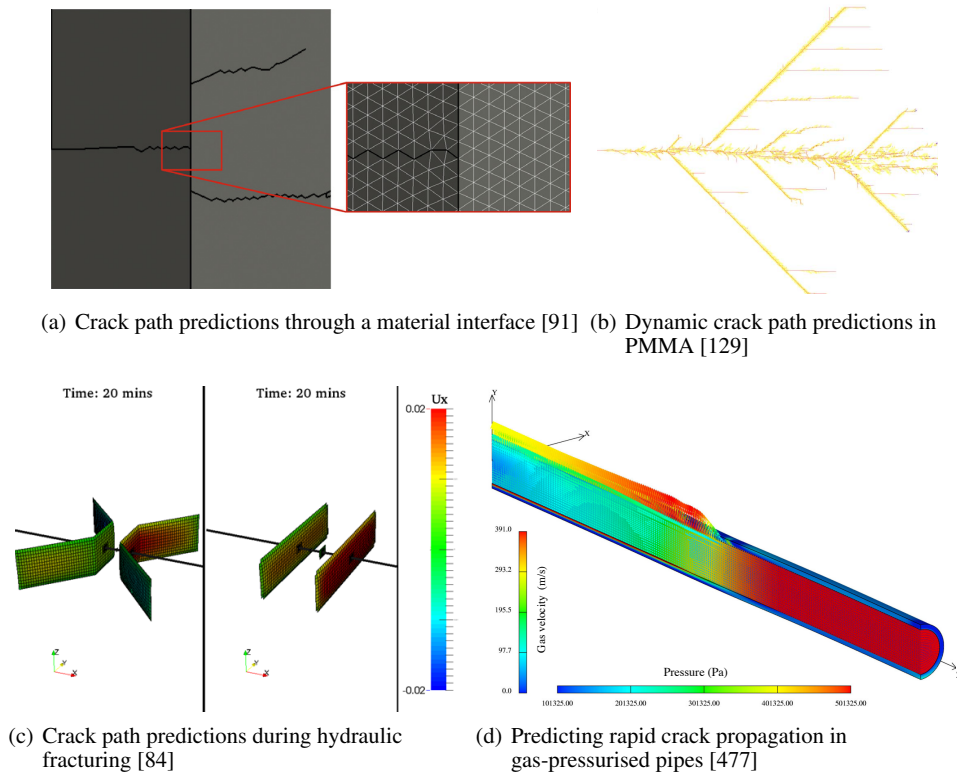


Figure 26. Fracture and adhesive joint examples

- COMET / STAR-CD (commercial software) [29, 41, 44, 46, 57, 58, 95, 97, 100, 120, 136, 137, 147, 148, 151–153, 161, 197, 201, 590–595, 598, 599];
- FOAM / OpenFOAM (open-source software) [25, 28, 30, 77, 78, 80, 83, 84, 88, 91, 94, 96, 98, 99, 101, 104, 105, 113, 140, 155, 156, 158–160, 162, 164, 193, 194, 196, 208, 447, 451, 452, 458, 459, 463, 464, 468, 469, 489, 491–495, 498, 555, 584];
- GTEA (in-house software) [298];
- MulPhys (in-house software) [260];
- NASIR (in-house software) [502, 600–608];
- PHOENICS (commercial software) [13–15, 17, 316–322];
- PHYSICA (in-house software) [241, 265–267, 609];
- TRANSPORE (in-house software) [294].

## 7. CONCLUSIONS AND CHALLENGES

The various finite volume approaches to solid mechanics can be seen to share many similarities, and in fact can all be described in a general unified manner (Section 3.5). When comparing the finite volume approach with the finite element approach, the likenesses are clear: both approaches adopt the same general strategy to discretise space into cells/elements, both use similar data storage structures, and both follow similar approaches to assemble their corresponding characteristic

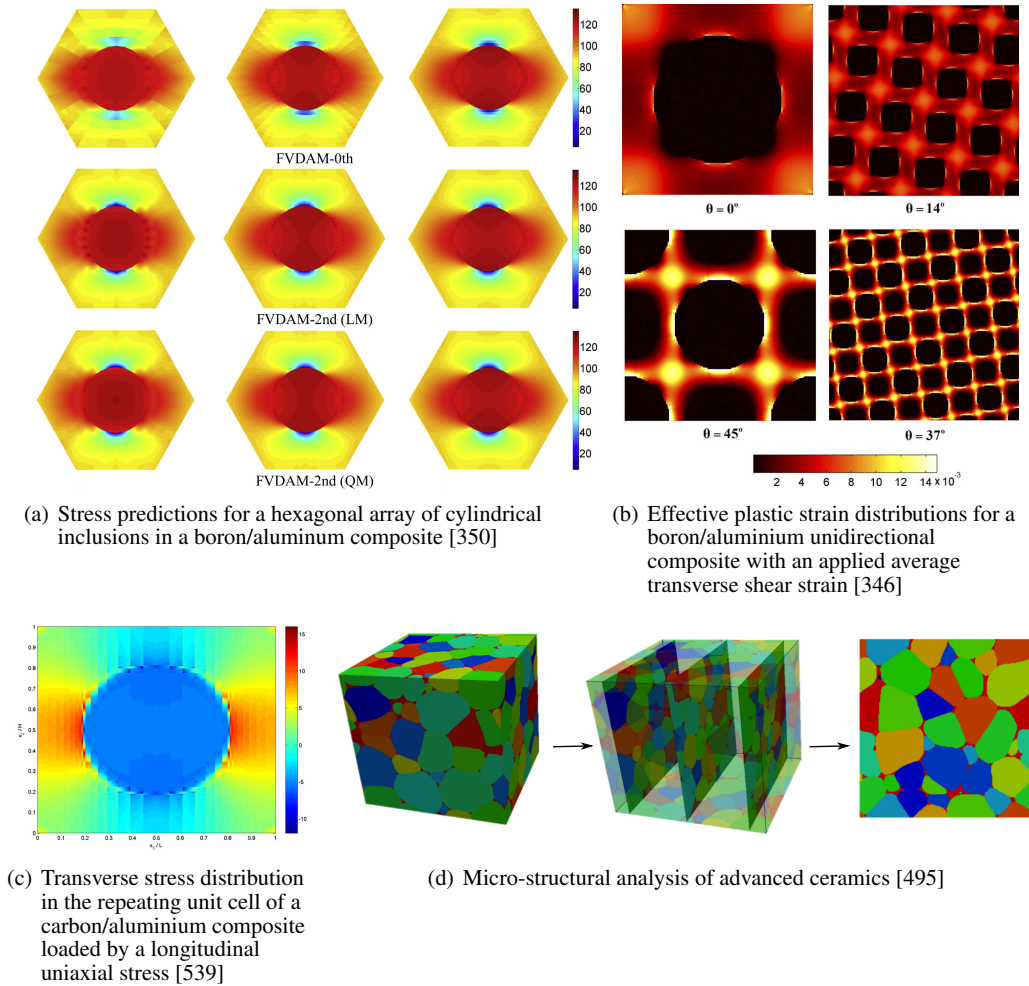


Figure 27. Microstructure analysis examples

matrices. The main differences lie in how the local integration domains are constructed, how the local integration is performed, and their fundamental philosophy: finite volume approaches are rooted in balance laws, where the governing equation is enforced by summing forces/fluxes acting on a control volume; in contrast, finite element methods adopt a more mathematical approach, based on variational methods, where the weak form of the governing equation is imposed in a volumetrically-averaged sense.

To end this article, we state three main challenges we see for the development of finite volume solid mechanics, such that its strengths and weaknesses may be rigorously explored in the context of solid mechanics, and its merits, relative to other similar approaches, may become clear to the computational solid mechanics community at large:

#### 1. Awareness:

Three decades after the first contributions to the field, there is still a general lack of awareness around the capabilities of the finite volume method in the sphere of solid mechanics; consequently, in the worst case, prestigious journals inadvertently assign inappropriate reviewers, reviewers who, having only limited knowledge of the area, accept poor or reject

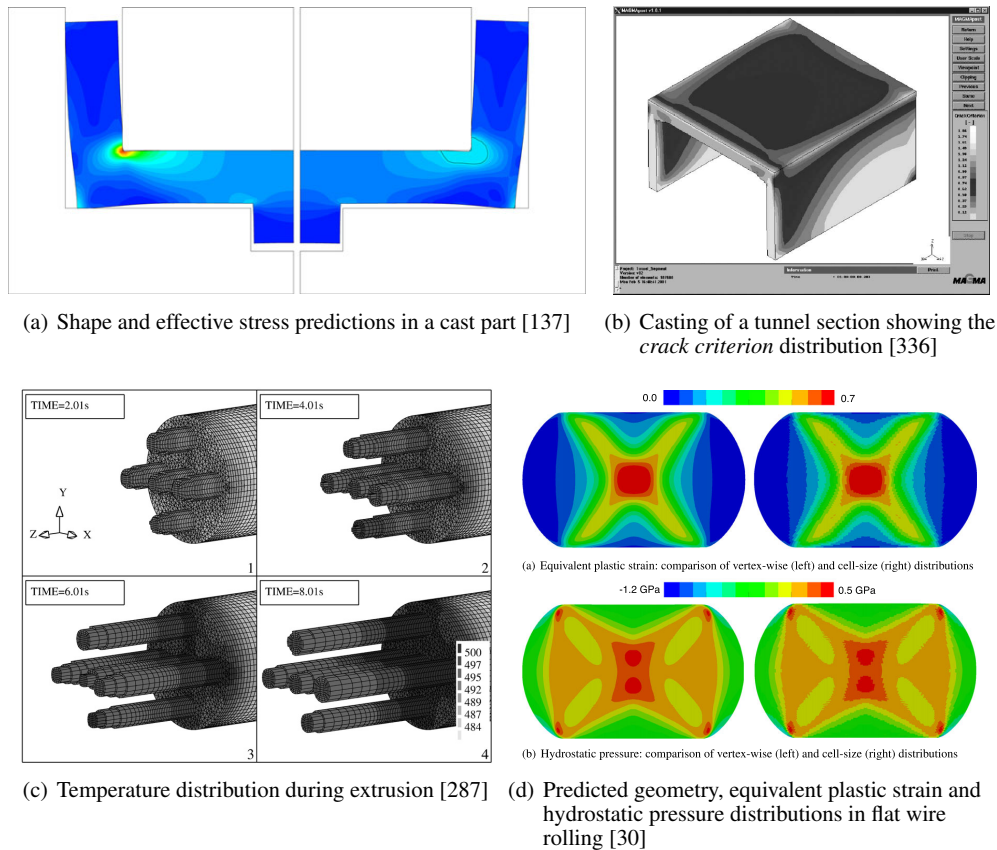


Figure 28. Metal forming and casting examples

good articles, for example, see [35], and authors are unaware of major developments in the field when surveying the literature.

## 2. Benchmarking:

As should be clear from this review, numerous differing finite volume formulations are possible; although some variants have been developed specifically for specialised applications, the comparison of the differing approaches on standard benchmarks is rare. Without such comparisons, in terms of efficiency, accuracy and robustness, it will not be possible to determine which approaches are optimal for certain classes of problems. Furthermore, given the trends in modern computing, the suitability of proposed approaches for execution on large-scale distributed memory clusters (>1000s CPU cores) should be further explored. Simulations using hundreds of millions of cells are commonplace at CFD conferences: clearly finite volume-based solid mechanics procedures have great potential. Similarly, finite volume variants should be benchmarked against alternative approaches, such as the finite element method, to determine relative merits, not just on academic standard cases but on complex industrial cases to test robustness. Processes such as *round robin* benchmarking series, for example [610], may offer one solution.

## 3. Code dissemination:

Where possible, code for published procedures should be shared for academic scrutiny: such

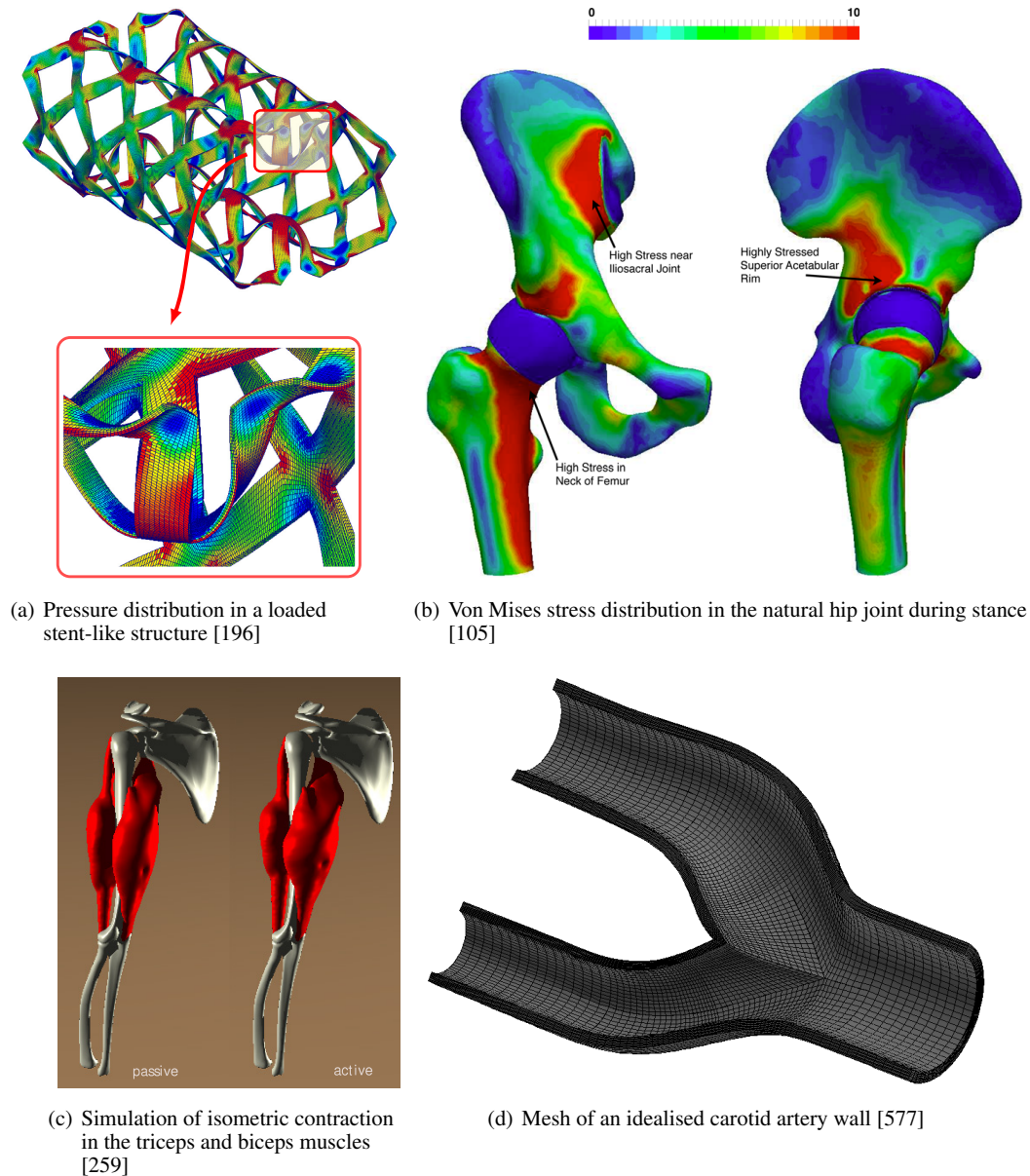


Figure 29. Biomechanics examples

distribution has the potential to: (a) accelerate academic progress, as others learn from and build on methods, as well as aiding in the discovery and resolution of errors; (b) facilitate ease of understanding and ease of implementation; (c) allow direct comparison of methods; (d) provide insight into the algorithm intricacies that may not be clear from academic articles; and (e) allow faster integration into commercial software and industrial use.

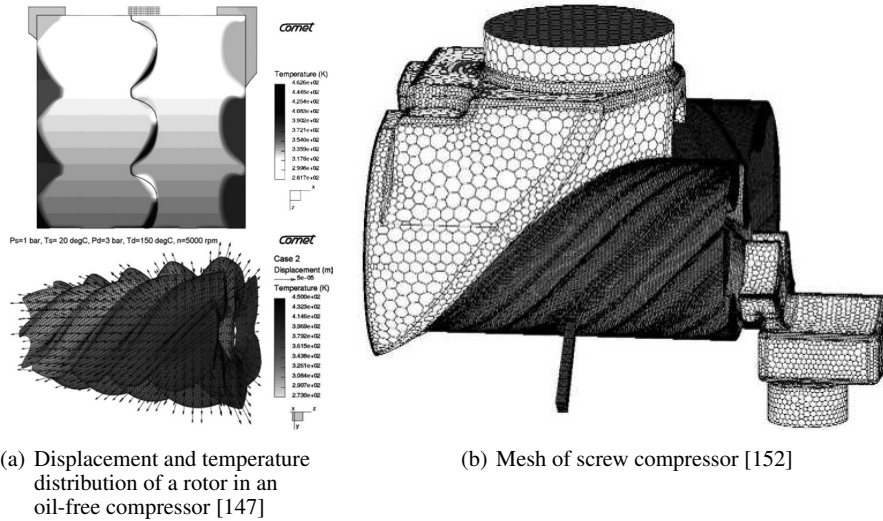


Figure 30. Screw compressor examples

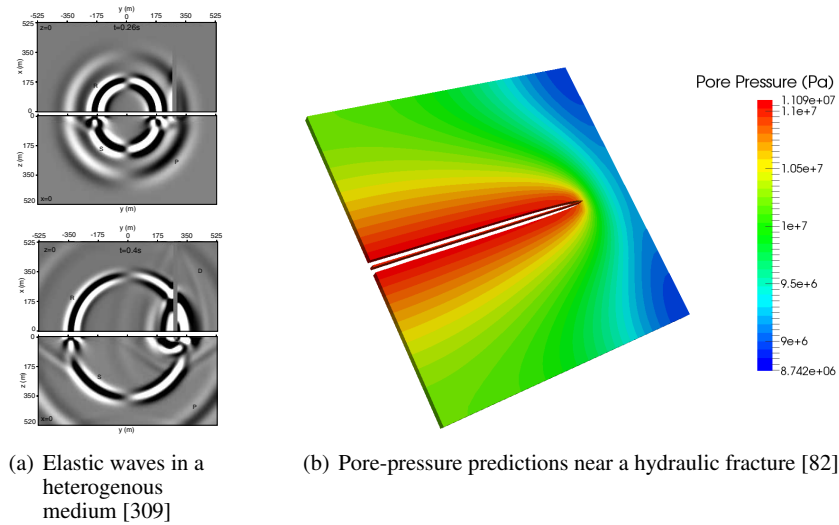


Figure 31. Geomechanics and poroelasticity examples

### A. APPENDIX A: TABLE OF MOST CITED ARTICLES RELATED TO THE FINITE VOLUME METHOD FOR SOLID MECHANICS

Table I lists the most cited articles related to the finite volume method for solid mechanics; the references have been listed in order of decreasing number of citations, and only articles with greater than fifty citations have been included, according to Google Scholar citations on 25<sup>th</sup> August 2018. As noted in the body of the article, care should be taken when interpreting the data, as the number of citations may not be directly proportional to impact on the field; for example, Weller et al. [193] has by far the greatest number of citations; however, a significant percentage of its received citations are related to its computational fluid mechanics developments, rather than its solid mechanics contributions.

Reference	Formulation-type	Number of citations
Weller et al. [193]	cell-centred	1988
Demirdžić and Muzaferija [29]	cell-centred	408
Idelsohn and Oñate [11]	vertex-centred and cell-centred	221
Demirdžić and Muzaferija [41]	cell-centred	189
Jasak and Weller [194]	cell-centred	185
Pindera et al. [352]	HFGMC/HOTFGM/FVDAM	185
Demirdžić and Martinović [3]	cell-centred	172
Bailey and Cross [24]	vertex-centred	143
Oñate et al. [12]	vertex-centred and cell-centred	128
Fryer et al. [5]	vertex-centred	103
Slone et al. [272]	vertex-centred	101
Slone et al. [273]	vertex-centred	97
Bansal and Pindera [346]	HFGMC/HOTFGM/FVDAM	94
Voller [611]	vertex-centred	91
Bijelonja et al. [97]	cell-centred	87
Taylor et al. [251]	vertex-centred	86
Cavalcante et al. [520]	HFGMC/HOTFGM/FVDAM	80
Taylor et al. [241]	vertex-centred	70
Khatam and Pindera [532]	HFGMC/HOTFGM/FVDAM	70
Fallah et al. [255]	vertex-centred	64
Ivanković et al. [119]	cell-centred	61
Karač et al. [132]	cell-centred	59
Taylor et al. [289]	vertex-centred	58
Bailey et al. [267]	vertex-centred	57
Slone et al. [274]	vertex-centred	56
Murphy and Ivanković [128]	cell-centred	55
Tuković and Jasak [112]	cell-centred	54
Demirdžić et al. [197]	cell-centred	52
Bailey et al. [264]	vertex-centred	51

Table I. Most cited articles related to the finite volume method for solid mechanics from Google Scholar citations on 25<sup>th</sup> August 2018. Approaches for heterogeneous periodic microstructures are indicated by HFGMC/HOTFGM/FVDAM.

## B. APPENDIX B: OVERVIEW OF THE DISCRETISATION USED IN HOTFGM/HFGMC/FVDAM APPROACHES

There are a variety of related methods with finite volume attributes which have been designed for the analysis of heterogenous microstructures. The related methods include the *higher-order theory for functionally graded material* (HOTFGM) [340], the *high-fidelity generalised method of cells* (HFGMC) [341–344], and the *finite volume direct averaging micromechanics* (FVDAM) theory

[345, 346]. A brief summary of the methods is given here, and readers are referred to Aboudi et al. [340], Bansal and Pindera [346] and Cavalcante et al. [38] for further details.

The HOTFGM and HFGMC approaches start by spatially discretising the solution domain into rectangular so-called *generic cells*, which are further split into a second discretisation level containing four rectangular sub-cells (Figure 32); for brevity and clarity, the description here has been limited to two dimensions; however, the approaches have been extended to three dimensions, as described in Aboudi et al. [340]. As a consequence of the assumed orthogonal Cartesian mesh, curved interfaces between material phases are approximated in a castellated *staircase* manner, as shown in Figure 32; this limitation was later removed by the FVDAM approach with extension to unstructured quadrilateral meshes. By considering the unit cell of a periodic material, the

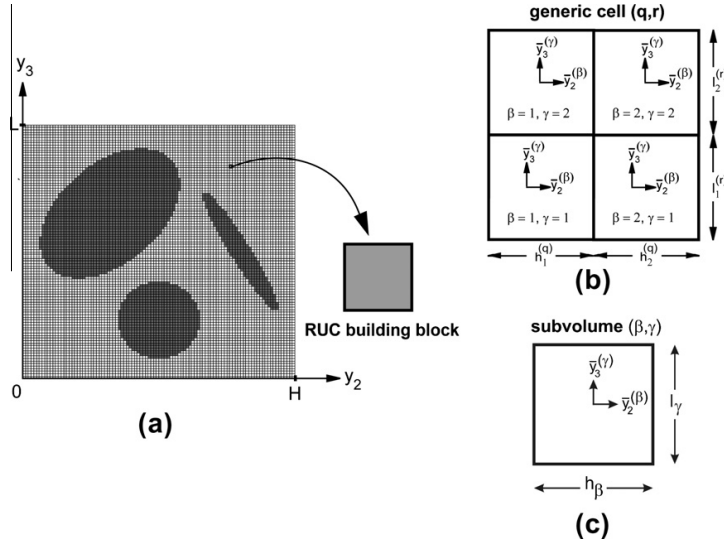


Figure 32. (a) Unit cell of a periodic material with microstructure discretised into rectangular building blocks. (b) Two-level discretisation employed by HFGMC into  $(q, r)$  generic cells further subdivided into four  $(b, c)$  subcells. (c) Single-level discretisation employed in the FVDAM theory into stand-alone  $(b, c)$  sub-volumes. Figure taken from Cavalcante et al. [38]

displacement field can be decomposed into average and fluctuating components,  $\mathbf{u} = \bar{\mathbf{u}} + \mathbf{u}'$ , where the average displacement is determined from the specified macroscopic average strains,  $\bar{\mathbf{u}} = \bar{\boldsymbol{\epsilon}}\mathbf{x}$ . Within each sub-cell, the fluctuating displacement is then assumed to vary quadratically as a function of the local coordinates,  $\bar{y}_2$  and  $\bar{y}_3$ :

$$\mathbf{u}'(\bar{y}_2, \bar{y}_3) = \mathbf{W}_{00} + \bar{y}_2 \mathbf{W}_{10} + \bar{y}_3 \mathbf{W}_{01} + \frac{1}{2} \left( 3\bar{y}_2^2 - \frac{h^2}{4} \right) \mathbf{W}_{20} + \frac{1}{2} \left( 3\bar{y}_3^2 - \frac{l^2}{4} \right) \mathbf{W}_{02} \quad (82)$$

where  $h$  and  $l$  are the width and height respectively of the sub-cell;  $\mathbf{W}_{00}$ ,  $\mathbf{W}_{10}$ ,  $\mathbf{W}_{01}$ ,  $\mathbf{W}_{20}$ , and  $\mathbf{W}_{02}$  are unknown vector displacement coefficients, each with three components; the  $\mathbf{W}_{00}$  component corresponds to the unknown displacement at the centre of the sub-cell, while the remaining coefficients correspond to higher-order displacement contributions within the sub-cell. Accordingly, there are  $5 \times 3 = 15$  unknown displacement coefficients within each sub-cell and hence  $4 \times 15 = 60$  within each generic cell; in three dimensions, there are 168 unknown quantities. For brevity here, the  $(\gamma)$  and  $(\beta)$  superscripts indicating the sub-cell have been dropped *i.e.*  $\bar{y}_2 = \bar{y}_2^{(\beta)}$ ,  $\bar{y}_3 = \bar{y}_3^{(\gamma)}$ , *etc.* It is also worth pointing out that although the approach has been developed

for periodic microstructures, the method can also be used for general structural stress analysis by assuming the average displacement  $\bar{\mathbf{u}}$  to be zero.

To determine the unknown displacement coefficients, the  $0^{th}$ ,  $1^{st}$  and  $2^{nd}$  *moments* of momentum conservation are applied to each sub-cell, in addition to the enforcement of traction and displacement continuity between sub-cells and generic cells, and inclusion of boundary conditions. A characteristic of the method, which is not possessed by the other finite volume variants, is the enforcement of these so-called *moments* of the governing equation. To achieve this, the governing equation (Equation 1), where temporal and body force terms have been neglected, is written in terms of a so-called stress moment  $\mathbf{S}$ :

$$\oint_{\Gamma} \mathbf{n} \cdot \mathbf{S} \, d\Gamma = \mathbf{0} \quad (83)$$

with the stress moment is defined as:

$$\mathbf{S} = \frac{1}{hl} \int_{-\frac{h}{2}}^{\frac{h}{2}} \int_{-\frac{l}{2}}^{\frac{l}{2}} [\boldsymbol{\sigma} \bar{y}_2^m \bar{y}_3^n] \, d\bar{y}_2 \, d\bar{y}_3 \quad (84)$$

The exponents  $m$  and  $n$  indicate the order of the equation; for example, when  $m = n = 0$ , the relation reduces to conservation of force; when  $m = 1$  and  $n = 1$  the relation represents conservation of angular momentum; while for  $m > 1$  and  $n > 1$  the relation represents conservation of higher stress moments. Note:  $m$  is not related to the time-step counter in Equation 4.

In this way, it is possible to assemble a system of  $60N$  algebraic equations of the standard form,  $[\mathbf{K}][\mathbf{U}] = [\mathbf{F}]$ , where  $N$  is the number of generic cells in the solution domain,  $[\mathbf{U}]$  is a vector of unknown displacement coefficients  $\mathbf{W}$ , the global stiffness matrix  $[\mathbf{K}]$  is a function of the sub-cell dimensions and mechanical properties, and the global force vector  $[\mathbf{F}]$  contains contributions from boundary condition and nonlinear material stresses. The linear system is inverted to give the displacements distributions within the sub-cells.

The HOTFGM and HFGMC approaches described above provide the basis for the subsequent FVDAM approach; the FVDAM approach differs from the HOTFGM and HFGMC methods in a number of ways:

- (a) The two-level spatial domain decomposition (generic cells and sub-cells) of the HOTFGM/HFGMC methods is replaced by one-level of discretisation/cells;
- (b) The displacement coefficients within each cell  $\mathbf{W}$  are expressed in terms of surface-averaged displacements *i.e.* displacement averaged at each cell surface;
- (c) Higher order moments of the equilibrium equation are not used;
- (d) In the parametric form of the FVDAM, the use of parametric mapping with a parent/reference cell allows the use of an unstructured mesh (similar to the finite element method), instead of the orthogonal Cartesian mesh of the HOTFGM/HFGMC approaches (see Figure ??);
- (e) In the assembled system of algebraic equations  $[\mathbf{K}][\mathbf{U}] = [\mathbf{F}]$ , the solution vector  $[\mathbf{U}]$  contains cell surface-averaged displacements, as opposed to sub-cell displacement coefficients.

Further technicals details of the HOTFGM, HFGMC and FVDAM methods can be found in Cavalcante et al. [38], Aboudi et al. [340], Aboudi [341], Aboudi et al. [342], Haj-Ali and Aboudi [343, 344], Bansal and Pindera [345, 346] and Cavalcante and Pindera [350].

## REFERENCES

- [1] A. K. Runchal. Tributes to an exceptional life: D. Brian Spalding, 9 January 1923 - 27 November 2016. Available at: [https://www.astfe.org/doc/Brian\\_Spalding-Tributes\\_to\\_an\\_Exceptional\\_Life.pdf](https://www.astfe.org/doc/Brian_Spalding-Tributes_to_an_Exceptional_Life.pdf), 2017.
- [2] I. Demirdžić, D. Martinović, and A. Ivanković. Numerical simulation of thermal deformation in welded workpiece. *Zavarivanje*, 31:209–219, 1988. In Croatian. English translation available at [https://www.researchgate.net/profile/Alojz\\_Ivankovic/publication/296148474\\_Numerical\\_simulation\\_of\\_thermal\\_deformation\\_in\\_welded\\_workpiece/links/5d07642ba6fdcc39f12219eb/Numerical-simulation-of-thermal-deformation-in-welded-workpiece.pdf](https://www.researchgate.net/profile/Alojz_Ivankovic/publication/296148474_Numerical_simulation_of_thermal_deformation_in_welded_workpiece/links/5d07642ba6fdcc39f12219eb/Numerical-simulation-of-thermal-deformation-in-welded-workpiece.pdf).
- [3] I. Demirdžić and D. Martinović. Finite volume method for thermo-elasto-plastic stress analysis. *Computer Methods in Applied Mechanics and Engineering*, 109:331–349, 1993.
- [4] C. Bailey, Y.D. Fryer, M. Cross, and P. Chow. Predicting the deformation of castings in moulds using a control volume approach on unstructured meshes. In M. Cross, J. F. T. Pittman, and R. D. Wood., editors, *Mathematical modelling for materials processing : based on the proceedings of a conference on Mathematical Modelling of Materials Processing, organized by the Institute of Mathematics and its Applications*, University of Bristol, September, 1991.
- [5] Y. D. Fryer, C. Bailey, M. Cross, and C.-H. Lai. A control volume procedure for solving the elastic stress-strain equations on an unstructured mesh. *Applied Mathematical Modelling*, 15: 639–645, 1991.
- [6] O. C. Zienkiewicz and E. Oñate. Finite volumes vs finite elements: Is there really a choice? *Nonlinear Computational Mechanics. State of the Art*, pages 240–254, 1991.
- [7] M. Cross, C. Bailey, P. Chow, and K. Peircleous. Towards an integrated control volume unstructured mesh code for the simulation of all macroscopic processes involved in shape casting. In R. D. Wood Chenot and O. C. Zienkiewicz, editors, *Numerical Methods in Industrial Processes NUMIFORM 92*, pages 787–792, Rotterdam, 1992. Belkema.
- [8] E. Oñate, M. Cervera, and O. C. Zienkiewicz. A study of the finite volume format for structural mechanics. Technical report, Internal Report Publication No. 15, CIMNE, Barcelona, 1992.
- [9] M. Cross. Development of novel computational technique for the next generation of software tools for casting simulation. In L. Katgerman T.S Piwonka, V.R. Voller, editor, *Modelling of Casting, Welding and Advanced Solidification Processes VI, TMS*, pages 115–126, 1993.

- [10] Y. D. Fryer, C. Bailey, M. Cross, and P. Chow. Predicting micro-porosity in shape casting using an integrated control volume unstructured mesh framework. In V. R. Voller T.S. Pivonka and L. Katgerman, editors, *Modelling of Casting, Welding and Advanced Solidification Processes VI*, pages 143–152, 1993.
- [11] S. R. Idelsohn and E. Oñate. Finite volumes and finite elements: Two ‘good friends’. *International Journal for Numerical Methods in Engineering*, 37:3323–3341, 1994.
- [12] E. Oñate, M. Cervera, and O. C. Zienkiewicz. A finite volume format for structural mechanics. *International Journal for Numerical Methods in Engineering*, 37:181–201, 1994.
- [13] S. B. Beale and S. R. Elias. Numerical solution of two-dimensional elasticity problems by means of a SIMPLE-based finite-difference scheme. Technical report, Institute for Mechanical Engineering, National Research Council, Ottawa, Ont. TR-LT-020 (NRC No. 32090), 1990.
- [14] S. B. Beale and S. R. Elias. Stress distribution in a plate subject to uniaxial loading. *PHOENICS Journal of Computational Fluid Dynamics*, 3(3):255–287, 1990.
- [15] K. M. Bukhari, H. Q. Qin, and D. B. Spalding. Progress report (to Rolls-Royce Ltd) on the calculation of thermal stresses in bodies of revolution. Technical report, CHAM Ltd, 1990.
- [16] J. H. Hattel and P. N. Hansen. FDM solutions of the thermoelastic equations using a staggered grid. In *Danish-German-Polish Workshop on Application of Computer Methods in Practice*, Warsaw, Poland, Oct. 1990.
- [17] K. M. Bukhari, I. S. Hamill, H. Q. Qin, and D. B. Spalding. Stress-analysis simulations in PHOENICS. Technical report, CHAM Ltd, 1991.
- [18] J. H. Hattel. Analysis of thermal induced stresses in die molds. In J. T. Cross Lacaze, M. Rappaz, G. Sciama, and I. Svensson, editors, *Examples of European Expertise in the Computer Simulation of Solidification and Casting*. B–18, Ecole de Mines, Nancy, France, 1992.
- [19] J. H. Hattel, P. N. Hansen, and L. F. Hansen. Analysis of thermal induced stresses in die casting using a novel control volume technique. In V. R. Voller T.S. Pivonka and L. Katgerman, editors, *Modelling of Casting, Welding and Advanced Solidification Processes VI, TMS*, pages 585–592, Palm Coast, Florida, USA, 1993.
- [20] R. Sevilla, M. Giacomini, and A. Huerta. A face-centred finite volume method for second-order elliptic problems. *International Journal for Numerical Methods in Engineering*, 0: 1–29, 2018.
- [21] R. Sevilla, M. Giacomini, and A. Huerta. A locking-free face-centred finite volume (FCFV) method for linear elasticity. *preprint*, 2018. arXiv:1806.07500v1 [math.NA], available at: <https://arxiv.org/pdf/1806.07500>.
- [22] M. Ebrahimnejad, N. Fallah, and A. R. Khoei. New approximation functions in the meshless finite volume method for 2D elasticity problems. *Engineering Analysis with Boundary Elements*, 46:10–22, 2014.

- [23] N. Fallah and M. Delzendeh. Free vibration analysis of laminated composite plates using meshless finite volume method. *Engineering Analysis with Boundary Elements*, 88:132–144, 2018.
- [24] C. Bailey and M. Cross. A finite volume procedure to solve elastic solid mechanics problems in three dimensions on an unstructured mesh. *International Journal for Numerical Methods in Engineering*, 38:1757–1776, 1995.
- [25] P. Cardiff, Tuković, H. Jasak, and A. Ivanković. A block-coupled finite volume methodology for linear elasticity and unstructured meshes. *Computers & Structures*, 175:100–122, 2016. doi: 10.1016/j.compstruc.2016.07.004.
- [26] G. Kluth and B. Després. Discretization of hyperelasticity on unstructured mesh with a cell-centered Lagrangian scheme. *Journal of Computational Physics*, 229:9092–9118, 2010.
- [27] C. H. Lee, A. J. Gil, and J. Bonet. Development of a cell centred upwind finite volume algorithm for a new conservation law formulation in structural dynamics. *Computers & Structures*, 118:13–38, 2013.
- [28] J. Haider, C. H. Lee, A. J. Gil, and J. Bonet. A first order hyperbolic framework for large strain computational solid dynamics: An upwind cell centred total Lagrangian scheme. *International Journal for Numerical Methods in Engineering*, 109:407–456, 2017.
- [29] I. Demirdžić and S. Muzafertija. Numerical method for coupled fluid flow, heat transfer and stress analysis using unstructured moving meshes with cells of arbitrary topology. *Computer Methods in Applied Mechanics and Engineering*, 125:235–255, 1995.
- [30] P. Cardiff, Tuković, P. De Jaeger, M. Clancy, and A. Ivanković. A Lagrangian cell-centred finite volume method for metal forming simulation. *International journal for numerical methods in engineering*, 109(13):1777–1803, 2016. doi: 10.1002/nme.5345.
- [31] M. Aguirre, A. J. Gil, J. Bonet, and A. A. Carre no. A vertex centred finite volume Jameson-Schmidt-Turkel (JST) algorithm for a mixed conservation formulation in solid dynamics. *Journal of Computational Physics*, 259:672 – 699, 2014. ISSN 0021-9991. doi: 10.1016/j.jcp.2013.12.012. URL <http://www.sciencedirect.com/science/article/pii/S0021999113008115>.
- [32] R. LeVeque. *Finite Volume Methods for Hyperbolic Problems*. Cambridge University Press, 2004.
- [33] B. R. Baliga and N. Atabaki. *Control-Volume-Based Finite-Difference and Finite-Element Methods*, chapter 6, pages 191–224. Wiley-Blackwell, 2009. ISBN 9780470172599. doi: 10.1002/9780470172599.ch6. URL <https://onlinelibrary.wiley.com/doi/abs/10.1002/9780470172599.ch6>.
- [34] R. Courant, K. Friedrichs, and H. Lewy. On the partial difference equations of mathematical physics. *Mathematische Annalen*, 100:32–74, 1928.

- [35] I. Demirdžić. On the discretization of the diffusion term in finite-volume continuum mechanics. *Numerical Heat Transfer, Part B: Fundamentals: An International Journal of Computation and Methodology*, 68:1:1–10, 2015. doi: 10.1080/10407790.2014.985992.
- [36] K. Maneeratana. *Development of the finite volume method for non-linear structural applications*. PhD thesis, Imperial College London, 2000.
- [37] M. Vaz Jr., P. A. Mu noz Rojas, and G. Filippini. On the accuracy of nodal stress computation in plane elasticity using finite volumes and finite elements. *Computers & Structures*, 87: 1044–1057, 2009.
- [38] M. A. A. Cavalcante, M.-J. Pindera, and H. Khatam. Finite-volume micromechanics of periodic materials: Past, present and future. *Composites Part B: Engineering*, 43:2521–2543, 2012.
- [39] N. J. Van Eck and L. Waltman. VOS: a new method for visualizing similarities between objects. In *Advances in Data Analysis: Proceedings of the 30<sup>th</sup> Annual Conference of the German Classification Society*, pages 299–306. Springer, 2007.
- [40] J. A. Trangenstein and P. Colella. A higher-order Godunov method for modeling finite deformation in elastic-plastic solids. *Communications on Pure and Applied Mathematics*, 44:41–100, 1991.
- [41] I. Demirdžić and S. Muzaferija. Finite volume method for stress analysis in complex domains. *International Journal for Numerical Methods in Engineering*, 37:3751–3766, 1994.
- [42] N. Dioh, A. Ivanković, P. Leever, and J. G. Williams. The high strain rate behaviour of polymers. *Journal de Physique IV*, 04 (C8), 1994. doi: 10.1051/jp4:1994818. C8-119-C8-124.
- [43] C. J. Rente and P. J. Oliveira. Extension of a finite volume method in solid stress analysis to cater for non-linear elasto-plastic effects. In J.L. Tassoulas, editor, *Proceedings of EM 14<sup>th</sup> Engineering Mechanics Conference*, University of Texas at Austin, USA, 2000.
- [44] A. Teskeredžić, I. Demirdžić, and S. Muzaferija. Numerical method for heat transfer, fluid flow, and stress analysis in phase-change problems. *Numerical Heat Transfer, Part B: Fundamentals*, 42:437–459, 2002.
- [45] A. Teskeredžić. *Application of the Finite Volume Method to Casting Problems*. PhD thesis, University of Sarajevo, 2004.
- [46] H. Bašić, I. Demirdžić, and S. Muzaferija. Finite volume method for simulation of extrusion processes. *International Journal for Numerical Methods in Engineering*, 62:475–494, 2005.
- [47] M. M. Martins, J. D. Bressan, S. T. Button, and A. Ivanković. Extrusion process by finite volume method using OpenFOAM software. In Y. Chastel Chinesta and M. El Mansori, editors, *International Conference on Advances in Material and Processing Technologies - AMPT2010*, pages 1461–1466. American Institute of Physics, Paris, France, 2010.

- [48] J. D. Bressan, M. M. Martins, and M. Vaz Jr. Stress evolution and thermal shock computation using the finite volume method. *Journal of Thermal Stresses*, 33:533–558, 2010.
- [49] M. Leonard, N. Murphy, A. Karač, and A. Ivanković. A numerical investigation of spherical void growth in an elastic-plastic continuum. *Computational Materials Science*, 64:38–40, 2012.
- [50] J. D. Bressan, M. M. Martins, and S. T. Button. Analysis of aluminium hot extrusion by finite volume method. *Materials Today: Proceedings*, 2(10, Part A):4740–4747, 2015.
- [51] M. M. Martins, J. D. Bressan, and S. T. Button. Analysis of aluminum extrusion in a 90° die by finite volume method. *Advanced Materials Research*, 1135:153–160, 2016.
- [52] M. M. Martins, J. D. Bressan, and S. T. Button. Finite volume analysis with the maccormack method applied to metal flow in forward extrusion. *Universal Journal of Mechanical Engineering*, 5:1–8, 2017.
- [53] P. Cardiff, T. Tang, Z. Tukovic, H. Jasak, A. Ivankovic, and P. De Jaeger. An Eulerian-inspired Lagrangian finite volume method for wire drawing simulations. In *IUTAM Symposium on Multi-scale Fatigue, Fracture and Damage of Materials in Harsh Environments*, Galway, Ireland, 2017. National University of Ireland Galway.
- [54] J. D. Bressan, M. M. Martins, and S. T. Button. Analysis of metal extrusion by the finite volume method. *Procedia Engineering*, 207:425–430, 2017.
- [55] K. Zarrabi and A. Basu. An axisymmetric finite volume formulation for creep analysis. *Journal of the Mechanical Behavior of Materials*, 10:325–340, 1999.
- [56] K. Zarrabi and A. Basu. A finite volume element formulation for solution of elastic axisymmetric pressurized components. *International Journal of Pressure Vessels and Piping*, 77:479–484, 2000.
- [57] E. Džuferović, A. Ivanković, and I. Demirdžić. Finite volume modelling of linear viscoelastic deformation. In *Proceedings of 3<sup>rd</sup> Congress of Croatian Society of Mechanics*, Dubrovnik, Croatia, 2000.
- [58] I. Demirdžić, E. Džuferović, and A. Ivanković. Finite-volume approach to thermoviscoelasticity. *Numerical Heat Transfer, Part B: Fundamentals*, 47:213–237, 2005.
- [59] S. Das, S. R. Mathur, and J. Y. Murthy. Finite-volume method for creep analysis of thin RF MEMS devices using the theory of plates. *Numerical Heat Transfer, Part B: Fundamentals*, 61:71–90, 2012.
- [60] A. Safari, Ž. Tuković, P. Cardiff, M. Walter, E. Casey, and A. Ivanković. Interfacial separation of a mature biofilm from a glass surface—a combined experimental and cohesive zone modelling approach. *Journal of the mechanical behavior of biomedical materials*, 54: 205–218, 2016.

- [61] I. Demirdžić, A. Ivanković, D. Martinović, and S. Muzaferija. Numerical method for solving linear and non-linear solid body problems. In *Proceedings of 1<sup>st</sup> Congress of Croatian Society of Mechanics*, Pula, Croatia, 1994.
- [62] I. Demirdžić. Finite volumes in solid mechanics. In *NAFEMS ASME Seminar - Alternative Strategies in Computational Mechanics*, London, February 1996.
- [63] H. Osman, S. Ahmad, and K. A. Arshad. A one-dimensional simulation of an electrofusion welding process. *International Conference on Modeling, Simulation and Applied Optimization (ICMSAO)*, 4:1–5, 2011.
- [64] H. G. D. Junior, C. R. Xavier, J. A. de Castro, M. F. Campos, A. A. Palmeira, and A. F. Habibe. Mathematical modeling and experimental investigation of the stress evolution at the steel welding. *Cadernos UniFOA*, 8:59–66, 2013.
- [65] K. S. Bibin and A. Ramarajan. Unstructured finite volume approach for 3-D unsteady thermo-structural analysis using bi-conjugate gradient stabilized method. *International Journal of Innovative Research in Science Engineering and Technology*, 2:1389–1400, 2013.
- [66] D. Martinović and I. Horman. Numerical simulation of clay bricks drying process. In *II Meunarodni nauno-struni skup Proizvodnja i prerada nemetalnih mineralnih sirovina i njihova primjena u industriji*, Zenica, Bosnia and Herzegovina, 1998. In Bosnian.
- [67] I. Demirdžić, I. Horman, and D. Martinović. Finite volume analysis of stress and deformation in hygro-thermo-elastic orthotropic body. *Computer Methods in Applied Mechanics and Engineering*, 190:1221–1232, 2000.
- [68] D. Martinović and I. Horman. Drying induced stresses in clay bricks an hygro-thermo-elastic model. In *International scientific and expert symposium Nonmetal Inorganic Materials*, pages 249–257, Zenica, Bosnia-Herzegovina, 2000.
- [69] D. Martinović, I. Horman, and I. Demirdžić. Numerical and experimental analysis of wood drying process. *Wood Science and Technology*, 35:143–156, 2001.
- [70] D. Martinović. *A numerical method for analysis of thermo-deformational processes during the welding*. PhD thesis, University of Sarajevo, 2002. In Bosnian.
- [71] I. Horman, D. Martinović, and S. Hajdarević. Numerical analysis of a phenomena in the wood caused by heat. In *Moisture or External Load, in: Proceedings of International scientific conference: Challenges in forestry and wood technology in the*, volume 21, pages 31–34, University of Zagreb, Faculty of Forestry, Zageb, 2008.
- [72] D. Martinović, I. Horman, and S. Hajdarević. Stress distribution in wooden corner joints. *Strojarstvo*, 50:193–204, 2008.
- [73] I. Horman, D. Martinović, and S. Hajdarević. Finite volume method for analysis of stress and strain in wood. *Drvna industrija*, 60:27–32, 2009.
- [74] I. Horman, S. Hajdarević, D. Martinović, and N. Vukas. Numerical analysis of stress and strain in a wooden chair. *Drvna industrija*, 61:151–158, 2010.

- [75] I. Horman, D. Martinović, I. Bijelonja, and S. Hajdarević. Wood subjected to hygro-thermal and/or mechanical loads. In *Finite Volume Method - Powerful Means of Engineering Design*. Finite Volume Method - Powerful Means of Engineering Design, R. Petrova (ed) 5, 2012.
- [76] R. Fu. *Thermo-Mechanical Coupling for Ablation*. PhD thesis, University of Kentucky, 2018.
- [77] T. Holzmann, A. Ludwig, and P. Raninger. Yield strength prediction in 3D during local heat treatment of structural A356 alloy components in combination with thermal-stress analysis. *Lambotte G., Lee J., Allanore A., Wagstaff S. (eds) Materials Processing Fundamentals. The Minerals, Metals & Materials Series*, 2018.
- [78] T. Tang, O. Hededal, and P. Cardiff. On finite volume method implementation of poro-elasto-plasticity soil model. *International journal for numerical and analytical methods in geomechanics*, 39:1410–1430, 2015. doi: 10.1002/nag.2361.
- [79] E. C. Bryant, J. Hwang, and M. M. Sharma. Arbitrary fracture propagation in heterogeneous poroelastic formations using a finite volume-based cohesive zone model. In *SPE Hydraulic Fracturing Technology Conference*, The Woodlands, Texas, February, 2015.
- [80] P. Cardiff, R. Manchanda, E. C. Bryant, D. Lee, A. Ivanković, and M. M. Sharma. Simulation of fractures in OpenFOAM: From adhesive joints to hydraulic fractures. In *10<sup>th</sup> OpenFOAM Workshop*, University of Michigan, Ann Arbor, MI, USA, 2015.
- [81] P. Cardiff, R. Manchanda, E. C. Bryant, A. Ivanković, and M. M. Sharma. Finite volume method for the simulation of hydraulic fractures. In *Joint Symposium of Irish Mechanics Society & Irish Society for Scientific & Engineering Computation Advances in Mechanics*, University College Dublin, Dublin, Ireland, 2015.
- [82] D. Lee, P. Cardiff, E. C. Bryant, R. Manchanda, H. Wang, and A. M. M. Sharma. New model for hydraulic fracture growth in unconsolidated sands with plasticity and leak-off. *SPE Annual Technical Conference and Exhibition*, pages 28–30, September 2015. 18174818-MS.
- [83] H. Elsafti and H. Oumeraci. A numerical hydro-geotechnical model for marine gravity structures. *Computers and Geotechnics*, 79:105 – 129, 2016. doi: 10.1016/j.compgeo.2016.05.025.
- [84] R. Manchanda, E. C. Bryant, P. Bhardwaj, P. Cardiff, and M. M. Sharma. Strategies for effective stimulation of multiple perforation clusters in horizontal wells. *SPE*, preprint:28–30, December 2017. doi: 10.2118/179126-PA.
- [85] M. Asadollahi. Finite volume method for poroelasticity. Master’s thesis, Delft University of Technology, 2017.
- [86] J. Fainberg and H. J. Leister. Finite volume multigrid solver for thermo-elastic stress analysis in anisotropic materials. *Computer Methods in Applied Mechanics and Engineering*, 137: 167–174, 1996.
- [87] I. Horman. *Finite volume method for analysis of timber drying*. PhD thesis, University of Sarajevo, 1999. In Bosnian.

- [88] P. Cardiff, A. Karač, and A. Ivanković. A large strain finite volume method for orthotropic bodies with general material orientations. *Computer Methods in Applied Mechanics and Engineering*, 268:318–335, 2014. doi: 10.1016/j.cma.2013.09.008.
- [89] A. Golubović, I. Demirdžić, and S. Muzaferija. Finite volume analysis of laminated composite plates. *International Journal for Numerical Methods in Engineering*, 109(11): 1607–1620, 2017. ISSN 1097-0207. doi: 10.1002/nme.5347. URL 10.1002/nme.5347.
- [90] Ž. Tuković, A. Ivanković, and A. Karač. Finite-volume stress analysis in multi-material linear elastic body. *International Journal for Numerical Methods in Engineering*, 93:400–419, 2012.
- [91] D. Carolan, Ž. Tuković, N. Murphy, and A. Ivanković. Arbitrary crack propagation in multi-phase materials using the finite volume method. *Computational Materials Science*, 69:153–159, 2013.
- [92] P. Cardiff. *Development of the Finite Volume Method for Hip Joint Stress Analysis*. PhD thesis, University College Dublin, 2012. URL [https://www.researchgate.net/publication/262772501\\_Development\\_of\\_the\\_Finite\\_Volume\\_Method\\_for\\_Hip\\_Joint\\_Stress\\_Analysis](https://www.researchgate.net/publication/262772501_Development_of_the_Finite_Volume_Method_for_Hip_Joint_Stress_Analysis).
- [93] C. J. Greenshields, H. G. Weller, and A. Ivanković. The finite volume formulation for fluid structure interaction. In R. Vilsmeier Haenel and F. Benkhaldoun, editors, *Finite Volumes for Complex Applications, II - Problems and Perspectives*, pages 467–474. Hermes Science, 1999.
- [94] C. J. Greenshields, H. G. Weller, and A. Ivanković. The finite volume method for coupled fluid flow and stress analysis. *Computer Modeling and Simulation in Engineering*, 4:213–218, 1999.
- [95] I. Bijelonja, I. Demirdžić, and S. Muzaferija. A finite volume method for large strain analysis of incompressible hyperelastic materials. *International Journal for Numerical Methods in Engineering*, 64:1594–1609, 2005.
- [96] C. J. Greenshields and H. G. Weller. A unified formulation for continuum mechanics applied to fluid-structure interaction in flexible tubes. *International Journal for Numerical Methods in Engineering*, 64:1575–1593, 2005.
- [97] I. Bijelonja, I. Demirdžić, and S. Muzaferija. A finite volume method for incompressible linear elasticity. *Computer Methods in Applied Mechanics and Engineering*, 195:6378–6390, 2006.
- [98] C. G. Giannopapa and G. Papadakis. New formulations of the dynamic equations of elastic solids suitable for a unified methodology for fluid-structure interaction problems. *Computer Methods in Applied Mechanics and Engineering*, 2006.
- [99] C. G. Giannopapa and G. Papadakis. Linear stability analysis and application of a new solution method of the elastodynamic equations suitable for a unified fluid-structure-interaction approach. *ASME Journal Pressure Vessels Technology*, 130:31303–1, 2008.

- [100] I. Bijelonja, I. Demirdžić, and S. Muzaferija. Mixed finite volume method for linear thermoelasticity at all Poisson's ratios. *Numerical Heat Transfer, Part A: Applications*, 72: 215–235, 2017.
- [101] H. Jasak and H. G. Weller. Finite volume methodology for contact problems of linear elastic solids. In *Proceedings of 3<sup>rd</sup> Congress of Croatian Society of Mechanics*, pages 253–260, Dubrovnik, Croatia, 2000.
- [102] P. Cardiff, A. Karač, R. Flavin, D. FitzPatrick, and A. Ivanković. Contact stress analysis in OpenFOAM - application to hip joint bones. In *OpenFOAM Workshop, Penn State University*, Penn State, PA, USA, 2011.
- [103] P. Cardiff, A. Karač, and A. Ivanković. Development of a finite volume methodology for linear elastic contact problems. In *21<sup>st</sup> International Workshop on Computational Mechanics of Materials, IWCMM, Limerick*, Limerick, Ireland, 2011.
- [104] P. Cardiff, A. Karač, and A. Ivanković. Development of a finite volume contact solver based on the penalty method. *Computational Materials Science*, 64:283 – 284, 2012.
- [105] P. Cardiff, A. Karač, D. FitzPatrick, R. Flavin, and A. Ivanković. Development of a hip joint model for finite volume simulations. *Journal of Biomechanical Engineering*, 136:1–8, 2014. doi: 10.1115/1.4025776.
- [106] K. Maneeratana and A. Ivanković. Finite volume method for structural applications involving material and geometrical non-linearities. In *European Council of Computational Mechanics Technische Universität München, Proceedings of the European Conference on Computational Mechanics (ECCM'99)*, pages 874–875, 1999.
- [107] K. Maneeratana and A. Ivanković. Finite volume method for geometrically non-linear stress analysis applications. In *Proceedings of the Seventh Annual Conference of the Association for Computational Mechanics in Engineering (ACME'1999)*, 1999.
- [108] K. Maneeratana and A. Ivanković. Finite volume method for large deformation with linear hypoelastic materials. In R. Vilsmeier and F. Benkhaldoun, editors, *Second International Symposium on Finite Volumes for Complex Applications (FVCA II) for Complex Applications II: Problems and Perspectives*, pages 459–466, University Duisburg, Germany, 1999. Hermes Science Publication.
- [109] K. Maneeratana and A. Ivanković. Modelling of high strain rate behaviour of a series 7108 aluminium alloy. In *Proceedings of the 14<sup>th</sup> Conference of the Mechanical Engineering Network of Thailand*, pages 227–233, 2000.
- [110] H. Bašić. *Application of the finite volume method to the analysis of plastic metal flow in extrusion technologies*. PhD thesis, University of Sarajevo, 2002. In Bosnian.
- [111] I. Bijelonja. *Finite volume method for incremental analysis of small and large thermo-elasto-plastic deformations*. PhD thesis, University of Sarajevo, 2002. In Bosnian.

- [112] Ž. Tuković and H. Jasak. Updated Lagrangian finite volume solver for large deformation dynamic response of elastic body. *Transactions of FAMENA*, 31:55–70, 2007.
- [113] Ž. Tuković and H. Jasak. FVM for fluid-structure interaction with large structural displacements. In *2<sup>nd</sup> OpenFOAM Workshop*, Zagreb, Croatia, 2007.
- [114] P. Cardiff, A. Karač, Ž. Tuković, and A. Ivanković. Development of a finite volume based structural solver for large rotation of non-orthogonal meshes. In *7<sup>th</sup> OpenFOAM Workshop*, Darmstadt, Germany, 2012.
- [115] P. Cardiff, A. Karač, Z. Tuković, and A. Ivanković. An open-source finite method for computational solid mechanics. In *Joint Symposium of Irish Mechanics Society and Irish Society for Scientific and Engineering Computation*, University College Dublin, Dublin, Ireland, 2013.
- [116] P. Cardiff, Ž. Tuković, A. Karač, and A. Ivanković. Nonlinear solid mechanics in OpenFOAM. In *9<sup>th</sup> OpenFOAM Workshop*, University of Zagreb, Croatia, 2014.
- [117] Q. Liu, P.-J. Ming, and W.-P. Zhang. Research on the nonlinear finite volume numerical method for the large rotating of disk. *Journal of Harbin Engineering University*, 39:1012–1018, 2018.
- [118] A. Ivanković, I. Demirdžić, J. G. Williams, and P. S. Leever. A new numerical method for analysing dynamic fracture problems. In *ESIS Symposium on Impact and Dynamic Fracture of Polymers and Composites*, Potro Cervo, Sardinia, Italy, 1993.
- [119] A. Ivanković, I. Demirdžić, J. G. Williams, and P. S. Leever. Application of the finite volume method to the analysis of dynamic fracture problems. *International Journal of Fracture*, 66:357–371, 1994.
- [120] A. Ivanković, S. Muzaferija, and I. Demirdžić. Finite volume method and multigrid acceleration in modelling of rapid crack propagation in full-scale pipe test. *Computational Mechanics*, 20:46–52, 1997.
- [121] A. Ivanković and G. P. Venizelos. Rapid crack propagation in plastic pipe: Predicting full-scale critical pressure from S4 test results. *Engineering Fracture Mechanics*, 59:607–622, 1998.
- [122] A. Ivanković. Finite volume modelling of dynamic fracture problems. *Computer Modelling and Simulation in Engineering*, 4:227–235, 1999.
- [123] A. Ivanković and S. Hillmansen. Evoluton of dynamic fractures in PMMA. *Plastics, Rubber and Composites*, 30:88–93, 2001.
- [124] V. Stylianou and A. Ivanković. Finite volume analysis of dynamic fracture phenomena I: A node release methodology. *International Journal of Fracture*, 113:107–123, 2002.
- [125] V. Stylianou and A. Ivanković. Finite volume analysis of dynamic fracture phenomena II: A cohesive zone type methodology. *International Journal of Fracture*, 113:125–151, 2002.

- [126] A. Ivanković and J. G. Williams K. C. Pandya. Crack growth predictions in polyethylene using measured traction-separation curves. *Engineering Fracture Mechanics*, pages 657–668, 2004.
- [127] A. Rager, J. G. Williams, and A. Ivanković. Numerical analysis of the three point bend impact test for polymers. *International Journal of Fracture*, 135(1-4):199–215, 2005.
- [128] N. Murphy and A. Ivanković. The prediction of dynamic fracture evolution in PMMA using a cohesive zone model. *Engineering Fracture Mechanics*, 72:861–875, 2005.
- [129] N. Murphy, M. Ali, and A. Ivanković. Dynamic crack bifurcation in PMMA. *Engineering Fracture Mechanics*, 73(16):2569–2587, 2006.
- [130] V. Tropša, I. Georgiou, A. Ivanković, A. J. Kinloch, and J. G. Williams. OpenFOAM in non-linear stress analysis: modelling of adhesive joints. In *1<sup>st</sup> OpenFOAM Workshop, Zagreb, Croatia*, 2006.
- [131] Ž. Tuković. Arbitrary crack propagation model in OpenFOAM, . Technical report, Faculty of Mechanical Engineering and Naval Architecture, University of Zagreb, in association with the School of Mechanical and Materials Engineering, University College Dublin, 2010.
- [132] A. Karač, B. R. K. Blackman, V. Cooper, A. J. Kinloch, S. Rodriguez Sanchez, W. S. Teo, and A. Ivanković. Modelling the fracture behaviour of adhesively-bonded joints as a function of test rate. *Engineering Fracture Mechanics*, 78:973–989, 2011.
- [133] A. Ivanković, V. Tropša, and J. G. Williams. Finite volume modelling of residual stresses in cast plastic slabs. In *Fifth international conference on residual stresses ICRS-5*, pages 392–399, Linköping Sweden, 1997.
- [134] V. Tropša, A. Ivankovic, and J. G. Williams. Predicting residual stresses due to solidification in cast plastic plates. *Plastics, Rubber and Composites*, 29(9):468–474, 2000. doi: 10.1179/146580100101541319. URL <https://doi.org/10.1179/146580100101541319>.
- [135] A. Sato, I. Ohnaka, and J. Iwane. Stress analysis by finite volume method for prediction of porosity and deformation defects of spheroidal graphite castings. *Journal of Japan Foundry Engineering Society*, 78:231–237, 2006. In Japanese.
- [136] A. Teskeredžić, I. Demirdžić, and S. Muzaferija. Numerical method for calculation of complete casting process - part I: Theory. *Numerical Heat Transfer, Part B: Fundamentals: An International Journal of Computation and Methodology*, 68:295–316, 2015.
- [137] A. Teskeredžić, I. Demirdžić, and S. Muzaferija. Numerical method for calculation of complete casting process - part II: Validation and application. *Numerical Heat Transfer, Part B: Fundamentals: An International Journal of Computation and Methodology*, 68:317–335, 2015.
- [138] F. S. Henry and M. W. Collins. A novel predictive model with compliance for arterial flows. *BED-Vol. 26, Advances in Bioengineering, ASME*, 1993.

- [139] F. S. Henry and M. W. Collins. Prediction of transient wall movement of an incompressible elastic tube using finite volume procedure. In *Proceedings of BIOMED93*, Bath, UK, 1993.
- [140] C. J. Greenshields, G. P. Vanizelos, and A. Ivanković. A fluid-structure model for fast brittle fracture in plastic pipes. *Journal of Fluids and Structures*, 14:221–234, 2000.
- [141] A. Ivanković, A. Karač, E. Dendrinis, and K. Parker. Blood flow in deformable arteries: The finite volume method for fluid-structure interaction problem. In *Proceedings of the 9<sup>th</sup> ACME Conference on Computational Mechanics in Engineering*, Birmingham, UK, 2001.
- [142] M. Schäfer and I. Teschauer. Numerical simulation of coupled fluid-solid problems. *Computer Methods in Applied Mechanics and Engineering*, 190:3645–3667, 2001.
- [143] M. Schäfer, I. Teschauer, L. Kadinski, and M. Selder. A numerical approach for the solution of coupled fluid-solid and thermal stress problems in crystal growth processes. *Computational Materials Science*, 24:409–419, 2002.
- [144] A. Ivanković, A. Karač, E. Dendrinis, and K. Parker. Towards early diagnosis of arterosclerosis: The finite volume method for fluid-structure interaction. *Biorheology*, 39: 401–407, 2002.
- [145] M. Torlak and S. Muzaferija. Finite volume approach to computation of elastic plates and their interaction with fluid flows. In *Finite Volumes for Complex Applications III - Problems and Perspectives*. Kogan Page Science, 2002.
- [146] M. Torlak, S. Muzaferija, and M. Perić. Application of a finite volume method to the computation of interaction between thin linearly elastic structures and incompressible fluid flows. In *VDI-Berichte 1862, VDI Tagung Fluid-Struktur-Wechselwirkung, Wiesloch*, 2002.
- [147] A. Kovačević, N. Stošić, I. K. Smith, and A. Numerical. A numerical study of fluid - solid interaction in screw compressors. *International Journal on Computer Application in Technology*, 21:148–158, 2004. doi: 10.1504/IJCAT.2004.006651.
- [148] N. Stošić, I. Smith, and A. Kovačević. *Screw Compressors*. Springer, Berlin, 2005.
- [149] G. Shaw and T. Stone. Finite volume methods for coupled stress/fluid flow in commercial reservoir simulations. In *SPE Reservoir Simulation Symposium, Houston, Texas*, 2005. SPE 93430.
- [150] M. Torlak. *A Finite-Volume Method for Coupled Numerical Analysis of Incompressible Fluid Flow and Linear Deformation of Elastic Structures*. PhD thesis, Technischen Universitaet Hamburg-Harburg, 2006.
- [151] A. Kovačević, N. Stošić, and I. K. Smith. Numerical simulation of combined screw compressor-expander machines for use in high pressure refrigeration systems. *Simulation Modelling Practice and Theory*, 14:1143–1154, 2006.
- [152] A. Kovačević, N. Stošić, E. Mujić, and I. K. Smith. CFD integrated design of screw compressors. *Journal of Engineering Applications of Computational Fluid Mechanics*, 1: 96–108, 2007.

- [153] N. Stošić, I. Smith, and A. Kovačević. Screw compressors. *Three Dimensional Computational Fluid Dynamics and Solid Fluid Interaction, Springer, Berlin*, 2007.
- [154] G. Papadakis. A novel pressure-velocity formulation and solution method for fluid-structure interaction problems. *Journal of Computational Physics*, 227:3383–3404, 2008.
- [155] H. Jasak, A. Jemcov, and Ž. Tuković. OpenFOAM: A C++ library for complex physics simulations. In *International Workshop on Coupled Methods in Numerical Dynamics*, Dubrovnik, Croatia, 2007.
- [156] V. Kanyanta, A. Ivanković, and A. Karač. Validation of a fluid-structure interaction numerical model for predicting flow transients in arteries. *Journal of Biomechanics*, 42:1705–1712, 2009.
- [157] P. Jagad, B. P. Puranik, and A. W. Date. A finite volume procedure on unstructured meshes for fluid-structure interaction problems. *World Academy of Science, Engineering and Technology International Journal of Mechanical, Aerospace, Industrial Mechatronic and Manufacturing Engineering*, 5:1406–1412, 2011.
- [158] W. Wiedemair, Ž. Tuković, H. Jasak, D. Poulidakos, and V. Kurtcuoglu. On ultrasound-induced microbubble oscillation in acapillary blood vessel and its implications for the blood-brain barrier. *Physics in Medicine & Biology*, 57:1019–1045, 2012.
- [159] C. Habchi, S. Russeil, D. Bougeard, J.-L. Harion, T. Lemenand, A. Ghanem, D. Della Valle, and H. Peerhossaini. Partitioned solver for strongly coupled fluid-structure interaction. *Computers & Fluids*, 71:306–319, 2013.
- [160] Ž. Tuković, P. Cardiff, A. Ivanković, and A. Karač. OpenFOAM library for fluid structure interaction. In *9<sup>th</sup> OpenFOAM Workshop, Zagreb, Croatia, Zagreb, Croatia*, 2014.
- [161] I. Smith, N. Stošić, and A. Kovačević. *Power Recovery From Low Grade Heat Sources by the Use of Screw Expanders*. Chandos Publishing, 2014.
- [162] B. Šekutkovski, I. Kostić, A. Simonović, P. Cardiff, and V. Jazarević. Three-dimensional fluid-structure interaction simulation with a hybrid RANS-LES turbulence model for applications in transonic flow domain. *Aerospace Science and Technology*, 49:1 – 16, 2016.
- [163] P. Jagad. A numerical procedure for elastic solids. *GIT-Journal of Engineering and Technology*, 9:113–124, 2016.
- [164] P. Cardiff, A. Karač, P. De Jaeger, H. Jasak, J. Nagy, A. Ivanković, and Ž. Tuković. Towards the development of an extendable solid mechanics and fluid-solid interactions toolbox for OpenFOAM. In *12th OpenFOAM Workshop*, volume 12, University of Exeter, UK, 2017.
- [165] P. Jagad, B.P. Puranik, and A.W. Date. A numerical analysis of fluid-structure interaction problem with a flow channel embedded in a structural material. *Proceedings of the Indian National Science Academy*, 83:655–667, 2017.

- [166] P. Jagad, B.P. Puranik, and A.W. Date. A finite volume procedure for fluid flow, heat transfer and solid-body stress analysis. *International Journal for Computational Methods in Engineering Science and Mechanics*, April 2018. doi: 10.1080/15502287.2018.1434839.
- [167] I. Demirdžić and A. Ivanković. Finite volume approach to modelling of plates. In *Proceedings of 2<sup>nd</sup> Congress of Croatian Society of Mechanics*, pages 101–108, Brac, Croatia, 1997.
- [168] N. Fallah. A cell vertex and cell centred finite volume method for plate bending analysis. *Computer Methods in Applied Mechanics and Engineering*, 193:3457–3470, 2004.
- [169] N. Fallah. A finite volume method for plate buckling analysis. In C. A. Mota Soares et.al, editor, *III European Conference on Computational Mechanics, Solids, Structures and Coupled Problems in Engineering.*, pages 5–8, Lisbon, Portugal, 2006.
- [170] N. Fallah, F. Hatami, and A. Displacement. Formulation based on finite volume method for analysis of Timoshenko beam. In *Proceedings of the 7<sup>th</sup> international conference on civil engineering*, pages 8–10, Tehran, Iran, May 2006.
- [171] N. Fallah. On the use of shape functions in the cell centered finite volume formulation for plate bending analysis based on Mindlin-Reissner plate theory. *Computers & Structures*, 84: 1664–1672, 2006.
- [172] N. Fallah and F. Hatami. Extension of the finite volume method for instability analysis of columns with shear effects. In *Proceedings of the Eighth International Conference on Computational Structures Technology*, Stirlingshire, Scotland, 2006. Civil-Comp Press. Paper 192.
- [173] F. Hatami, N. Fallah, and S. Pourzeynali. Application of the finite volume method for shell analysis: A membrane study. In B. H. V. Topping, G. Montero, and R. Montenegro, editors, *Proceedings of the Eighth International Conference on Computational Structures Technology*. Civil-Comp Press, Stirlingshire, UK, 2006. doi: 10.4203/ccp.83.160. Paper 160.
- [174] S. Isić, V. Doleček, and I. Karabegović. A comparison between finite element and finite volume methods on the problem of stability of timoshenko beam. In *The 12th International Conference on Problems of Material Engineering*, Jasna, Slovakia, 2007. Mechanics and Design.
- [175] S. Isić, V. Doleček, and I. Karabegović. Numerical and experimental analysis of postbuckling behaviour of prismatic beam under displacement dependent loading. In *Proceedings of the First Serbian Congress on Theoretical and Applied Mechanics*, Kopaonik, Serbia, 2007.
- [176] S. Isić, V. Doleček, and I. Karabegović. A comparison of finite element and finite volume method on stability analysis of rectangular plate. In V. Doleček Karabegović and M. Jurković, editors, *I. 6<sup>th</sup> International Scientific Conference on Production Engineering, Development and Modernization of Production*, RIM Bihac, BiH, 2007.
- [177] S. Isić. *Numerical and experimental analysis of nonlinear stability phenomena in elastic systems*. PhD thesis, University of Bihac, Bosnia and Herzegovina, 2008. In Bosnian.

- [178] N. Fallah. Finite volume method for determining the natural characteristics of structures. *Journal of Engineering Science and Technology*, 8:93–106, 2013.
- [179] N. Fallah and A. Parayandeh-Shahrestany. A novel finite volume based formulation for the elasto-plastic analysis of plates. *Thin-Walled Structures*, 77:153–164, 2014.
- [180] N. Fallah and M. Ebrahimnejad. Finite volume analysis of adaptive beams with piezoelectric sensors and actuators. *Applied Mathematical Modelling*, 38:727–737, 2014.
- [181] L.-L. Jing, P.-J. Ming, W.-P. Zhang, L.-R. Fu, and Y.-P. Cao. Static and free vibration analysis of functionally graded beams by combination Timoshenko theory and finite volume method. *Composite Structures*, 138:192–213, 2016.
- [182] N. Fallah and A. Ghanbari. A displacement finite volume formulation for the static and dynamic analysis of shear deformable circular curved beams. *Scientia Iranica*, pages –, 2017. ISSN 1026-3098. doi: 10.24200/sci.2017.4259. URL [http://scientiairanica.sharif.edu/article\\_4259.html](http://scientiairanica.sharif.edu/article_4259.html).
- [183] N. Fallah, A. Parayandeh-Shahrestany, and H. Golkoubi. A finite volume formulation for the elasto-plastic analysis of rectangular Mindlin-Reissner plates, a non-layered approach. *Civil Engineering Infrastructures Journal*, 50:293–310, 2017.
- [184] B. Mohebi, A. R. Kaboudan, and O. Yazdanpanah. Damage detection in beam-like structures using finite volume method. *Journal of Rehabilitation in Civil Engineering*, 5:77–92, 2017.
- [185] N. Fallah and A. Ghanbary. A displacement finite volume formulation for the static and dynamic analysis of shear deformable curved beams. *Scientia Iranica*, 25(3):999–1014, 2018.
- [186] A. Amraei and N. Fallah. A cell-centered finite volume formulation for the calculation of stress intensity factors in Mindlin-Reissner cracked plates. *Civil Engineering Journal*, 3: 1366–1385, 2018.
- [187] Ž. Tuković, P. De Jaeger, P. Cardiff, and A. Ivanković. A finite volume solver for geometrically exact Simo-Reissner beams. In *ECCOMAS MSF 2019, Thematic conference*, Sarajevo, Bosnian and Herzegovina, 2019.
- [188] S. Das, S. R. Mathur, and J. Y. Murthy. An unstructured finite-volume method for structure-electrostatic interactions in MEMS. *Numerical Heat Transfer, Part B: Fundamentals*, 60: 425–451, 2011.
- [189] S. Das, M. Koslowski, S. R. Mathur, and J. Y. Murthy. Finite volume method for simulation of creep in RF MEMS devices. In *ASME 2011 International Mechanical Engineering Congress and Exposition: Nano and Micro Materials, Devices and Systems; Microsystems Integration*, volume 11, Denver, Colorado, USA, 2011.
- [190] N. N. Dioh, A. Ivanković, and I. Demirdžić. Dynamic thermo elastic plastic deformation of solids using finite volume technique. In E. Oñate D.R.J. Owen, editor, *Computational Plasticity, Fundamentals and Applications*, pages 1947–1957. Pineridge Press, 1995.

- [191] N. N. Diod, A. Ivanković, P. S. Leever, and J. G. Williams. Stress wave propagation effects in split hopkinson pressure bar tests. In *Proceedings of The Royal Society; Proceedings: Mathematical and Physical Sciences*, pages 187–204. 449, 1995.
- [192] L. Djapic Oosterkamp, A. Ivankovic, and G. Venizelos. High strain rate properties of selected aluminium alloys. *Materials Science and Engineering: A*, 278(1):225 – 235, 2000. ISSN 0921-5093. doi: [https://doi.org/10.1016/S0921-5093\(99\)00570-5](https://doi.org/10.1016/S0921-5093(99)00570-5). URL <http://www.sciencedirect.com/science/article/pii/S0921509399005705>.
- [193] H. G. Weller, G. Tabor, H. Jasak, and C. Fureby. A tensorial approach to computational continuum mechanics using object orientated techniques. *Computers in Physics*, 12:620–631, 1998.
- [194] H. Jasak and H. G. Weller. Application of the finite volume method and unstructured meshes to linear elasticity. *International Journal for Numerical Methods in Engineering*, 48:267–287, 2000.
- [195] C. Suvanjumrat and E. Chaichanasiri. Implementation and validation of finite volume C++ codes for plane stress analysis. In *CST02, The Second TSME*, Krabi, 2011. International Conference on Mechanical Engineering.
- [196] J. Haider, C. H. Lee, A. J. Gil, A. Huerta, and J. Bonet. An upwind cell centred total Lagrangian finite volume algorithm for nearly incompressible explicit fast solid dynamic applications. *Computer Methods in Applied Mechanics and Engineering*, 340:684–727, 2018.
- [197] I. Demirdžić, S. Muzaferija, and M. Perić. Benchmark solutions of some structural analysis problems using finite-volume method and multigrid acceleration. *International Journal for Numerical Methods in Engineering*, 40:1893–1908, 1997.
- [198] P. Cardiff, Ž. Tuković, H. Jasak, and A. A. Ivanković. Block-coupled finite volume methodology for linear elasticity. In *9<sup>th</sup> OpenFOAM Workshop*, volume 9, University of Zagreb, Croatia, 2014.
- [199] I. González, A. Naseri, J. Chiva, J. Rigola, and C. D. Pérez-Segarra. An enhanced finite volume based solver for thermoelastic materials in fluid-structure coupled problems. In *6<sup>th</sup> European Conference on Computational Mechanics (ECCM 6)*, *7<sup>th</sup> European Conference on Computational Fluid Dynamics (ECFD 7)*, Glasgow, UK, 15 June 2018.
- [200] B. L. Fowler and R. K. Yee. Application of finite volume method for solid mechanics. In *Proceedings of the ASME IMECE Conference International Mechanical Engineering Congress and RD&D Expo*, pages 15–21, November 2003. IMECE2003-44297.
- [201] I. Bijelonja. A numerical method for almost incompressible body problem. In Katalinić, editor, *Proceedings of the 22<sup>nd</sup> International DAAAM Symposium*, pages 321–322, Vienna, Austria, 2011.
- [202] P. J. Oliveira and C. J. Rente. Development and application of a finite volume method for static and transient stress analysis. In *Proceedings of NAFEMS World Congress'99 on Effective Engineering Analysis*, pages 297–309, 1999.

- [203] I. Demirdžić. A fourth-order finite volume method for structural analysis. *Applied Mathematical Modelling*, 40:3104–3114, 2016.
- [204] N. Fallah. A method for calculation of face gradients in two-dimensional cell centred finite volume formulation for stress analysis in solid problems. *Scientia Iranica*, 15:286–294, 2008.
- [205] J. M. Nordbotten. Cell-centered finite volume discretizations for deformable porous media. *International Journal for Numerical Methods in Engineering*, 100:399–418, 2014.
- [206] J. M. Nordbotten. Convergence of a cell-centered finite volume discretization for linear elasticity. *SIAM Journal on Numerical Analysis*, 53:2605–2625, 2015.
- [207] E. Keilegavlen and J. M. Nordbotten. Finite volume methods for elasticity with weak symmetry. *International Journal for Numerical Methods in Engineering*, 2017. doi: 10.1002/nme.5538.
- [208] Ž. Tuković, A. Karač, P. Cardiff, H. Jasak, and A. Ivanković. OpenFOAM finite volume solver for fluid-solid interaction. *Transactions of FAMENA*, 42(3):1–31, 2018. doi: 10.21278/TOF.42301.
- [209] N. Fallah. Finite Volume Based Formulations for the Analysis of Bernoulli and Timoshenko Beams. *Journal of Numerical Simulation in Engineering*, 1(3):259–268, Winter 2008.
- [210] A. Golubović. *Finite volume analysis of laminated composite plates*. PhD thesis, University of Sarajevo, 2017.
- [211] S. K. Godunov. A difference method for numerical calculation of discontinuous solutions of the equations of hydrodynamics. *Matematicheskii Sbornik*, 47:271–306, 1959.
- [212] S. K. Godunov. The problem of a generalized solution in the theory of quasi-linear equations and in gas dynamics. *Russian Mathematical Surveys*, 17:145–156, 1962.
- [213] J. A. Trangenstein and R. B. Pember. Numerical algorithms for strong discontinuities in elastic-plastic solids. *Journal of Computational Physics*, 103(1):63–89, 1992.
- [214] J. A. Trangenstein. Second-order Godunov algorithm for two-dimensional solid mechanics. *Computational Mechanics*, 13:343–359, 1994.
- [215] G. H. Miller and E. G. Puckett. A high-order Godunov method for multiple condensed phases. *Journal of Computational Physics*, 128:134–164, 1996.
- [216] H. Tang and F. Sotiropoulos. A second-order Godunov method for wave problems in coupled solid water gas systems. *Journal of Computational Physics*, 151:790–815, 1999.
- [217] A. Berezovski and G. A. Maugin. Simulation of thermoelastic wave propagation by means of a composite wave-propagation algorithm. *Journal of Computational Physics*, 168:249–264, 2001.
- [218] B. P. Howell and G. J. Ball. A free-Lagrange augmented Godunov method for the simulation of elastic-plastic solids. *Journal of Computational Physics*, 175:128–167, 2002.

- [219] A. Berezovski and G. A. Maugin. Simulation of wave and front propagation in thermoelastic materials with phase transformation. *Computational Materials Science*, 28:478–485, 2003.
- [220] G. Kluth and B. Després. F. V. schemes for hyperelastic-plastic models in finite deformations. In Reymard and J.-M. Hérard, editors, *Finite Volumes for Complex Applications V-Problems & Perspectives*. John Wiley & Sons, 2008.
- [221] G. Carré, S. Del Pino, B. Després, and E. Labourasse. A cell-centered Lagrangian hydrodynamics scheme on general unstructured meshes in arbitrary dimension. *Journal of Computational Physics*, 228:5160–5183, 2009.
- [222] P.-H. Maire, R. Abgrall, J. Breil, R. Loubère, and B. Rebourcet. A nominally second-order cell-centered Lagrangian scheme for simulating elastic-plastic flows on two-dimensional unstructured grids. *Journal of Computational Physics*, 235:626–665, 2013.
- [223] S. K. Sambasivan, M.-J. Shashkov, and D. E. Burton. A finite volume cell-centered lagrangian hydrodynamics approach for solids in general unstructured grids. *International Journal for Numerical Methods in Fluids*, 72:770–810, 2013.
- [224] C. D. Sijoy and Shashank Chaturvedi. An Eulerian multi-material scheme for elastic-plastic impact and penetration problems involving large material deformations. *European Journal of Mechanics - B/Fluids*, 53:85 – 100, 2015. ISSN 0997-7546. doi: 10.1016/j.euromechflu.2015.04.004. URL <http://www.sciencedirect.com/science/article/pii/S0997754615000527>.
- [225] B. Després and E. Labourasse. Angular momentum preserving cell-centered Lagrangian and Eulerian schemes on arbitrary grids. *Journal of Computational Physics*, 290:28 – 54, 2015. ISSN 0021-9991. doi: 10.1016/j.jcp.2015.02.032. URL <http://www.sciencedirect.com/science/article/pii/S0021999115001023>.
- [226] S. Ndanou, N. Favrie, and S. Gavriluk. Multi-solid and multi-fluid diffuse interface model: Applications to dynamic fracture and fragmentation. *Journal of Computational Physics*, 295:523 – 555, 2015. ISSN 0021-9991. doi: 10.1016/j.jcp.2015.04.024. URL <http://www.sciencedirect.com/science/article/pii/S0021999115002806>.
- [227] Jun-Bo Cheng, Eleuterio F. Toro, Song Jiang, Ming Yu, and Weijun Tang. A high-order cell-centered Lagrangian scheme for one-dimensional elastic-plastic problems. *Computers & Fluids*, 122:136 – 152, 2015. ISSN 0045-7930. doi: 10.1016/j.compfluid.2015.08.029. URL <http://www.sciencedirect.com/science/article/pii/S0045793015003059>.
- [228] R. Loubere, P.-H. Maire, and B. Rebourcet. Chapter 13 - staggered and colocated finite volume schemes for Lagrangian hydrodynamics. In R. Abgrall and C.-W. Shu, editors, *Handbook of Numerical Methods for Hyperbolic Problems*, volume 17 of *Handbook of Numerical Analysis*, pages 319 – 352. Elsevier, 2016. doi: 10.1016/bs.hna.2016.07.003. URL <http://www.sciencedirect.com/science/article/pii/S1570865916300059>.

- [229] W. Boscheri, M Dumbser, and R. Loubère. Cell centered direct Arbitrary-Lagrangian-Eulerian ADER-WENO finite volume schemes for nonlinear hyperelasticity. *Computers & Fluids*, 134-135:111 – 129, 2016. ISSN 0045-7930. doi: 10.1016/j.compfluid.2016.05.004. URL <http://www.sciencedirect.com/science/article/pii/S004579301630144X>.
- [230] F. Vilar, C.-W. Shu, and P.-H. Maire. Positivity-preserving cell-centered Lagrangian schemes for multi-material compressible flows: From first-order to high-orders. part I: The one-dimensional case. *Journal of Computational Physics*, 312:385 – 415, 2016. ISSN 0021-9991. doi: 10.1016/j.jcp.2016.02.027. URL <http://www.sciencedirect.com/science/article/pii/S0021999116000917>.
- [231] G. Georges, J. Breil, and P.-H. Maire. A 3D finite volume scheme for solving the updated Lagrangian form of hyperelasticity. *International Journal for Numerical Methods in Fluids*, 84(1):41–54, 2017. doi: 10.1002/flid.4336. URL <https://onlinelibrary.wiley.com/doi/abs/10.1002/flid.4336>.
- [232] T. Heuzé. Lax-Wendroff and TVD finite volume methods for unidimensional thermomechanical numerical simulations of impacts on elastic-plastic solids. *Journal of Computational Physics*, 346:369 – 388, 2017. ISSN 0021-9991. doi: 10.1016/j.jcp.2017.06.027. URL <http://www.sciencedirect.com/science/article/pii/S0021999117304722>.
- [233] Jun-Bo Cheng, Yueling Jia, Song Jiang, Eleuterio F. Toro, and Ming Yu. A second-order cell-centered Lagrangian method for two-dimensional elastic-plastic flows. *Communications in Computational Physics*, 22(5):1224–1257, 2017. doi: 10.4208/cicp.OA-2016-0173.
- [234] Jun-Bo Cheng, Weizhang Huang, Song Jiang, and Baolin Tian. A third-order moving mesh cell-centered scheme for one-dimensional elastic-plastic flows. *Journal of Computational Physics*, 349:137 – 153, 2017. ISSN 0021-9991. doi: 10.1016/j.jcp.2017.08.018. URL <http://www.sciencedirect.com/science/article/pii/S0021999117305892>.
- [235] David Fridrich, Richard Liska, and Burton Wendroff. Cell-centered Lagrangian Lax-Wendroff HLL hybrid method for elasto-plastic flows. *Computers & Fluids*, 157:164 – 174, 2017. ISSN 0045-7930. doi: 10.1016/j.compfluid.2017.08.030. URL <http://www.sciencedirect.com/science/article/pii/S0045793017303080>.
- [236] T. Heuzé. Simulation of impacts on elastic-viscoplastic solids with the flux-difference splitting finite volume method applied to non-uniform quadrilateral meshes. *Advanced Modeling and Simulation in Engineering Sciences*, 5(1):9, 2018. ISSN 2213-7467. doi: 10.1186/s40323-018-0101-z. URL [10.1186/s40323-018-0101-z](https://doi.org/10.1186/s40323-018-0101-z).
- [237] M. Aguirre, A. J. Gil, J. Bonet, and C. H. Lee. An upwind vertex centred finite volume solver for Lagrangian solid dynamics. *Journal of Computational Physics*, 300:387–422, 2015.

- [238] M. M. Selim, R. P. Koomullil, and D. R. McDaniel. Linear elasticity finite volume based structural dynamics solver. In *AIAA Modeling and Simulation Technologies Conference*, Washington, D.C., USA, June 2016. doi: 10.2514/6.2016-4418.
- [239] M. M. Selim, R. Koomullil, and D. R. McDaniel. Finite volume based fluid-structure interaction solver. In *58<sup>th</sup> AIAA/ASCE/AHS/ASC Structures, Structural Dynamics, and Materials Conference, Grapevine, Texas, 2017*.
- [240] B. R. Baliga and S. V. Patankar. A new finite-element formulation for convection-diffusion problems. *Numerical Heat Transfer, Part B: Fundamentals*, 3:4:393–409, 1980. doi: 10.1080/01495728008961767.
- [241] G. A. Taylor, C. Bailey, and M. Cross. A vertex-based finite volume method applied to non-linear material problems in computational solid mechanics. *International Journal for Numerical Methods in Engineering*, 56:507–529, 2003.
- [242] M. A. Wheel. A geometrically versatile finite volume formulation for plane elastostatic stress analysis. *The Journal of Strain Analysis for Engineering Design*, 31:111–116, 1996.
- [243] M. A. Wheel. A finite-volume approach to the stress analysis of pressurised axisymmetric structures. *International Journal of Pressure Vessels and Piping*, 68:311–317, 1996.
- [244] M. A. Wheel. Applying the finite volume approach to structural analysis. In P. E. O’Donoghue S. N. Atluri, editor, *Modelling and Simulation in Engineering*, pages 229–234. 1, 1998.
- [245] M. A. Wheel. A mixed finite volume formulation for determining the small strain deformation of incompressible materials. *International Journal for Numerical Methods in Engineering*, 44:1843–1861, 1999.
- [246] V. A. F. Costa and A. C. M. Sousa. A control volume-based fem for the solution of the three-dimensional, elastic stress-strain equations. In *WSEAS Proceedings 2<sup>nd</sup> World MCME (Mathematics & Computers in Mechanical Engineering, MCME 2000)*, Vouliagmeni, Greece, 2000.
- [247] N. Fallah. *Using shape function in cell centred finite volume formulation for two dimensional stress analysis, Lecture series on computer and computational sciences (ICCMSE 2005)*, volume 4. Brill Academic Publishers, The Netherlands, 2005.
- [248] G. H. Xia, Y. Zhao, J. H. Yeo, and X. Lv. A 3D implicit unstructured-grid finite volume method for structural dynamics. *Computational Mechanics*, 40:299–312, 2007.
- [249] Y.-Y. Tsui, Y.-C. Huang, C.-L. Huang, and S.-W. Lin. A finite-volume-based approach for dynamic fluid-structure interaction. *Numerical Heat Transfer, Part B: Fundamentals*, 64(4): 326–349, 2013. doi: 10.1080/10407790.2013.806691.
- [250] Y. Wu, X. Xie, and L. Chen. Hybrid stress finite volume method for linear elasticity problems. *International Journal of Numerical Analysis and Modeling*, 10:634–656, 2013.

- [251] G. A. Taylor, C. Bailey, and M. Cross. Solution of the elastic/visco-plastic constitutive equations: A finite volume approach. *Applied Mathematical Modelling*, 19:746–760, 1995.
- [252] W. J. Ferguson. The control volume finite element numerical solution technique applied to creep in softwoods. *International Journal of Solids and Structures*, 35:1325–1338, 1998.
- [253] J.P. Hambleton, S.W. Sloan, A.V. Pyatigorets, and V.R. Voller. Lower bound limit analysis using the control volume finite element method. In *13th International Conference of the IACMAG*, pages 88–93, Melbourne, Australia, 2011.
- [254] N. Fallah, C. Bailey, and M. Cross. Finite volume method for stress analysis. In *Proceedings ASME The 7<sup>th</sup> annual conference of the association for computational mechanics in engineering*, volume 99, pages 135–138, Durham, UK, 1999.
- [255] N. Fallah, C. Bailey, M. Cross, and G. A. Taylor. Comparison of finite element and finite volume methods application in geometrically nonlinear stress analysis. *Applied Mathematical Modelling*, 24:439–455, 2000.
- [256] N. Fallah, C. Bailey, and M. Cross. CFD approach for solid mechanics analysis. In *European Congress on Computational Methods in Applied Sciences and Engineering, ECCOMAS 2000*, Barcelona, Spain, 11-14 September 2000.
- [257] N. Fallah. *Computational stress analysis using finite volume methods*. PhD thesis, University of Greenwich, 2000.
- [258] A. K. Slone, N. Fallah, C. Bailey, and M. Cross. A finite volume approach to geometrically nonlinear stress analysis. In *Third International Symposium on Finite Volumes for Complex Applications - Problems and Perspectives*, pages 663–670, 2002. ISBN 1-9039-9634-1.
- [259] J. Teran, S. Blemker, V. N. T. Hing, and R. Fedkiw. Finite volume methods for the simulation of skeletal muscle. In *Eurographics/SIGGRAPH Symposium on Computer Animation*, 2003.
- [260] A. C. Limache and S. R. Idelsohn. On the development of finite volume methods for computational solid mechanics. *Mecánica Computacional*, 26:827–843, 2007.
- [261] M. A. Wheel. A finite volume method for analyzing the bending deformation of thick and thin plates. *Computer Methods in Applied Mechanics and Engineering*, 147:199–208, 1997.
- [262] A. J. Beveridge and M. Wheel. A control volume based formulation of the discrete Kirchoff triangular thin plate bending element. In *The 17<sup>th</sup> UK National Conference on Computational Mechanics in Engineering*, pages 287–290, Nottingham, UK, 2009.
- [263] G. A. Taylor. *A vertex based discretisation scheme applied to material non-linearity within a multi-physics framework*. PhD thesis, University of Greenwich, 1996.
- [264] C. Bailey, P. Chow, M. Cross, Y. Fryer, and K. Pericleous. Multiphysics modelling of metals casting process. *Proceedings of the Royal Society of London A: Mathematical, Physical and Engineering Sciences*, pages 459–486, 1996.

- [265] C. Bailey, G. A. Taylor, S. M. Bounds, G. Moran, and M. Cross. PHYSICA: a multiphysics computational framework and its application to casting. *Mineral & Metal Processing and Power Generation*, pages 419–425, 1997.
- [266] C. Bailey, S. Bounds, M. Cross, G. Moran, K. Pericleous, and G. A. Taylor. Multiphysics modeling and its application to the casting process. *Computer Modelling and Simulation in Engineering*, 4:206–212, 1999.
- [267] C. Bailey, G. A. Taylor, M. Cross, and P. Chow. Discretisation procedures for for multiphysics phenomena. *Journal of Computational and Applied Mathematics*, 103:3–17, 1999.
- [268] A. B. Oldroyd, M. A. Wheel, and T. J. Scanlon. An integrated volume based approach for analysing flow induced vibrations. In *Proceedings European Conference on Computational Mechanics (ECCM)*, Munich, Germany, September 1999.
- [269] M. A. Wheel, A. Oldroyd, T. J. Scanlon, and P. Wenke. Integrating finite volume based structural analysis procedures with CFD software to analyse fluid structure interaction. In *Proceedings of 2<sup>nd</sup> Int. Conf. on Finite Volumes for Complex Applications*, Duisburg, Germany, 1999.
- [270] A. K. Slone. *A finite volume unstructured mesh approach to dynamic fluid-structure interactions between fluids and linear elastic solids*. PhD thesis, University of Greenwich, 2000.
- [271] A. K. Slone, K. Pericleous, C. Bailey, and M. Cross. Details of an integrated approach to three- dimensional dynamic fluid structure interaction. In *Fluid Structure Interaction*, pages 57–66. WIT Press, 2001. ISBN 1-85312-881-3. <https://www.witpress.com/books/978-1-85312-881-3>.
- [272] A. K. Slone, K. Pericleous, C. Bailey, and M. Cross. Dynamic fluid-structure interaction using finite volume unstructured mesh procedures. *Computers & Structures*, 80:371–390, 2002.
- [273] A. K. Slone, C. Bailey, and M. Cross. Dynamic solid mechanics using finite volume methods. *Applied Mathematical Modelling*, 27:69–87, 2003.
- [274] A. K. Slone, K. Pericleous, C. Bailey, M. Cross, and C. Bennett. A finite volume unstructured mesh approach to dynamic fluid-structure interaction: An assessment of the challenge of predicting the onset of flutter. *Applied Mathematical Modelling*, 28:211–239, 2004.
- [275] A. K. Slone, T. N. Croft, A. J. Williams, and M. Cross. An alternative mixed eulerian lagrangian approach to high speed collision between solid structures on parallel clusters. *Advances in Engineering Software*, 38(4):244 – 255, 2007. ISSN 0965-9978. doi: <https://doi.org/10.1016/j.advengsoft.2006.09.015>. URL <http://www.sciencedirect.com/science/article/pii/S0965997806001542>.
- [276] M. Cross, T. N. Croft, A. K. Slone, A. J. Williams, N. Christakis, M. K. Patel, C. Bailey, and K. Pericleous. Computational modelling of multi-physics and multi-scale processes

- in parallel. *International Journal for Computational Methods in Engineering Science and Mechanics*, 8(2):63–74, 2007. doi: 10.1080/15502280601149510. URL <https://doi.org/10.1080/15502280601149510>.
- [277] X. Lv, Y. Zhao, X. Y. Huang, G. H. Xia, and X. H. Su. A matrix-free implicit unstructured multigrid finite volume method for simulating structural dynamics and fluid-structure interaction. *Journal of Computational Physics*, 225:120–144, 2007.
- [278] T. N. Croft, A. J. Williams, A. K. Slone, and M. Cross. A two-dimensional prototype multi-physics model of the right ventricle of the heart. *International Journal for Numerical Methods in Fluids*, 57(5):583–600, 2008. doi: 10.1002/flid.1764. URL <https://onlinelibrary.wiley.com/doi/abs/10.1002/flid.1764>.
- [279] G. H. Xia and C. I. Lin. An unstructured finite volume approach for structural dynamics in response to fluid motions. *Computers & Structures*, 86:684–701, 2008.
- [280] K. Hejranfar and M. H. Azampour. Simulation of 2D fluid–structure interaction in inviscid compressible flows using a cell-vertex central difference finite volume method. *Journal of Fluids and Structures*, 67:190–218, 2016.
- [281] G. A. Taylor. Material non-linearity within a finite volume framework for the simulation of a metal casting process. *Computational Plasticity: Fundamentals and Applications II*, pages 1459–1470, 1995.
- [282] G. A. Taylor, C. Bailey, and M. Cross. A three dimensional finite volume approach to the thermomechanical modelling of the shape casting of metals. In *Proceedings of 8<sup>th</sup> Int. Conf. on Modelling of Casting, Welding and Advanced Solidification Processes*, 1998.
- [283] M. Cross. Computational issues in the modelling of materials-based manufacturing processes. *Journal of Computer-Aided Materials Design*, 3:100–116, 1996.
- [284] S. Bounds, G. Moran, K. Pericleous, M. Cross, and T. N. Croft. A computational model for defect prediction in shape castings based on the interaction of free surface flow, heat transfer, and solidification phenomena. *Metallurgical and Materials Transactions B*, 31:515–527, 2000.
- [285] A. J. Williams, T. N. Croft, and M. Cross. Computational modelling of metals extrusion and forging processes. In M. Cross, J. W. Ewans, and C. Bailey, editors, *Computational Modelling of Materials, Minerals and Metals Processing, TMS*, pages 481–490. Materials Society, 2001.
- [286] A. J. Williams, T. N. Croft, and M. Cross. Computational modelling of metal extrusion and forging processes. *Journal of Materials Processing Technology*, 125:573–582, 2002. doi: 10.1016/S0924-0136(02)00401-6. URL <http://www.sciencedirect.com/science/article/pii/S0924013602004016>.
- [287] A. J. Williams, A. K. Slone, T. N. Croft, and M. Cross. A mixed Eulerian-Lagrangian method for modelling metal extrusion processes. *Computer Methods in Applied Mechanics and Engineering*, 199:2123–2134, 2010.

- [288] G. A. Taylor, M. Hughes, N. Strusevich, and K. Pericleous. The application of three dimensional finite volume methods to the modelling of welding phenomena. In Sahn, P. N. Hansen, and J. G. Conley, editors, *Modeling of Casting, Welding and Advanced Solidification Processes IX*, 2000.
- [289] G. A. Taylor, M. Hughes, N. Strusevich, and K. Pericleous. The application of three-dimensional finite volume methods to the modelling of welding phenomena. *Applied Mathematical Modelling*, 26:309–320, 2002.
- [290] G. A. Taylor, M. Hughes, N. Strusevich, and K. Pericleous. Finite volume methods applied to the computational modelling of welding phenomena. *Applied Mathematical Modelling*, 26:309–320, 2002.
- [291] G. A. Taylor, V. Breiguine, C. Bailey, and M. Cross. An augmented Lagrangian contact algorithm employing a vertex-based finite volume method. In *ACME*, 2000. Available at: [http://www.brunel.ac.uk/~eesrgat/research/ps\\_pubs](http://www.brunel.ac.uk/~eesrgat/research/ps_pubs).
- [292] J.-F. Gong, L.-K. Xuan, P.-J. Ming, and W.-P. Zhang. Thermoelastic analysis of functionally graded solids using a staggered finite volume method. *Composite Structures*, 104:134–143, 2013.
- [293] J.-F. Gong, P.-J. Ming, L.-K. Xuan, and W.-P. Zhang. Thermoelastic analysis of three-dimensional functionally graded rotating disks based on finite volume method. *Journal of Mechanical Engineering Science*, 2014.
- [294] P. Perré and J. Passard. A control-volume procedure compared with the finite-element method for calculating stress and strain during wood drying. *Drying Technology*, 13:635–660, 1995.
- [295] C. Salinas, C. Chávez, Y. Gatica, and R. Ananias. Two-dimensional wood drying stress simulation using control control-volume mixed finite element methods (CVFEM). *Ingeniería e Investigacion*, 31:171–183, 2011.
- [296] M. A. Wheel. A control volume-based finite element method for plane micropolar elasticity. *International Journal for Numerical Methods in Engineering*, 75:992–1006, 2008.
- [297] A. J Beveridge, M. Wheel, and D. Nash. A higher order control volume based finite element method to predict the deformation of heterogeneous materials. *Computers & Structures*, 129: 56–62, 2013.
- [298] M. Zhu, P.-J. Ming, L. Xuan, and W.-P. Zhang. An unstructured finite volume time domain method for structural dynamics. *Applied Mathematical Modelling*, 36:183–192, 2012.
- [299] L. Xuan, P.-J. Ming, J. Gong, D. Zheng, and W.-P. Zhang. A finite volume time domain method for in-plane vibration on mixed grids. *Journal of Vibration and Acoustics*, 136, 2014.
- [300] L. Xuan, P.-J. Ming, W.-P. Zhang, G. Jin, and J. Gong. Time domain finite volume method for the transient response and natural characteristics of structural-acoustic coupling in an enclosed cavity. *Shengxue Xuebao/Acta Acustica*, 39:215–225, 2014.

- [301] P. Wenke and M. A. Wheel. A finite volume method for solid mechanics incorporating rotational degrees of freedom. *Computers & Structures*, 81:321–329, 2003.
- [302] W. Pan, M. Wheel, and Y. Qin. Six-node triangle finite volume method for solids with a rotational degree of freedom for incompressible material. *Computers & Structures*, 88:1506–1511, 2010.
- [303] W. Pan and M. Wheel. A finite-volume method for solids with a rotational degrees of freedom based on the 6-node triangle. *International Journal of Numerical Methods in Biomedical Engineering*, 27:1411–1426, 2011.
- [304] K. McManus, M. Cross, C. Walshaw, S. Johnson, P. Leggett, and A. Scalable. Strategy for the parallelization of multiphysics unstructured mesh-iterative codes on distributed-memory systems. *International Journal of High Performance Computing Applications*, 14:137–174, 2000.
- [305] K. McManus, M. Cross, C. Walshaw, T. N. Croft, and A. J. Williams. Parallel performance in multi-physics simulation. In *ICCS '02 Proceedings of the International Conference on Computational Science-Part II*, pages 806–815, London, 2002. Springer-Verlag.
- [306] J. F. Maitre, A. Rezgui, H. Souhail, and A. M. Zine. High order finite volume schemes: Application to non-linear elasticity problems. In *Finite volumes for complex applications, III (Porquerolles)*, *Hermes Sci. Publ., Paris*, pages 391–398, 2002.
- [307] H. Souhail. *Schéma volumes finis: Estimation derreur a posteriori hiérarchique par éléments finis mixtes. Résolution de problèmes d'élasticité non-linéaire*. PhD thesis, Ecole Centrale de Lyon, 2004.
- [308] J. Zhang and T. Liu. P-SV wave propagation in heterogeneous media: Grid method. *Geophysical Journal International*, 136:431–438, 1999.
- [309] J. Zhang and T. Liu. Elastic wave modelling in 3-D heterogeneous media: 3-D grid method. *Geophysical Journal International*, 150:780–799, 2002.
- [310] J. Zhang. Wave propagation across fluid-solid interfaces: A grid method approach. *Geophysical Journal International*, 159:240–252, 2004.
- [311] T. Liu, K. Liu, and J. Zhang. Unstructured grid method for stress wave propagation in elastic media. *Computer Methods in Applied Mechanics and Engineering*, 193:2427–2452, 2004.
- [312] T. Liu, K. Liu, and J. Zhang. Triangular grid method for stress-wave propagation in 2-D orthotropic materials. *Archive of Applied Mechanics*, 74:477–488, 2005.
- [313] H. Gao and J. Zhang. Parallel 3-D simulation of seismic wave propagation in heterogeneous anisotropic media: A grid method approach. *Geophysical Journal International*, 165:875–888, 2006.
- [314] E. Dormy and A. Tarantola. Numerical simulation of elastic wave propagation using a finite volume method. *Journal of geophysical research*, 100:2123–2133, 1995. doi: 10.1029/94JB02648.

- [315] F. H. Harlow and J. E. Welch. Numerical calculation of the time-dependent viscous incompressible flow of fluid with free surface. *Physics of Fluids*, 8, 1965.
- [316] D. B. Spalding. Simulation of fluid flow, heat transfer and solid deformation simultaneously. In *NAFEMS Conference No 4*, Brighton, UK, 1993.
- [317] D. B. Spalding. Simultaneous fluid-flow, heat-transfer and solid-stress computation in a single computer code. In *Keynote lecture 4<sup>th</sup> International Colloquium on Process Simulation*, Helsinki University of Technology, Espoo, Finland, 1997.
- [318] D. B. Spalding. Fluid-structure interaction in the presence of heat transfer and chemical reaction. In *ASME/JSME Joint Pressure Vessels and Piping Conference*, San Diego, CA, USA, 1998.
- [319] D. B. Spalding. Fluid-structure interaction in the presence of heat transfer and chemical reaction. In V. Kudriavtsev and W. Cheng, editors, *V. Computational Technologies for Fluid/Thermal/Structural/Chemical Systems With Industrial Applications*, 1998.
- [320] D. B. Spalding. Simultaneous prediction of solid stress, heat transfer and fluid flow by a single algorithm. In *ASME Pressure Vessels and Piping Conference*, Vancouver, British Columbia, Canada, March 2002.
- [321] D. B. Spalding. Extending the boundaries of heat transfer. In *The 13th International Heat Transfer Conference, Sydney, Australia, August 16, 2006*.
- [322] D. B. Spalding. Enlarging the frontiers of computational fluid dynamics. In *International Symposium Heat & Mass Transfer & Hydrodynamics in Swirling Flow*, Moscow, Russia, 2008.
- [323] S. V. Patankar and D. B. Spalding. A calculation procedure for heat, mass, and momentum transfer in three-dimensional parabolic flows. *International Journal of Heat and Mass Transfer*, 15:1787, 1972.
- [324] S. V. Patankar. *Numerical Heat Transfer and Fluid Flow*. Hemisphere Publishing Corporation, McGraw-Hill Book Company, Washington, 1980.
- [325] J. H. Hattel, P. Hansen, and L. F. Hansen. Analysis of thermally induced stresses in die casting using a novel control volume technique. In T. Pivonka, editor, *Modelling of Casting and Welding and Advanced Solidification Processes Advanced Solidification Processes Minerals Advanced Solidification Processes Minerals Metals and Materials Society*. Modelling of Casting, Welding and Advanced Solidification Processes, Minerals, Metals & Materials Society, TMS, 1993.
- [326] J. H. Hattel, P. N. Hansen, and S. Andersen. Modeling of thermal induced stresses in high pressure die casting dies. In *NADCA 19<sup>th</sup> International die casting congress, NADC, Transactions*, Rosemont, IL, USA, 1993.
- [327] J. H. Hattel. Stress calculations using a control volume based finite difference method. *Revedannelse og Brudmekanik, DMS Vintermøderbog*, 1993.

- [328] J. H. Hattel. *Control volume based finite difference method - Numerical modeling of thermal and mechanical conditions in casting and heat treatment processes*. PhD thesis, Institute of Manufacturing Engineering, Technical University of Denmark, 1993.
- [329] J. H. Hattel and P. N. Hansen. 1-D analytical model for the thermally induced stresses in the mold surface during die casting. *Applied Mathematical Modeling*, 18:550–559, 1994.
- [330] J. H. Hattel and P. N. Hansen. A control volume-based finite difference method for solving the equilibrium equations in terms of displacements. *Applied Mathematical Modelling*, 19: 210–243, 1995.
- [331] J. H. Hattel. Numerical modelling of stresses and deformations in casting processes. In *Proceedings of CASTING 1997*, Helsinki University of Technology, 1997. Int. ADI and Simulation Conf. Helsinki.
- [332] N. Pryds and J. H. Hattel. Numerical modelling of rapid solidification. *Modelling and Simulation in Materials Science and Engineering*, 5(5):451–472, 1997.
- [333] J. H. Hattel, J. Thorborg, and S. Andersen. Stress/strain modelling of casting processes in the framework of the control-volume method. In *Modeling of Casting and Advanced Solidification Processes VIII, Warrendale, USA : TMS, The Minerals, Metals and Materials Society*, pages 763–770, 1998.
- [334] J. H. Hattel and N. Pryds. Modelling rapid solidification with the control volume method. In *A.R. Dinesen, M. Eldrup, D. Juul Jensen, S. Linderoth, T.B. Pedersen, N.H. Pryds, A. Schrder Pedersen, J.A. Wert, Proceedings of Science of Metastable and Nanocrystalline Alloys - Structure, Properties and Modelling, Roskilde, Ris National Laboratory*, pages 241–247, 2001.
- [335] J. Thorborg. *Nonlinear constitutive modelling in thermomechanical processes with the control volume method*. PhD thesis, Department of Manufacturing Engineering, Technical University of Denmark, 2001.
- [336] J. H. Hattel and J. Thorborg. A numerical model for predicting the thermomechanical conditions during hydration of early-age concrete. *Applied Mathematical Modelling*, 27: 1–26, 2003.
- [337] J. Thorborg and J. H. Hattel. Thermo-elasto-plasticity in solidification processes using the control volume method on staggered grid. In Stefanescu et. al., editor, *Modelling of Casting, Welding and Advanced Solidification Processes, Warrendale: TMS - The Minerals, Metals & Materials Society*, 2003.
- [338] L. Wang and R. Melnik. Finite volume analysis of nonlinear thermo-mechanical dynamics of shape memory alloys. *Heat and Mass Transfer*, 43, 2007.
- [339] K. R. Rajagopal, A. R. Srinivasa, and A. Ponnalagu. Thermo-inelastic response of polymeric solids. Technical report, Final Report, Texas Engineering Experiment Station, Harvey Mitchell Parkway South, Suite 300, College Station, TX, 2014.

- [340] J. Aboudi, M.-J. Pindera, and S.M. Arnold. Higher-order theory for functionally graded materials. *Composites Part B: Engineering*, 30:777–832, 1999.
- [341] J. Aboudi. Micromechanical analysis of fully coupled electro-magneto-thermo-elastic multiphase composites. *Smart Materials and Structures*, 10:867–877, 2001.
- [342] J. Aboudi, M.-J. Pindera, and S.M. Arnold. Linear thermoelastic higher-order theory for periodic multiphase materials. *ASME Journal of Applied Mechanics*, 68:697–707, 2001.
- [343] R. Haj-Ali and J. Aboudi. Nonlinear micromechanical formulation of the high fidelity generalized method of cells. *International Journal of Solids and Structures*, 46:2577–2592, 2009.
- [344] R. Haj-Ali and J. Aboudi. Discussion paper: Has renaming the high fidelity generalized method of cells been justified? *International Journal of Solids and Structures*, 49:2051–2058, 2012.
- [345] Y. Bansal and M.-J. Pindera. A second look at the higher-order theory for periodic multiphase materials. *ASME Journal of Applied Mechanics*, 72:177–195, 2005.
- [346] Y. Bansal and M.-J. Pindera. Finite-volume direct averaging micromechanics of heterogeneous materials with elastic-plastic phases. *International Journal of Plasticity*, 22:775–825, 2006.
- [347] J. Aboudi. A continuum theory for fiber-reinforced elastic viscoplastic composites. *International Journal of Engineering Science*, 20:605–621, 1982.
- [348] J. Aboudi. *Mechanics of Composite Materials: A Unified Micromechanical Approach*. Elsevier, Amsterdam, Netherlands, 1991.
- [349] M. Paley and J. Aboudi. Micromechanical analysis of composites by the generalized cells model. *Mechanics of Materials*, 14:127–139, 1992.
- [350] M. A. A. Cavalcante and M.-J. Pindera. Generalized FVDAM theory for elastic-plastic periodic materials. *International Journal of Plasticity*, 77:90–117, 2016.
- [351] J. Aboudi. The generalized method of cells and high-fidelity generalized method of cells micromechanical models: a review. *Mechanics of Advanced Materials and Structures*, 11:329–366, 2004.
- [352] M.-J. Pindera, H. Khatam, A. S. Drago, and Y. Bansal. Micromechanics of spatially uniform heterogeneous media: A critical review and emerging approaches. *Composites Part B: Engineering*, 40:349–378, 2009.
- [353] N. Charalambakis and F. Murat. Homogenization of stratified thermoviscoplastic materials. *Quarterly of Applied Mathematics*, 64(2):359–99, 2006.
- [354] J. Aboudi, S. M. Arnold, and B. A. Bednarczyk. *Micromechanical analyses of smart composite materials*. Nova Science Publishers, New York, USA, 2007.

- [355] J. Aboudi. Finite strain micromechanical modeling of multiphase composites. *International Journal for Multiscale Computational Engineering*, 6:411–434, 2008.
- [356] S. N. Atluri and S. Shen. The meshless local Petrov-Galerkin (MLPG) method: a simple & less-costly alternative to the finite element and boundary element methods. *Computer Modeling in Engineering and Sciences*, 3:11–51, 2002.
- [357] S. N. Atluri and T. Zhu. A new meshless local Petrov-Galerkin (MLPG) approach in computational mechanics. *Computational Mechanics*, 22:117–127, 1998. doi: 10.1007/s004660050346.
- [358] H.-K. Ching and R. C. Batra. Determination of Crack Tip Fields in Linear Elastostatics by the Meshless Local Petrov-Galerkin (MLPG) Method. *Computer Modeling in Engineering and Sciences*, 2:273–289, 2001.
- [359] A. Warlock, H.-K. Ching, A. K. Kapila, and R. C. Batra. Plane strain deformations of an elastic material compressed in a rough rectangular cavity. *International Journal of Engineering Science*, 40:991–1010, 2002.
- [360] L. Qian, R. Batra, and L. Chen. Elastostatic deformations of a thick plate by using a higher-order shear and normal deformable plate theory and two meshless local Petrov-Galerkin (MLPG) methods. *Computer Modeling in Engineering and Sciences*, 4(1):161–76, 2003.
- [361] I. Raju and D. Phillips. Further developments in the MLPG method for beam problems. *Computer Modeling in Engineering and Sciences*, 4(1):141–60, 2003.
- [362] S. N. Atluri, Z. Han, and A. Rajendran. A new implementation of the meshless finite volume method, through the MLPG “mixed” approach. *Computer Modeling in Engineering and Sciences*, 6(6):491–514, 2004.
- [363] Z. Han and S. N. Atluri. Meshless local Petrov-Galerkin (MLPG) approaches for solving 3D problems in elasto-statics. *Computer Modeling in Engineering and Sciences*, 6:169–88, 2004.
- [364] R. C. Batra, M. Porfiri, and D. Spinello. Treatment of material discontinuity in two meshless local Petrov-Galerkin (MLPG) formulations of axisymmetric transient heat conduction. *International Journal for Numerical Methods in Engineering*, 61:2461–2479, 2004.
- [365] Z. Han, A. Rajendran, and S. N. Atluri. Meshless local Petrov-Galerkin (MLPG) approaches for solving nonlinear problems with large deformations and rotations. *Computer Modeling in Engineering and Sciences*, 10(1):1, 2005.
- [366] Jan Sladek, Vladimir Sladek, Peter Solec, and Andres Saez. Dynamic 3D axisymmetric problems in continuously non-homogeneous piezoelectric solids. *International Journal of Solids and Structures*, 45(16):4523 – 4542, 2008. ISSN 0020-7683. doi: 10.1016/j.ijsolstr.2008.03.027. URL <http://www.sciencedirect.com/science/article/pii/S0020768308001376>.

- [367] M. R. Moosavi and A. Khelil. Accuracy and computational efficiency of the finite volume method combined with the meshless local Petrov-Galerkin in comparison with the finite element method in elasto-static problem. *ICCES*, 5:211–38, 2008.
- [368] M. R. Moosavi and A. Khelil. Finite volume meshless local Petrov-Galerkin method in elastodynamic problems. *Engineering Analysis with Boundary Elements*, 33:1016–1021, 2009.
- [369] M. R. Moosavi, F. Delfanian, and A. Khelil. Orthogonal meshless finite volume method in elasticity. *Thin-Walled Structures*, 49:708–712, 2011.
- [370] M. R. Moosavi, F. Delfanian, and A. Khelil. The orthogonal meshless finite volume method for solving Euler-Bernoulli beam and thin plate problems. *Thin-Walled Structures*, 49:923–932, 2011.
- [371] Seyed Mahmoud Hosseini, Jan Sladek, and Vladimir Sladek. Meshless local Petrov-Galerkin method for coupled thermoelasticity analysis of a functionally graded thick hollow cylinder. *Engineering Analysis with Boundary Elements*, 35(6):827 – 835, 2011. ISSN 0955-7997. doi: 10.1016/j.enganabound.2011.02.001. URL <http://www.sciencedirect.com/science/article/pii/S0955799711000233>.
- [372] D. Soares, V. Sladek, and J. Sladek. Modified meshless local Petrov-Galerkin formulations for elastodynamics. *International Journal for Numerical Methods in Engineering*, 90(12): 1508–1828, 2012. doi: 10.1002/nme.3373. URL <https://onlinelibrary.wiley.com/doi/abs/10.1002/nme.3373>.
- [373] M. R. Moosavi, F. Delfanian, and A. Khelil. Orthogonal meshless finite volume method applied to crack problems. *Thin-Walled Structures*, 52:61–65, 2012.
- [374] M. Moosavi, F. Delfanian, and A. Khelil. Orthogonal meshless finite volume method in shell analysis. *Finite Elements in Analysis and Design*, 62:1–7, 2012.
- [375] M. R. Moosavi. Orthogonal meshless finite volume method applied to elastodynamic crack problems. *International Journal of Fracture*, 179:1–7, 2013. doi: 10.1007/s10704-012-9752-9.
- [376] M. Ebrahimnejad, N. Fallah, and A. R. Khoei. Adaptive refinement in the meshless finite volume method for elasticity problems. *Computers & Mathematics with Applications*, 69, 2015.
- [377] M. Ebrahimnejad, N. Fallah, and A.R. Khoei. Three types of meshless finite volume method for the analysis of two-dimensional elasticity problems. *Computational and Applied Mathematics*, 36(2):971–990, 2017.
- [378] N. Fallah. Mesh-free and mesh based finite volume methods for solid mechanics analysis. In *41<sup>st</sup> Solid Mechanics Conference (SOLMECH 2018)*, Warsaw, Poland, 2018.
- [379] A. Davoudi-Kia and N. Fallah. Comparison of enriched meshless finite-volume and element-free Galerkin methods for the analysis of heterogeneous media. *Engineering*

- with Computers*, Dec 2017. ISSN 1435-5663. doi: 10.1007/s00366-017-0573-3. URL 10.1007/s00366-017-0573-3.
- [380] A. Davoudi-Kia and N. Fallah. An enriched meshless finite volume method for the modeling of material discontinuity problems in 2D elasticity. *Latin American Journal of Solids and Structures*, 15(2):209–219, April 2018. doi: 10.1590/1679-78254121.
- [381] N. Fallah and N. Nikraftar. Meshless finite volume method for the analysis of fracture problems in orthotropic media. *Engineering Fracture Mechanics*, 2018. doi: 10.1016/j.engfractmech.2018.09.029. In press.
- [382] H. Bašić, I. Demirdžić, and S. Muzaferija. Analysis of plastic flow of metals during extrusion processes using finite volume method. In *Proceedings of 3<sup>rd</sup> International Conference on Industrial Tools*, pages 22–26, Slovenia, 2001. Rogaska Slatina.
- [383] H. Bašić. Friction models comparison in finite volume method simulation of bulk metal forming technologies. *Journal for Technology of Plasticity*, 33:113–122, 2008.
- [384] H. Bašić. The constitutive models in numerical simulation of steady-state metal forming processes. *Journal for Technology of Plasticity*, 34:27–36, 2009.
- [385] Z.Z. Chen, Z.L. Lou, and X.Y. Ruan. Finite volume simulation and mould optimization of aluminum profile extrusion. *Journal of Materials Processing Technology*, 190(1-3):382 – 386, 2007. doi: 10.1016/j.jmatprotec.2007.01.032.
- [386] M. R. Jafari, S. M. Zebarjad, and F. Kolahan. Simulation of thixoformability of A356 aluminum alloy using finite volume method. *Materials Science and Engineering A*, 454: 558–563, 2007. doi: 10.1016/j.msea.2006.11.124.
- [387] S. Lou, G. Zhao, R. Wang, and X. Wu. Modeling of aluminum alloy profile extrusion process using finite volume method. *Journal of Materials Processing Technology*, 206:481–490, 2008.
- [388] K.S. Al-Athel and M.S. Gadala. Eulerian volume of solid (VOS) approach in solid mechanics and metal forming. *Computer methods in applied mechanics and engineering*, 200:2145–2159, 2011.
- [389] R. Wang and H. Z. Li. Modeling of aluminum extrusion process using non-orthogonal block structured grids based FVM. *Advanced Materials Research*, 189:1749–1752, 2011.
- [390] R. Wang. Body fitted grids based FVM simulation of aluminum extrusion process. *Advanced Materials Research*, 418:2102–2105, 2012.
- [391] J. D. Bressan, M. M. Martins, and S. T. Button. Aluminium extrusion analysis by the finite volume method. In Oñate, D. R. J. Owen, D. Peric, and B. Suárez, editors, *XII International Conference on Computational Plasticity. Fundamentals and Applications COMPLAS XII*, 2013.

- [392] C. Zhang, H. Chen, G. Zhao, L. Zhang, and S. Lou. Optimization of porthole extrusion dies with the developed algorithm based on finite volume method. *The International Journal of Advanced Manufacturing Technology*, pages 1–13, 2016.
- [393] A. de Brauer, A. Iollo, and T. Milcent. A Cartesian scheme for compressible multimaterial models in 3D. *Journal of Computational Physics*, 313:121 – 143, 2016. ISSN 0021-9991. doi: 10.1016/j.jcp.2016.02.032. URL <http://www.sciencedirect.com/science/article/pii/S0021999116000966>.
- [394] A. de Brauer, A. Iollo, and T. Milcent. A Cartesian scheme for compressible multimaterial hyperelastic models with plasticity. *Communications in Computational Physics*, 22(5): 1362?1384, 2017. doi: 10.4208/cicp.OA-2017-0018.
- [395] J. G. Teng, S. F. Chen, and J. L. Hu. A finite volume method for deformation analysis of woven fabrics. *International Journal for Numerical Methods in Engineering*, 46:2061–2098, 1999.
- [396] S. F. Chen, J. L. Hu, and J. G. Teng. A finite-volume method for contact drape simulation of woven fabrics and garments. *Finite Elements in Analysis and Design*, 37:513–531, 2001.
- [397] B. Martin and F. Pascal. Discrete duality finite volume method applied to linear elasticity. *Finite Volumes for Complex Applications VI: Problems & Perspectives*, 4:663–671, 2011.
- [398] B. Martin. *Elaboration de solveurs volumes finis 2D/3D pour résoudre le problème de l'élasticité linéaire*. PhD thesis, Ecole normale supérieure de Cachan - ENS Cachan, Français, 2012.
- [399] D. A. Di Pietro, R. Eymard, S. Lemaire, and R. Masson. Hybrid finite volume discretization of linear elasticity models on general meshes. In J. Fürst, J. Halama, R. Herbin, and F. Hubert, editors, *Finite Volumes for Complex Applications: VI Problems & Perspectives, Volume 4 of Springer Proceedings in Mathematics, Springer Berlin Heidelberg*, pages 331–339, 2011.
- [400] M. L. Wilkins. Calculation of elastic-plastic flow, T3 - UCRL; 7322. Technical report, Lawrence Radiation Laboratory, Lawrence Livermore Laboratory, University of California, Berkeley, 1963. <https://catalog.hathitrust.org/Record/007293160>.
- [401] M. L. Wilkins. Calculations of elastic-plastic flow. *Methods of Computational Physics*, 3, 1964. Edited by B. Adler, S. Fernback, and M. Rotenberg.
- [402] M. L. Wilkins. *Computer simulation of dynamic phenomena*. Springer-Verlag, Berlin Heidelberg New York, 1999.
- [403] N. M. Bessonov, S. F. Golovashchenko, and V. A. Volpert. Numerical modelling of contact elastic-plastic flows. *Mathematical Modelling of Natural Phenomena*, 4(1):44–87, 2009. URL <http://eudml.org/doc/222347>.
- [404] C. M. Rhie and W. L. Chow. Numerical study of the turbulent flow past an airfoil with trailing edge separation. *AIAA Journal*, 21:1525–1532, November 1983. doi: 10.2514/3.8284.

- [405] A. Jameson, W. Schmidt, and E. Turkel. Numerical solution of the Euler equations by finite volume methods using Runge-Kutta time-stepping schemes. In *AIAA 5<sup>th</sup> Computational Fluid Dynamics Conference*, volume 81, page 1259, 1981.
- [406] D. A. H. Jacobs. Preconditioned conjugate gradient methods for solving systems of algebraic equations. Technical report, Central Electricity Research Laboratories Report (RD/L/N193/80), 1980.
- [407] O. I. I. Hassan. *A vertex centred Finite Volume algorithm for fast solid dynamics: Total and Updated Lagrangian descriptions*. PhD thesis, University of Swansea, 2019.
- [408] T. Belytschko, W. K. Liu, B. Moran, and K. I. Elkhodary. *Nonlinear Finite Elements for Continua and Structures*. Wiley, Chichester, West Sussex, 2<sup>nd</sup> edition, 2014.
- [409] K. J. Bathe. *Finite element procedures*. Prentice Hall, New Jersey, 1996.
- [410] M. Schäfer. *Computational Engineering - Introduction to Numerical Methods*. Springer-Verlag, Berlin, Heidelberg, 2006. ISBN 3540306854.
- [411] O. C. Zienkiewicz and R. L. Taylor. *The finite element method, volume 2, solid mechanics*. Butterworth Heinemann, Oxford, 5<sup>th</sup> edition, 2000.
- [412] T. A. Laursen. *Computational Contact and Impact Mechanics*. Springer-Verlag Berlin Heidelberg GmbH, 2002.
- [413] Dassault Systèmes Simulia Corp. Abaqus 6.14. [http://www.simulia.com/products/abaqus\\_fea.html](http://www.simulia.com/products/abaqus_fea.html), 2018.
- [414] E. Oñate and M. Cervera. Derivation of thin plate bending elements with one degree of freedom per node. *Engineering Computations*, 10:543–561, 1993.
- [415] E. Oñate. Elementos finitos y volúmenes finitos puntos de encuentro y posibilidad de nuevas aplicaciones. Technical report, CIMNE, Barcelona, 1998.
- [416] E. Oñate and F. Zarate. Rotation-free triangular plate and shell elements. *International Journal for Numerical Methods in Engineering*, 47:557–603, 2000.
- [417] O. C. Zienkiewicz. Origins, milestones and directions of the finite element method: A personal view. *Archives of Computational Methods in Engineering State of the art reviews*, 2(1):1–48, 1995.
- [418] A. Lahrmann. An element formulation for the classical finite difference and finite volume method applied to arbitrarily shaped domains. *International Journal for Numerical Methods in Engineering*, 35:893–913, 1992.
- [419] D. M. Harrild and C. S. Henriquez. A finite volume model of cardiac propagation. *Annals of Biomedical Engineering*, 25:315–334, 1997.
- [420] Q. Fang, T. Tsuchiya, and T. Yamamoto. Finite difference, finite element and finite volume methods applied to two-point boundary value problems. *Journal of Computational and Applied Mathematics*, 139:9–19, 2002.

- [421] T. Yamamoto, Q. Fang, T. Tsuchiya, and Finite Difference. Finite element and finite volume methods applied to two-point boundary value problems. *Journal of Computational and Applied Mathematics*, 139:9–19, 2002.
- [422] V. Jacquemet and C. S. Henriquez. Finite Volume Stiffness Matrix for Solving Anisotropic Cardiac Propagation in 2-D and 3-D Unstructured Meshes. *IEEE Transactions on Biomedical Engineering*, 52:1490–1492, 2005.
- [423] V. Jacquemet. Link between the FEM and FVM formulations of anisotropic cardiac propagation in unstructured meshes. Technical report, ITS Technical Report, TR-ITS 2005.021, 2005.
- [424] G. Filippini, C. R. Maliska, and M. Vaz Jr. A physical perspective of the element-based finite volume method and FEM-Galerkin methods within the framework of the space of finite elements. *International Journal for Numerical Methods in Engineering*, 98:24–43, 2014.
- [425] I. Demirdžić. Finite volumes vs finite elements. there is a choice. *Coupled Systems Mechanics*, 9(1):5–28, 2020. doi: 10.12989/csm.2020.9.1.005.
- [426] Osama I. Hassan, Ataollah Ghavamian, Chun Hean Lee, Antonio J. Gil, Javier Bonet, and Ferdinando Auricchio. An upwind vertex centred finite volume algorithm for nearly and truly incompressible explicit fast solid dynamic applications: Total and updated lagrangian formulations. *Journal of Computational Physics: X*, 3:100025, 2019. ISSN 2590-0552. doi: <https://doi.org/10.1016/j.jcp.2019.100025>. URL <http://www.sciencedirect.com/science/article/pii/S2590055219300411>.
- [427] I. M. Smith, D. V. Griffiths, and L. Margetts. *Programming the Finite Element Method*. Wiley, 5<sup>th</sup> edition, 2013.
- [428] W. H. Reed and T. R. Hill. Triangular mesh methods for the neutron transport equation. Technical report, Los Alamos Scientific Lab., N.Mex. (USA), 1973. Technical Report 836, LA-UR-73-479; CONF-730414-2.
- [429] B. Cockburn. Discontinuous galerkin methods. Technical report, School of Mathematics, Univeristy of Minnesota, 2003.
- [430] B. Cockburn, J. Gopalakrishnan, and R. Lazarov. Unified hybridization of discontinuous galerkin, mixed, and continuous galerkin methods for second order elliptic problems. *SIAM Journal on Numerical Analysis*, 47:1319–1365, 2009. doi: 10.1137/070706616.
- [431] G. Fu, B. Cockburn, and H. Stolarski. Analysis of an hdg method for linear elasticity. *International Journal for Numerical Methods in Engineering*, 102(3-4):551–575, 2015. doi: 10.1002/nme.4781. URL <https://onlinelibrary.wiley.com/doi/abs/10.1002/nme.4781>.
- [432] W. Qiu, J. Shen, and K. Shi. An hdg method for linear elasticity with strong symmetric stresses. *Math. Comp.*, 87:69–93, 2018. doi: 10.1090/mcom/3249.

- [433] R. Sevilla, M. Giacomini, A. Karkoulas, and A. Huerta. A superconvergent hybridisable discontinuous galerkin method for linear elasticity. *International Journal for Numerical Methods in Engineering*, 116:91–116, 2018. doi: 10.1002/nme.5916.
- [434] J. S. Hesthaven and T. Warburton. *Nodal Discontinuous Galerkin Methods: Algorithms, Analysis, and Applications (Texts in Applied Mathematics)*. Springer, New York, USA, 2007.
- [435] A. K. Slone, K. Pericleous, C. Bailey, and M. Cross. Dynamic fluid structure interactions using finite volume unstructured mesh procedures. In *International Forum on Aero-elasticity and Structural Dynamics*, pages 417–424, June 1997.
- [436] I. Demirdžić. Finite volume approach to multi-physics problems. In S.N. Alturi and P. E. O’Donoghue, editors, *Modelling and Simulation Based Engineering*, pages 1757–1762. Tech Science Press, Palmdale, 1998.
- [437] M. Schäfer, S. Meynen, R. Sieber, and I. Teschauer. Multigrid methods for coupled fluid-solid problems. In *European Congress on Computational Methods in Applied Sciences and Engineering, ECCOMAS 2000*, Barcelona, Spain, 2000.
- [438] A. K. Slone, M. Cross, K. Pericleous, and C. Bailey. A finite volume approach to dynamic fluid structure interaction. In *8th Annual Conference of the Association for Computational Mechanics in Engineering (ACME 2000)*, pages 218–221, Greenwich University, London, UK, 2000.
- [439] A. K. Slone, K. Pericleous, C. Bailey, and M. Cross. Dynamic fluid structure interactions using finite volume unstructured mesh procedures. In *8th Symposium on Multidisciplinary Analysis and Optimization, Multidisciplinary Analysis Optimization Conferences*. American Institute of Aeronautics and Astronautics, 2000. doi: 10.2514/6.2000-4788.
- [440] A. K. Slone, K. Pericleous, C. Bailey, and M. Cross. Dynamic fluid structure interactions using finite volume unstructured mesh procedures. In *ECCOMAS Computational Fluid Dynamics Conference*, 2001. ISBN 0 905 091 12 4.
- [441] A. K. Slone, M. Cross, K. Pericleous, C. Bailey, and M. Cross. Using finite volume unstructured mesh approach to dynamic fluid structure interaction: An assessment of the challenge of flutter analysis. In W. A. Wall, K. U. Bletzinger, and K. Schweizerhof, editors, *Trends in Computational Structural Mechanics*, pages 741–750. CIMNE: International Centre for Numerical Methods in Engineering, 2001. ISBN 84-89925-77-1. [www.tib.eu/de/suchen/id/BLCP%3ACN050065390/A-finite-volume-unstructured-mesh-approach-to-dynamic/](http://www.tib.eu/de/suchen/id/BLCP%3ACN050065390/A-finite-volume-unstructured-mesh-approach-to-dynamic/).
- [442] E. Džuferović. *Interaction of viscoplastic fluid and viscoelastic solid - Numerical modelling*. PhD thesis, University of Sarajevo, 2002. In Bosnian.
- [443] A. Karač and A. Ivanković. Drop impact of fluid-filled plastic containers: finite volume method for coupled fluid-structure-fracture problems. In H.A. Mang, F. G. Rammerstorfer, and J. Eberhardsteiner, editors, *WCCM V, Fifth World Congress on Computational Mechanics*, Vienna, Austria, 2002.

- [444] A. K. Slone, T.cN. Croft, A. J. Williams, and M. Cross. A two fluid approach to high impact interaction amongst solid structures. In H. A. Mang, F. G. Rammerstorfer, and J. Eberhardsteiner, editors, *Fifth World Congress on Computational Mechanics Proceedings*, Vienna, Austria, 2002. Vienna University of Technology, Austria. ISBN 3-9501554-0-6.
- [445] A. K. Slone, D. Grossman, A.J. Williams, K. Pericleous, C. Bailey, and M. Cross. A time and space accurate numerical approach to closely coupled fluid structure interaction problems. In *11th International Colloquium on Numerical Analysis and Computer Science With Applications*, Plovdiv, Bulgaria, 2002.
- [446] A. Karač and A. Ivanković. Fully predictive model of the drop impact and fracture of fluid-filled plastic containers. In *Proceedings of 11th ACME conference on computational mechanics in engineering*, pages 113–116, Glasgow, 2003. University of Strathclyde Publishing.
- [447] A. Karač and A. Ivanković. Modelling the drop impact behaviour of fluid-filled polyethylene containers. In B. R. K. Blackman, A. Pavan, and J. G. Williams, editors, *Fracture of Polymers*, pages 253–264.ESIS publication 32, 2003. Composites and Adhesives.
- [448] A. Karač. *Drop impact of fluid-filled polyethylene containers*. PhD thesis, Imperial College London, 2003.
- [449] M. Cross, A. K. Slone, T. N. Croft, and A. J. Williams. Computational modelling of thermal fluid structure interaction processes. In B. H. V. Topping, editor, *Progress in Engineering Computational Technology*, page 111 – 126. Saxe-Coberg Publications, 2004.
- [450] A. Karač and A. Ivanković. Modelling drop impact and fracture of fluid-filled plastic containers. In *Proceedings of The 15<sup>th</sup> European Conference on Fracture - Advanced Fracture Mechanics for Life and Safety Assessments*, Stockholm, Sweden, 2004.
- [451] C. G. Giannopapa. *Fluid-Structure interaction in flexible vessels*. PhD thesis, University of London, 2004.
- [452] C. G. Giannopapa and G. Papadakis. A new formulation for solids suitable for a unified solution method for fluid-structure interaction problems. In *ASME PVP*, volume 491-1, pages 111–117, San Diego California, 2004.
- [453] A. K. Slone and M. Cross. A comparison of finite element and finite volume methods for computational structural mechanics and their application in multi-physics problems. In *5th International Conference on Engineering Computational Technology*. Civil-Comp Press, 2006. ISBN 0-948749-96-2. paper number 71.
- [454] A. K. Slone, T. N. Croft, A. J. Williams, and M. Cross. A mixed eulerian-lagrangian approach to high speed collision between solid structures on parallel clusters. In *5th International Conference on Engineering Computational Technology*. Civil-Comp Press, 2006. ISBN 1-905088-10-8. paper number 118.

- [455] M. Cross, T. N. Croft, D. McBride, A. K. Slone, and A. J. Williams. Using mixed discretisation schemes in multi-physics simulation. In *Innovation in Engineering Computational Technology*, pages 309–324. Saxe-Coburg Publications, 2006. [www.ctresources.info/csets/download/csets.315.pdf](http://www.ctresources.info/csets/download/csets.315.pdf).
- [456] G. Papadakis and C. G. Giannopapa. Towards a unified solution method for fluid-structure interaction problems: Progress and challenges. In *Proceedings of PVP 2006-ICPVT11 10<sup>th</sup> International Symposium on Emerging Technology in Fluids*, Vancouver, Canada, 2006.
- [457] C. G. Giannopapa and G. Papadakis. Indicative results and progress on the development of the unified single solution method for fluid-structure interaction problems. (CASA-report, No. 0711). Technical report, Technische Universiteit Eindhoven, Eindhoven, 2007.
- [458] A. Karač and A. Ivanković. Investigating the behaviour of fluid-filled polyethylene containers under base drop impact: A combined experimental/numerical approach. *International Journal of Impact Engineering*, 36:621–631, 2009.
- [459] A. Karač and A. Ivanković. Behaviour of fluid filled PE containers under impact: Theoretical and numerical investigation. *International Journal of Impact Engineering*, 36:621–631, 2009.
- [460] A. Safari, A. Ivanković, Ž. Tuković, and E. Casey M. Walter. A fluid-structure interaction study of biofilm detachment. In *1<sup>st</sup> International Conference on Mathematical and Computational Biomedical Engineering - CMBE2009, June 29 -July 1 Swansea, UK*. P. Nithiarasu, R. L., 2009.
- [461] A. K. Slone, A. J. Williams, T. N. Croft, and M. Cross. Dynamic fluid structure interaction in parallel: a challenge for scalability. In B. H. V. Topping and P. Ivanyi, editors, *Parallel, Distributed and Grid Computing for Engineering*, pages 329–350. Saxe-Coburg Publications, 2009. based upon an invited keynote presentation.
- [462] S. Das, S. R. Mathur, and J. Y. Murthy. An unstructured finite-volume method for structure-electrostatic interactions in MEMS. In *Proceedings of IMECE2010 2010 ASME International Mechanical Engineering Congress and Exposition*. Vancouver, Canada, 2010.
- [463] A. Kelly and M.-J. O’Rourke. Two system, single analysis, fluid-structure interaction modelling of the abdominal aortic aneurysms. *Proceedings of the Institution of Mechanical Engineers Part H - Journal of Engineering in Medicine*, 224(H8):955–970, 2010.
- [464] A. Kelly and M.-J. O’Rourke. Fluid, solid and fluid-structure interaction simulations on patient-based abdominal aortic aneurysm models. *Proceedings of the Institution of Mechanical Engineers Part H - Journal of Engineering in Medicine*, 226(4):288–304, 2012.
- [465] S. Das. *Fluid-Structure Interactions in Microstructures*. PhD thesis, University of Texas at Austin, 2013.
- [466] I. L. de Oliveira, J. L. Gasche, J. Militzer, and C. E. Baccin. Using FOAM-Extend to Assess the Influence of Fluid-Solid Interaction on the Flow in Intracranial Aneurysms. In *COBEM-2017-0851, 24<sup>th</sup> ABCM International Congress of Mechanical Engineering*, Curitiba, PR, Brazil, 2017.

- [467] I. L. de Oliveira. *Using FOAM-Extend to assess the influence of fluid-structure interaction on the rupture of intracranial aneurysms*. PhD thesis, Sao Paulo State University, Júlio De Mesquita Filho, 2017.
- [468] P. Cardiff, A. Karač, P. De Jaeger, H. Jasak, J. Nagy, A. Ivanković, and Ž. Tuković. Towards the development of an extendable solid mechanics and fluid-solid interactions toolbox for OpenFOAM. *preprint*, 2018. arXiv:1808.10736 [math.NA], available at <https://arxiv.org/abs/1808.10736>.
- [469] Ž. Tuković, M. Bukač, P. Cardiff, H. Jasak, and A. Ivanković. Added mass partitioned fluid-structure interaction solver based on a robin boundary condition for pressure. In *OpenFOAM Selected papers of the 11th Workshop*, pages 1–23. Springer International, 2018.
- [470] P. S. Leever, G. Venizelos, and A. Ivanković. Rapid crack propagation along pressurized pipe: small-scale testing and numerical modelling. *Construction and Building Materials*, 1993.
- [471] I. Demirdžić, A. Ivanković, H. J. MacGillivray, and K. Maneeratana. Numerical modelling of high-rate tensile tests using finite volume formulation. In *Proceedings of IUTAM Symposium on Innovative Computational Methods for Fracture and Damage*, Dublin, Ireland, 1996.
- [472] N. Murphy and A. Ivanković. Dynamic fracture simulation of brittle material characterised by microcrack-dominated failure mechanisms. In *Proceedings of 7<sup>th</sup> ACME Conf Comp Mech in Eng.*, pages 99–102, Durham, UK, 1999.
- [473] V. Stylianou. *Finite volume modelling of rapid crack propagation (RCP) in brittle polymers*. PhD thesis, Imperial College London, 1999.
- [474] K. C. Pandya, A. Ivanković, and J. G. Williams. Cohesive zone modelling of crack growth in polymers - part 2 - numerical simulation of crack growth. *Plastics, Rubber and Composites*, 29:447–452, 2000.
- [475] K. C. Pandya, A. Ivanković, and J. G. Williams. Predicting crack growth in tough polyethylene from measured cohesive zone traction-separation curves. In *Proceedings of 11th Int. Conf. on Deformation, Yield and Fracture of Polymers*, 2000.
- [476] K. C. Pandya, A. Ivanković, and J. G. Williams. Predictive fracture modelling in tough polyethylenes using experimentally measured cohesive zone traction curves. In *Proceedings of 13th European Conference on Fracture - ECF13*, San Sebastian, Spain, 2000.
- [477] A. Ivanković, H. Jasak, A. Karač, V. Tropša, and P. Leever. Fully predictive model of RCP in plastic pipes. In *Proceedings of 14<sup>th</sup> European Conference on Fracture*, Kracow, Poland, 2002.
- [478] A. Ivanković, H. Jasak, A. Karač, and V. Tropša. Prediction of dynamic fracture in pressurised plastic pipes. In *The Annual Conference of the Association of Computational Mechanics in Engineering*, volume 10, pages 173–176, 2002.

- [479] A. Ivanković, N. Murphy, and S. Hillmansen. Evolution of dynamic fractures in PMMA: experimental and numerical investigations. In M. H. Aliabadi and A. Ivanković, editors, *Advances in fracture mechanics, vol. 9*. WIT Press/Computational Mechanics Publications, Southampton, UK, 2004.
- [480] N. Murphy. *Dynamic Fracture of PMMA: A combined experimental and numerical investigation*. PhD thesis, University College Dublin, 2007.
- [481] D. McAuliffe, A. Karač, N. Murphy, and A. Ivanković. Transferability of adhesive fracture toughness measurements between peel and TDCB test methods for a nano-toughened epoxy. *Adhesion Society*, 2011. <http://hdl.handle.net/10197/4765>.
- [482] D. McAuliffe, A. Karač, N. Murphy, and A. Ivanković. Determination of the cohesive strength and toughening mechanisms of a nano-modified adhesive under a triaxial stress. *Adhesion Society*, 2012. <http://hdl.handle.net/10197/4785>.
- [483] D. McAuliffe. *Fracture Toughness Characterisation of a Nano-modified Structural Adhesives*. PhD thesis, University College Dublin, 2012.
- [484] V. Cooper, A. Ivankovic, A. Karač, D. McAuliffe, and N. Murphy. Effects of bond gap thickness on the fracture of nano-toughened epoxy adhesive joints. *Polymer*, 53(24):5540 – 5553, 2012. doi: 10.1016/j.polymer.2012.09.049.
- [485] I. Georgiou, A. Ivanković, A.J. Kinloch, and V. Tropsa. Rate dependent fracture behaviour of adhesively bonded joints. In A. Pavan B. R. K. Blackman and J. G. Williams, editors, *Fracture of Polymers, Composites and Adhesives II*, volume 32 of *European Structural Integrity Society*, pages 317 – 328. Elsevier, 2003.
- [486] I. Georgiou, H. Hadavinia, A. Ivanković, A. J. Kinloch, V. Tropsa, and J. G. Williams. Cohesive zone models and the plastically-deforming peel test. *The Journal of Adhesion*, 79:239–265, 2003.
- [487] V. Cooper, A. Ivanković, and A. Karač. A mode I fracture behaviour analysis of adhesively bonded joints. In *European conference on fracture*, volume 17, Brno, Czech Republic, 2008.
- [488] V. J. Cooper. *The Fracture Behaviour of Nano-toughened Structural Epoxy Adhesives*. PhD thesis, University College Dublin, 2010.
- [489] A. Tabaković, A. Karač, A. Ivanković, A. Gibney, C. McNally, and M. D. Gilchrist. Modelling the quasi-static behaviour of bituminous material using a cohesive zone model. *Engineering Fracture Mechanics*, 77:2403–2418, 2010.
- [490] D. Carolan. *Mechanical and Fracture Properties of PCBN as a Function of Rate and Temperature*. PhD thesis, University College Dublin, 2011.
- [491] M. Petrović. *The Behaviour of Polycrystalline Diamonds as a Function of Rate and Temperature*. PhD thesis, University College Dublin, 2011.
- [492] D. Carolan, A. Ivanković, and N. Murphy. Numerical investigation into dynamic fracture of pcbn. *Key Engineering Materials*, 488:553–556, 2012.

- [493] D. Carolan, A. Ivanković, and N. Murphy. A combined experimental-numerical investigation of fracture of polycrystalline cubic boron nitride. *Engineering Fracture Mechanics*, 99:101–117, 2013.
- [494] P. Alveen, D. McNamara, D. Carolan, N. Murphy, and A. Ivanković. Analysis of two-phase ceramic composites using micromechanical models. *Computational Materials Science*, 92:318–324, 2014.
- [495] D. McNamara, P. Alveen, D. Carolan, N. Murphy, and A. Ivanković. Micromechanical study of strength and toughness of advanced ceramics. *Procedia Materials Science*, 3:1810–1815, 2014.
- [496] P. Alveen. *An experimental-numerical investigation into the properties of polycrystalline cubic boron nitride towards materials optimisation*. PhD thesis, University College Dublin, 2015.
- [497] R. A general poro-elastic model for pad-scale fracturing of horizontal wells. *A general poro-elastic model for pad-scale fracturing of horizontal wells*. PhD thesis, University of Texas at Austin, 2015.
- [498] D. McNamara, P. Alveen, D. Carolan, N. Murphy, and A. Ivanković. Numerical analysis of the strength of polycrystalline diamond as a function of microstructure. *International Journal of Refractory Metals and Hard Materials*, 52:195–202, 2015.
- [499] D. McNamara. *The mechanical and fracture properties of polycrystalline diamond as a function of microstructure*. PhD thesis, University College Dublin, 2015.
- [500] D. Lee. *A Model for Hydraulic Fracturing and Proppant Placement in Unconsolidated Sands*. PhD thesis, University of Texas at Austin, 2017.
- [501] S. Shiting Yi. *Development of Computationally Efficient 2D and Pseudo-3D Multi-Fracture Models with Applications to Fracturing and Refracturing*. PhD thesis, University of Texas at Austin, 2018.
- [502] S. R. Sabbagh-Yazdi, A. Farhoud, and S. A. Gharebaghi. Simulation of 2D linear crack growth under constant load using GFVM and two-point displacement extrapolation method. *Applied Mathematical Modelling*, 2018. doi: 10.1016/j.apm.2018.05.022.
- [503] M.-J. Pindera. Local/global stiffness matrix formulation for composite materials and structures. *Composites Engineering*, 1(2):69–83, 1991.
- [504] J. Aboudi, M.-J. Pindera, and S.M. Arnold. Elastic response of metal matrix composites with tailored microstructures to thermal gradients. *International Journal of Solids and Structures*, 31:1393–1428, 1994.
- [505] J. Aboudi. Micromechanical analysis of the fully coupled finite thermoelastic response of rubberlike matrix composites. *International Journal of Solids and Structures*, 39:2587–2612, 2002.

- [506] J. Aboudi, M.-J. Pindera, and S.M. Arnold. High-fidelity generalized method of cells for inelastic periodic multiphase materials. Technical report, NASA TM-2002-211469, 2002.
- [507] Y. Zhong, M.-J. Pindera, and S. Arnold. Efficient reformulation of HOTFGM: Heat conduction with variable thermal conductivity. *NASA CR 2002-211910*, November 2002.
- [508] J. Aboudi, M.-J. Pindera, and S.M. Arnold. Higher-order theory for periodic multiphase materials with inelastic phases. *International Journal of Plasticity*, 19:805–847, 2003.
- [509] Y. Bansal and M.-J. Pindera. Efficient reformulation of the thermo-elastic higher-order theory for FGMs. *Journal of Thermal Stresses*, 26(11-12):1055–1092, 2003.
- [510] S.M. Arnold, B. Bednarczyk, and J. Aboudi. Comparison of the computational efficiency of the original versus reformulated high-fidelity generalized method of cells. Technical report, NASA/TM-2004-213438., 2004.
- [511] Y. Bansal and Pindera M.-J. Testing the predictive capability of the high-fidelity generalized method of cells using an efficient reformulation. Technical report, NASA/CR-2004-213043, 2004.
- [512] B.A. Bednarczyk, S.M. Arnold, J. Aboudi, and M.-J. Pindera. Local field effects in titanium matrix composites subject to fiber-matrix debonding. *International Journal of Plasticity*, 20: 1707–1737, 2004.
- [513] M.-J. Pindera, Y. Bansal, and Y. Zhong. Finite-Volume Direct Averaging Theory for Functionally Graded Materials (FVDAT-FGM). Technical report, NASA Disclosure of Invention and New Technology Form 1679, 2004.
- [514] Y. Zhong, Y. Bansal, and M.-J. Pindera. Efficient reformulation of the thermal higher-order theory for FGM's with variable thermal conductivity. *International Journal of Computational Engineering Science*, 5(4):795–831, 2004.
- [515] J. Aboudi. Micromechanically established constitutive equations for multiphase materials with viscoelastic-viscoplastic phases. *Mechanics of Time-Dependent Materials*, 9:121–145, 2005.
- [516] J. Aboudi and R. Gilat. Micromechanical analysis of lattice blocks. *International Journal of Solids and Structures*, 42:4372–4392, 2005.
- [517] M. A. A. Cavalcante. Modelling of the transient thermo-mechanical behavior of composite material structures by the finite-volume theory. Master's thesis, Federal University of Alagoas, Maceio, Alagoas, Brazil, 2006.
- [518] M.-J. Pindera and Y. Bansal. Finite volume direct averaging micromechanics of heterogeneous materials with elastic-plastic phases. *International Journal of Plasticity*, 22: 775–825, 2006.
- [519] H.A. Bruck, R. Gilat, J. Aboudi, and A.L. Gershon. A new approach for optimizing the mechanical behavior of porous microstructures for porous materials by design. *Modelling and Simulation in Materials Science and Engineering*, 15:653–674, 2007.

- [520] M. A. A. Cavalcante, S. P. C. Marques, and M.-J. Pindera. Parametric formulation of the finite-volume theory for functionally graded materials - part I: Analysis. *ASME Journal of Applied Mechanics*, 74:935–945, 2007.
- [521] M. A. A. Cavalcante, S. P. C. Marques, and M.-J. Pindera. Parametric formulation of the finite-volume theory for functionally graded materials - part II: Numerical results. *ASME Journal of Applied Mechanics*, 74:946–957, 2007.
- [522] A. S. Drago and M.-J. Pindera. Micro-macromechanical analysis of heterogeneous materials: macroscopically homogeneous vs periodic microstructures. *Composites Science and Technology*, 67(6):1243–63, 2007.
- [523] M. Gattu. Parametric finite volume theory for periodic heterogeneous materials. Master's thesis, University of Virginia, Charlottesville, Virginia, USA, 2007.
- [524] M.-J. Pindera and Y. Bansal. On the micromechanics-based simulation of metal matrix composite response. *Journal of Engineering Materials and Technology*, 129(3):468–82, 2007.
- [525] M. Ryvkin and J. Aboudi. The effect of fiber loss in periodic composites. *International Journal of Solids and Structures*, 44:3497–3513., 2007.
- [526] B.A. Bednarczyk, J. Aboudi, S.M. Arnold, and R.M. Sullivan. Analysis of space shuttle external tank spray-on foam insulation with internal pore pressure. *Journal of Engineering Materials Technology*, 130:041005–0410016, 2008.
- [527] M. A. A. Cavalcante, S. P. C. Marques, and M.-J. Pindera. Computational aspects of the parametric finite-volume theory for functionally graded materials. *Computational Materials Science*, 44:422–438, 2008.
- [528] M. Gattu, H. Khatam, A. S. Drago, and M.-J. Pindera. Parametric finite-volume micromechanics of uniaxial, continuously-reinforced periodic materials with elastic phases. *Journal of Engineering Materials and Technology*, 130:31015–31030, 2008.
- [529] G. H. Paulino, M.-J. Pindera, R. H. Dodds, F. E. Rochinha, E. V. Dave, and L. Chen. Multiscale and functionally graded materials. In *AIP conference proceedings*, volume 973, Melville, New York, 2008.
- [530] M. A. A. Cavalcante, S. P. C. Marques, and M.-J. Pindera. Transient thermo-mechanical analysis of a layered cylinder by the parametric finite-volume theory. *Journal of Thermal Stresses*, 32:112–134, 2009.
- [531] X. Gao, Y. Song, and Z. Sun. Quadrilateral subcell based finite volume micromechanics theory for multiscale analysis of elastic periodic materials. *ASME Journal of Applied Mechanics*, 76:011013–1, 2009.
- [532] H. Khatam and M.-J. Pindera. Parametric finite-volume micromechanics of periodic materials with elastoplastic phases. *International Journal of Plasticity*, 25:1386–1411, 2009.

- [533] H. Khatam and M.-J. Pindera. Thermo-elastic moduli of lamellar composites with wavy architectures. *Composites Part B: Engineering*, 40(1):50–64, 2009.
- [534] H. Khatam, L. Chen, and M.-J. Pindera. Elastic and plastic response of perforated plates with different porosity architectures. *Journal of Engineering Materials and Technology, Transactions of the ASME*, 131(3):031015–14, 2009.
- [535] J. Aboudi and Y. Freed. *Shape Memory Alloys: Manufacture Properties and Applications, Micromechanical modeling of shape memory alloy composites*. Nova Science Publishers, 2010.
- [536] B.A. Bednarczyk, J. Aboudi, S.M. Arnold, and R.M. Sullivan. Micromechanics modeling of composites subjected to multiaxial progressive damage in the constituents. *AIAA Journal*, 48:1367–1378, 2010.
- [537] R. Haj-Ali and J. Aboudi. Formulation of the high-fidelity generalized method of cells with arbitrary cell geometry for refined micromechanics and damage in composites. *International Journal of Solids and Structures*, 47:3447–3461, 2010.
- [538] H. Khatam and M.-J. Pindera. Plasticity-triggered architectural effects in periodic multilayers with wavy microstructures. *International Journal of Plasticity*, 26(2):273–287, 2010.
- [539] J. Aboudi. The effect of anisotropic damage evolution on the behavior of ductile and brittle matrix composites. *International Journal of Solids and Structures*, 48:2102–2119, 2011.
- [540] M. A. A. Cavalcante, S. P. C. Marques, and M.-J. Pindera. Transient finite-volume analysis of a graded cylindrical shell under thermal shock loading. *Mechanics of Advanced Materials and Structures*, 18:53–67, 2011.
- [541] M. A. A. Cavalcante, H. Khatam, and M.-J. Pindera. Homogenization of elastic-plastic periodic materials by FVDAM and FEM approaches - An assessment. *Composites Part B: Engineering*, 42:1713–1730, 2011.
- [542] J. Chareonsuk and P. Vessakosol. Numerical solution for functionally graded solids under thermal and mechanical loads using a high-order control volume finite element method. *Applied Thermal Engineering*, 31:213–27, 2011.
- [543] H. Khatam and M.-J. Pindera. Plastic deformation modes in perforated sheets and their relation to yield and limit surfaces. *International Journal of Plasticity*, 27(10):1537–59, 2011.
- [544] D. Carolan, Ž. Tuković, D. McNamara, P. Alveen, N. Murphy, and A. Ivanković. Effect of microstructure on the fracture toughness of polycrystalline cubic boron nitride. In *7<sup>th</sup> OpenFOAM Workshop*, Darmstadt, Germany, 2012.
- [545] M. A. A. Cavalcante and M.-J. Pindera. Generalized finite-volume theory for elastic stress analysis in solid mechanics - part I: Framework. *ASME Journal of Applied Mechanics*, 79, 2012.

- [546] M. A. A. Cavalcante and M.-J. Pindera. Generalized finite-volume theory for elastic stress analysis in solid mechanics - part II: Results. *ASME Journal of Applied Mechanics*, 79, 2012.
- [547] M. A. A. Cavalcante. *Generalized finite-volume micromechanics theory for heterogeneous materials*. PhD thesis, University of Virginia, 2012.
- [548] H. Khatam and M.-J. Pindera. Microstructural scale effects in the nonlinear elastic response of bio-inspired wavy multilayers undergoing finite deformation. *Composites Part B: Engineering*, 43(3):869–84, 2012.
- [549] M. A. A. Cavalcante and M.-J. Pindera. Generalized FVDAM theory for periodic materials with elastic- plastic phases. In *CILAMCE 2013 Proceedings of the XXXIV Iberian Latin-American Congress on Computational Methods in Engineering*, ABMEC, Pirenópolis, GO, Brazil, 2013.
- [550] M.A.A. Cavalcante and M.-J. Pindera. Generalized FVDAM theory for periodic materials undergoing finite deformations - part I: Framework. *ASME Journal of Applied Mechanics*, 81(2):021005–021010., 2014.
- [551] M.A.A. Cavalcante and M.-J. Pindera. Generalized FVDAM theory for periodic materials undergoing finite deformations - part II: numerical results. *ASME Journal of Applied Mechanics*, 81(2):021006–021012, 2014.
- [552] P. Cardiff, M. Leonard, N. Murphy, and A. Ivanković. Fracture toughness optimization of nano-toughened structural adhesives: A representative volume element approach. In *Proceedings of the 37<sup>th</sup> Annual Meeting of the Adhesion Society*, San Diego, CA, USA, 2014.
- [553] M. Leonard. *Micro-Mechanical Modelling of Toughening Mechanisms in Nano-Toughened Structural Adhesives*. PhD thesis, University College Dublin, 2014.
- [554] W. Tu and M.-J. Pindera. Cohesive zone-based damage evolution in periodic materials via finite volume homogenization. *ASME Journal of Applied Mechanics*, 81 (10):1–12, 01005, 2014.
- [555] D. Carolan, A. Ivankovic H. M. Chong, A. J. Kinloch, and A. C. Taylor. Co-continuous polymer systems: A numerical investigation. *Computational Materials Science*, 98:24–33, 2015.
- [556] W. Tu. *CZM-based Finite-Volume Homogenization and Optimization of Periodic Composites*. PhD thesis, University of Virginia, 2016.
- [557] Q. Chen, G. Wang, X. Chen, and J. Geng. Finite-volume homogenization of elastic/viscoelastic periodic materials. *Composite Structures*, 182:457–470, 2017.
- [558] Q. Chen, G. Wang, and M.-J. Pindera. Finite-volume homogenization and localization of nanoporous materials with cylindrical voids. part 1: Theory and validation. *European Journal of Mechanics / A Solids*, 2018. doi: 10.1016/j.euromechsol.2018.02.004.

- [559] Q. Chen, W. Tu, R. Liu, and X. Chen. Parametric multiphysics finite-volume theory for periodic composites with thermo-electro-elastic phases. *Journal of Intelligent Material Systems and Structures*, 29:530–552, 03 2018.
- [560] J. Ye, Y. Hong, H. Cai, Y. Wang, Z. Zhai, and B. Shi. A new three-dimensional parametric FVDAM for investigating the effective elastic moduli of particle-reinforced composites with interphase. *Mechanics of Advanced Materials and Structures*, 0(0):1–11, 2018. doi: 10.1080/15376494.2018.1452321. URL 10.1080/15376494.2018.1452321.
- [561] I. Bijelonja and S. Muzafherija Demirdžić. Some computational aspects of finite volume analysis of solid body deformation. In *Proceedings of 3<sup>rd</sup> Congress of Croatian Society of Mechanics*, pages 261–267, Dubrovnik, Croatia, 2000.
- [562] M. Cross, C. Walshaw, A. J. Williams, A. K. Slone, T. N. Croft, and K. McManus. Parallel processing for nonlinear problems. In E. Oñate and D. R. J. Owen, editors, *VII International Conference on Computational Plasticity*, Barcelona, Spain, 2003. CIMNE.
- [563] I. Demirdžić, E. Džaferović, and A. Ivanković. Predicting residual stresses due to solidification in cast plastic plates. In *4<sup>th</sup> International Congress of Croatian Society of Mechanics*, 2003.
- [564] A. J. Williams, A. K. Slone, T. N. Croft, and M. Cross. A mixed eulerian- lagrangian approach for metal forming. In *6th ESAFORM conference on Metal Forming*, Salerno, Italy, April 2003.
- [565] H. Kalkan. A combined experimental-numerical investigation on aluminium extrusion. Master’s thesis, Atilim University, Ankara, Turkey, 2011.
- [566] J. Mohan, A. Karač, N. Murphy, and A. Ivanković. An experimental and numerical investigation of the mixed-mode fracture toughness and lap shear strength of aerospace grade composite joints. *Key Engineering Materials*, 488:549–552, 2011.
- [567] P. Cardiff, P. De Jaeger, Ž. Tuković, and A. Ivanković. A finite approach to simulation of wire rolling. In *Joint Symposium of Irish Mechanics Society & Irish Society for Scientific & Engineering Computation, Galway*, 2014.
- [568] P. Cardiff, Ž. Tuković, A. Ivankovic, and P. De Jaeger. Development of an arbitrary Lagrangian-Eulerian finite volume method for metal forming simulation in OpenFOAM. In *The 13th OpenFOAM Workshop (OFW13)*, Shanghai, China, June 24-29 2018.
- [569] M. Clancy, P. Cardiff, P. De Jaeger, and A. Ivankovic. Implementation of advanced plasticity models in OpenFOAM. In *The 13th OpenFOAM Workshop (OFW13)*, Shanghai, China, June 24-29 2018.
- [570] D. Grossman, C. Bailey, K. Pericleous, and A. K. Slone. Computational modelling of blood flow and artery wall interaction. In *9th Workshop on the Finite Element Methods in Biomedical Engineering Biomechanics and Related Fields*, University of Ulm, Germany, 2002. ISBN 3-9806183-5-8.

- [571] C. M. Anthony. Finite volume modelling of the human leg. Master's thesis, Imperial College London, 2003.
- [572] O. Alakija, A. Ivanković, and A. Karač. Finite volume solution to high rate wave propagation through a lung alveoli stack. In *IUTAM Symposium on Impact Biomechanics: From Fundamental Insights to Applications*, pages 281–288, 2005.
- [573] N. M. Quinn, A. Ivanković, and A. Karač. An experimental and numerical investigation into the deformation profiles of mock arteries. In *ASME Summer Bioengineering Conference*, 2007.
- [574] N. M. Quinn, A. Ivanković, and A. Karač. A combined experimental and numerical investigation into early atherosclerosis. In *The Fifteenth UK Conference of the Association of Computational Mechanics in Engineering*, Glasgow, United Kingdom, 2-3 April, 2007. Civil-Comp Press. doi: 10.4203/ccp.85.11. Paper 11.
- [575] A. Safari, A. Ivanković, and Ž. Tuković. Numerical modelling of viscoelastic response of bacterial biofilm to mechanical stress. In *Bioengineering In Ireland Conference*, pages 25–26, Radisson Hotel, Sligo, January, 2008.
- [576] V. Kanyanta, A. Ivanković, and A. Karač. Accurate prediction of blood flow transients: A fluid-structure interaction approach in hemodynamic wall shear stress. In P. Nithiarasu, editor, *1<sup>st</sup> International Conference on Mathematical and Computational Biomedical Engineering - CMBE2009*, Swansea, UK, 2009.
- [577] V. Kanyanta. *Towards early diagnosis of atherosclerosis: Wall shear prediction*. PhD thesis, University College Dublin, Ireland, 2009.
- [578] S. Kelly. *Thrombus growth and its influence on the stress distribution in patient-based abdominal aortic aneurysm models*. PhD thesis, University College Dublin, 2009.
- [579] P. Cardiff, A. Karač, R. Flavin, D. FitzPatrick, and A. Ivanković. The development of a numerical model of the hip joint for complex soft tissue reconstructions around the hip joint. In *13<sup>th</sup> Annual Sir Bernard Crossland Symposium*, University College Dublin, Dublin, Ireland, 2010.
- [580] P. Cardiff, A. Karač, R. Flavin, D. FitzPatrick, and A. Ivanković. The development of a numerical model of the hip joint. In *17<sup>th</sup> Bioengineering In Ireland*, Galway, Ireland, 2011.
- [581] P. Cardiff, A. Karač, R. Flavin, D. FitzPatrick, and A. Ivanković. Numerical analysis of the hip joint bones in contact. In *ACME-UK, Heriott-Watt University*, Edinburgh, Scotland, 2011.
- [582] N. Quinn. *Towards early diagnosis of atherosclerosis: combined experimental and numerical investigation into the deformation of mock arterial models*. PhD thesis, University College Dublin, 2011.
- [583] P. Cardiff, A. Karač, R. Flavin, D. FitzPatrick, and A. Ivanković. Modelling the muscles for hip joint stress analysis using a finite volume methodology. In *18<sup>th</sup> Bioengineering In Ireland*, Belfast, Northern Ireland, 2012.

- [584] P. Cardiff, A. Karač, D. FitzPatrick, R. Flavin, and A. Ivanković. Development of mapped stress-field boundary conditions based on a Hill-type muscle model. *International Journal for Numerical Methods in Biomedical Engineering*, 2014. doi: 10.1002/cnm.
- [585] H. Khalili Parsa. *Compression tests on fluid-filled gelatine microcapsules: A combined experimental/numerical study*. PhD thesis, University College Dublin, 2014.
- [586] A. Safari. *A combined experimental and numerical study of biofilm detachment*. PhD thesis, University College Dublin, 2015.
- [587] K. Fitzgerald, P. Cardiff, R. Flavin, and A. Ivankovic. Calculation of hip joint contact pressures using a high resolution finite volume model with CT-based properties. In *Bioengineering in Ireland*, 2016.
- [588] K. Fitzgerald, P. Cardiff, R. Flavin, and A. Ivankovic. Towards in silico analysis of total hip arthroplasty mechanics. In *XXVI Congress of the International Society of Biomechanics*, Brisbane, Australia, 2017.
- [589] L. Muralidharan, P. Cardiff, R. Flavin, and A. Ivankovic. A numerical model for the calculation of ankle joint stresses. In *XXVI Congress of the International Society of Biomechanics*, Brisbane, Australia, 2017.
- [590] A. Kovačević, N. Stošić, and I. K. Smith. Solid-fluid interaction in screw compressors. In *XVI International Compressor Engineering Conference at Purdue*, 2002.
- [591] A. Kovačević, N. Stošić, and I. K. Smith. Three-dimensional modelling of solid-fluid interaction as a design tool in screw compressors. In *International Design Conference - DESIGN 2002*, Dubrovnik, Croatia, 2002.
- [592] A. Kovačević, N. Stošić, and I. K. Smith. The influence of rotor deflection upon the screw compressor process. In *Schraubecompressor tagung (Screw compressor meeting)*, Dortmund, Germany, 2002.
- [593] A. Kovačević, N. Stošić, and I. K. Smith. Numerical simulation of fluid flow and solid structure in screw compressors. In *Proceedings of 2002 ASME Congress*, New Orleans, USA, 2002. Symposium on the Analysis and Applications of Heat Pump and Refrigeration Systems.
- [594] A. Kovačević, N. Stošić, and I. K. Smith. Fluid-solid interaction for extension of range in screw machine application. In *Advances of CFD in Fluid Machinery Design, ImechE Seminar*, London, UK, 2003.
- [595] A. Kovačević, N. Stošić, I. K. Smith, and E. Mujić. Fluid-solid interaction in the design of multifunctional screw machines. In *8<sup>th</sup> International Design Conference - Design 2004*, volume 2, pages 1289–1295, Dubrovnik, Croatia, 2004.
- [596] A. Kovačević, E. Mujić, N. Stošić, and I. K. Smith. Extending the role of computational fluid dynamics in screw machines. *Journal of Process Mechanical Engineering, Part E, Proceedings of the Institution of Mechanical Engineers*, pages 83–97, 2011.

- [597] I. Bijelonja. A finite volume method for a geomechanics problem. In *Proceedings of the 22<sup>nd</sup> International DAAAM Symposium*, pages 323–324, 2011.
- [598] I. Demirdžić, S. Muzaferija, and M. Perić. Advances in computation of heat transfer, fluid flow, and solid body deformation using finite volume approaches. In E. M. Sparrow W. J. Minkowycz, editor, *Advances in Numerical Heat Transfer, Chapter 2*, pages 59–96. Taylor & Francis, 1997.
- [599] I. Bijelonja. Finite volume method analysis of large strain elasto-plastic deformation. In *The 16<sup>th</sup> DAAAM International Symposium*, Opatia, Croatia, 2005.
- [600] S. R. Sabbagh-Yazdi, M. T. Alkhamis, N. E. Mastorakis, and M. Esmaili. Finite volume analysis of two-dimensional strain in a thick pipe with internal fluid pressure. *International Journal of Mathematical Models and Methods in Applied Sciences*, 2:162–167, 2008.
- [601] S. R. Sabbagh-Yazdi, N. E. Mastorakis, and M. Esmaili. Explicit 2D matrix free Galerkin finite volume solution of plane strain structural problems on triangular meshes. *International Journal of Mathematics and Computers in Simulations*, 2:1–8, 2008.
- [602] M. T. Alkhamis, S. R. Sabbagh-Yazdi, M. Esmaili, and F. M. Wegian. Utilizing NASIR Galerkin finite volume analyzer for 2D plane strain problems under static and vibrating concentrated loads. *Jordan Journal of Civil Engineering*, 2:335–343, 2008.
- [603] S. R. Sabbagh-Yazdi, S. Alimohammadi, and N. E. Mastorakis. Comparison of finite element and finite volume solvers results for plane-stress displacements in plate with oval hole. In *Proceedings of the 4<sup>th</sup> IASME/WSEAS International Conference on Continuum Mechanics CM'09*, pages 168–173, 2009.
- [604] S. R. Sabbagh-Yazdi and T. Amiri-Saadatabadi. Sequential computations of two-dimensional temperature profiles and thermal stresses on an unstructured triangular mesh by GFVM method. *International Journal of Civil Engineering*, 9:171–182, 2011.
- [605] S. R. Sabbagh-Yazdi, M. Esmaili, and M. T. Alkhamis. Symmetric conditions for strain analysis in a long thick cylinder under internal pressure using NASIR unstructured GFVM solver. *Jordan Journal of Civil Engineering*, 5:258–267, 2011.
- [606] S. R. Sabbagh-Yazdi and S. Ali-Mohammadi. Performance evaluation of iterative GFVM on coarse unstructured triangular meshes and comparison with matrix manipulation based solution methods. *Scientia Iranica*, 18:131–138, 2011.
- [607] S. R. Sabbagh-Yazdi, S. AliMohammadi, and M. K. Pipelzadeh. Unstructured finite volume method for matrix-free explicit solution of stress-strain fields in two-dimensional problems with curved boundaries in equilibrium condition. *Applied Mathematical Modelling*, 36:2224–2236, 2012.
- [608] S. R. Sabbagh-Yazdi and M. Bayatlou. Equilibrium condition nonlinear modeling of a cracked concrete beam using a 2D Galerkin finite volume solver. *Computational Methods in Civil Engineering*, 3:63–76, 2012.

- [609] C. Bailey, P. Chow, M. Cross, K. Pericleous, G. A. Taylor, T. N. Croft, D. Wheeler, and H. Lu. Finite volume methods for multiphysics problems. In D. Haanel, R. Vilsmeirer, and F. Benkhaldoun, editors, *Finite Volumes for Complex Applications, II - Problems and Perspectives*, Duisburg, Germany, 1999. Hermes Science.
- [610] D. Hitchings, G. A. O. Davies, and A. Kamoulakos. *Linear static benchmarks*. International Association for the Engineering Analysis Community & National Agency for Finite Element Methods & Standards (NAFEMS), Glasgow, UK, 1987.
- [611] V. R. Voller. *Basic Control Volume Finite Element Methods for Fluids and Solids*. World Scientific, Singapore, 2009.